SOME ASPECTS OF COMBUSTION OF COAL IN FLUIDIZED BEDS

by

RABINDRA KUMAR CHAKRABORTY

A thesis

submitted for the

Degree of

Doctor of Philosophy

Department of Mechanical Engineering

The University of Aston in Birmingham, England

SEPTEMBER 1979

SOME ASPECTS OF COMBUSTION OF COAL IN FLUIDIZED BEDS

by

RABINDRA KUMAR CHAKRABORTY

A THESIS SUBMITTED FOR THE DEGREE OF DOCTOR OF PHILOSOPHY

1979

SUMMARY

This thesis presents an experimental study of the mechanism of combustion of carbon in shallow fluidized bed combustors. Burning rates and temperatures of electrode carbon spheres and burn-out times of batch charges of char particles were measured experimentally over a wider range of variables than reported hitherto. Bed temperature , carbon and inert particle size, superficial fluidizing velocity, oxygen concentration and static bed depth were the variables explored.

Combustion was found to be controlled mainly by chemical kinetics at a bed temperature of 800 °C, whereas at a bed temperature of 900 °C rate of transfer of oxygen to the carbon influenced combustion progressively as the inert particle size was increased. When the inert particle size approaches about 1000 μm, the rate of mass transfer of oxygen dominated the process entirely. Forced convection played an important role in the transfer of oxygen at high superficial fluidizing velocities.

Proposals have been presented to modify the existing models of combustion of single carbon particles, taking into account the effects of mass transfer by forced convection and the oxidation of carbon to carbon dioxide at the surface by oxygen. Predictions of this modified model were found to be in good agreement with experimental data. Burning rates and particle temperatures increased with increase in bed temperature, inert particle size, superficial fluidizing velocity and oxygen concentration.

Elutriation of unburnt carbon particles was minimal with large size of feed. The presence of a large number of burning carbon particles in a continuously-fed coal-fired fluidized bed combustor reduced burning rate and temperature of individual particles significantly by reducing local oxygen concentration within the bed. This helps to maintain the burning carbon particle temperatures to a value less than 100 K higher than the bed. The experiments showed that:

(i) Forced convection plays an important role to supply oxygen to burning carbon particles

(ii) Higher intensity of combustion (MW/m^3) could be achieved by larger size of carbon and inert particles, high bed temperature and high superficial fluidizing velocity

(iii) Better control of bed temperature may be achieved by recycling a part of exhaust gas through the bed to reduce rate of combustion.

The work demonstrates the relative importance of some design and operating parameters and suggests what needs to be done to improve future shallow fluidized bed combustors and where future research is required.

COMBUSTION MECHANISMS TEMPERATURES COAL FLUIDIZED BEDS

ACKNOWLEDGEMENTS

The author wishes to express his deepest gratitude, appreciation and sincere thanks to Dr. J. R. Howard for his constant encouragement, guidance, inspiration, invaluable advice and suggestions throughout the work.

The author also wishes to thank and acknowledge:

Dr.R.G.Temple, Department of Chemical Engineering, University of Aston for his assistance in analysing the char particle and Mr. Hepenstal, technical staff of the same department for conducting the proximate analysis tests;

Mr.A.R.Cooper, Department of Chemical Engineering, University of Aston for his suggestions and discussion in analysing some of the results;

Dr.P. Basu, Central Mechanical Engineering Research Institute, Durgapur, India for some of his suggestions and advice about the work;

Dr.J. Broughton, Engineering Development Department, NEI Mechanical Engineering Limited, Derby, England for his help in procuring the inert alumina particles;

Mr.Ian Ross, Research Student, Department of Chemical Engineering, University of Cambridge, Cambridge, England for his suggestions and discussion to interpret some of the results from a different point of view;

Mr. Mahendra Patel, Research Student, Department of Chemical Engineering, University of Cambridge, Cambridge, England for his help in procuring "Kanthal heating element";

The technical staff, Department of Mechanical Engineering, University

of Aston for their active co-operation and assistance for the experimental work, particularly to Mr. G. Rickers for his help in procuring materials, Mr. H. Smith for making the carbon spheres, Mr. H. Pratt, Mr. D. Green, Mr. L. Beddal and Mr. P. Pizer for constructing the experimental set-up, Mr. A. Evitts for his help in providing facilities for the experimental work, Mr. N. Moss, Mr. P. Hickman and Mr. E. Lawlor for their help in the laboratory at different times.

Mr. R. Howes, Mr. N. Haverly, Mr. T. F. Weir, Mr. A. Crowcombe and Mrs. S. Hunt, Communication Media Unit, University of Aston for their help in making films, photographs and slides.

Mrs.A.Breakspear, Mrs.M.Cousins and Mrs.D.Scott for typing the thesis.

The Commonwealth Scholarship Commission for financial help.

The author also acknowledges with gratitude the help of his brother-in-law, Mr. P. C. Chakraborty at the early stage of his educational career which helped the author to continue his education to this stage successfully.

Finally, the author wishes to thank his wife, Swapna, for her loving support and encouragement throughout the work.

DEDICATED TO

my parents:

Late N. K. Chakraborty and Mrs. Santilata Devi

and my son:

Indraneal (Neal)

NOMENCLATURE

A	Frequency (pre-exponential) factor,	(m/s)
b	Constant defining radius of carbon monoxide reaction zone around a burning carbon particle,	
c_p	Oxygen concentration in the particulate phase of the fluidized bed or in the bulk air far away from a burning carbon particle surface,	(k mol of oxygen/m^3)
c_s	Oxygen concentration at the burning carbon particle surface,	(k mol of oxygen/m^3)
d	Carbon particle diameter,	(m)
d_i	Carbon particle initial diameter before combustion,	(m)
d_p	Bed inert particle mean diameter,	(m)
D_G	Binary molecular diffusion coefficient in gas phase between air and oxygen,	(m^2/s)
E	Activation energy for combustion reaction between carbon and oxygen,	(k cal/k mol)
h	Heat transfer coefficient between fluidized bed and immersed object,	(W/m^2 K)
h_{gc}	Gas convective component of heat transfer coefficient between fluidized bed and immersed object,	(W/m^2 K)
h_{pc}	Particle convective component of heat transfer coefficient between fluidized bed and immersed object,	(W/m^2 K)
h_r	Radiative component of heat transfer coefficient between fluidized bed and immersed object,	(W/m^2 K)

NOMENCLATURE continued

K	Overall rate coefficient	(m/s)
$\frac{1}{K}$	Overall resistance to combustion,	(s/m)
k_g	Mass transfer coefficient,	(m/s)
$\frac{1}{k_g}$	Mass transfer resistance,	(s/m)
k_s	First order reaction rate constant at the carbon surface,	(m/s)
$\frac{1}{k_s}$	Kinetic resistance to combustion,	(s/m)
m	Mass of a carbon particle,	(kg)
m_i	Initial charge mass of fixed carbon in the batch charge of char particles,	(kg)
$\dot{m}$	Burning rate of a carbon particle,	(kg/s)
r	Radius of carbon monoxide reaction zone around a burning particle,	(m)
R	Universal gas constant, 1.986	$(\frac{k\ cal}{k\ mol\ K})$
Re	Reynolds Number of a burning carbon particle,	$(Re = \frac{Ud\rho_f}{\mu})$
Sc	Schmidt Number,	$(Sc = \frac{\mu}{\rho_f D_G})$
Sh	Sherwood Number of a burning carbon particle,	$(Sh = k_g \frac{d}{D_G})$
t	Time,	(s)
$t_{b_{batch}}$	Burn out time of batch charge of char particle,	(s)
$t_{b_{Diffusion}}$	Burn out time of a carbon particle under complete diffusion controlled rate of combustion,	(s)

NOMENCLATURE continued

$t_{b_{estimated}}$	Estimated burn out time of a char particle	(s)
$t_{b_{Kinetic}}$	Burn out time of a carbon particle under complete kinetically controlled rate of combustion,	(s)
t_b	Burn out time of a char particle	(s)
T_b	Bed temperature	(K)
T_s	Carbon particle surface temperature	(K)
U	Superficial fluidizing velocity	(m/s)
U_{mf}	Minimum fluidizing velocity	(m/s)

ε_m	Mean voidage around a burning carbon particle.	
μ	Dynamic viscosity of fluidizing gas,	(kg/m s)
ρ_c	Density of carbon particle,	(kg/m^3)
ρ_{char}	Density of char particle,	(kg/m^3)
ρ_f	Density of fluidizing gas,	(kg/m^3)
ρ_s	Density of inert particles,	(kg/m^3)
ϕ	A mechanism factor which takes the value 1 when carbon dioxide is transported away and 2 when carbon monoxide is transported away from the carbon surface.	

CONTENTS

CHAPTER FOUR: BURNING RATES OF SINGLE CARBON PARTICLES AND BURNING CARBON PARTICLE TEMPERATURES IN SHALLOW FLUIDIZED BEDS

PART A

CHAPTER FOUR: PART B

LIST OF FIGURES

LIST OF FIGURES continued

LIST OF FIGURES continued

LIST OF TABLES

CHAPTER ONE

INTRODUCTION

Fluidized bed combustion of coal has attracted much attention during the recent years from people concerned with future supply of energy resources and development of improved combustion systems. Increasingly high cost and utilisation of existing oil and gas reserves at a rate faster than that of discovery of new sources have caused a great concern for future energy supply. Known reserves of coal are much more abundant than those of oil and gas[1,2]. So following the era of cheap oil and gas, coal is now being reconsidered as an alternative to oil and gas; the latter two being regarded in long term as future premium fuels for applications where there is no reasonable alternative, e.g. air transport, internal combustion engine. Research for improved methods of burning coal during 1961-63 by *Elliott* while at C.E.G.B. and *Thurlow, Hoy & Wright* at BCURA[3-9] and subsequent extensive work in the U.K. and the U.S.A. has developed the fluidized bed combustion of coal to its present state. The incentive was to find a cheaper method than existing plant such as pulverised fuel boilers which could also reduce emissions of sulphur dioxide and oxides of nitrogen[9]. The fluidized bed combustion process also offers high heat transfer rate from the bed to its containment or immersed surfaces, high combustion intensity, low pollution from oxides of nitrogen and sulphur dioxide, flexibility of fuel usage by its capacity to cover a wide variety of solid fuels without recourse to major adjustments to the plants and reduced corrosion of boiler tubes[4,9-18].

The advantages and the technical feasibilities of fluidized bed combustion of coal are already well established[19]. Five successive International Conferences on Fluidized Bed Combustion in the U.S.A.[20-24], one International Symposium on Fluidized Combustion[25] and one International Conference on Fluidization[26], both in U.K. have shown the present accelerating development and interest in fluidized bed combustion of coal not only by the rate of growth of literature, but by the amount of monetary investment in demonstration plants[8,15,27-30]. In the U.S.A., for example, the ERDA 1977 budget for the development of fluidized combustion was of the order of $50 million[8]. Atmospheric and shallow fluidized bed industrial boilers are on the point of offering for sale by a number of commercial manufacturers who are prepared to give full commercial warranties[27-29]. Already a number of demonstration atmospheric fluidized bed boilers are operating satisfactorily[8,9,12-16, 30-33].

Pressurised fluidized bed combustion for combined gas and steam cycle power generation is under active development stage because of the higher thermal efficiency which can arise from such plant and significant reduction in size[8,9,11-15,34-36]. Improvement in efficiency of electric power generation, currently 36% in the best existing power stations can be raised to about 45%[37]. The International Energy Agency, financed by the U.S.A., Germany and the U.K. has started to build a demonstration pressurised fluidized bed rig at Grimethorpe in U.K. to investigate combustion, heat transfer, gas cleaning and energy recovery[6,8,9,34]. It is expected to be commissioned by 1979.

Research is also in progress on high intensity rotating fluidized beds[38-46]. In addition to the higher combustion intensities[41] (up to 240 MW/m^3 of bed when burning propane), wider range of turn-down, which is a limitation of a stationary fluidized beds, is achievable by altering the speed of rotation, as an extra control parameter. Gas and coal have been burned successfully in laboratory scale rotating fluidized beds[39,41,43,45,46].

Although a great deal of work has already been done to exploit the advantages of fluidized bed combustion and commercial units have been designed and constructed, the mechanisms of combustion of coal in fluidized beds, however, has not yet been established firmly, whether at atmospheric pressure or at elevated pressure[11,19]. The burning rates and temperatures of coal particles under differing design and operating conditions have also not been fully investigated. Information in these areas will be very helpful for the design and control of future fluidized bed combustion systems so that optimum performance can be achieved. The choices open to the investigators are:

(i) to perform experimental work over a wider range of bed operating conditions and compare the experimental results with predictions of existing models,

(ii) to suggest how these models might he modified to make them a more reliable tool for the combustion system designer.

Because some models were already in existence and there was, relatively little experimental data covering a range of variables of magnitudes

found in current fluidized bed combustion plants, it was decided to choose an experimental programme to gather more realistic data and then compare such data with predictions of existing models. Further it was hoped to suggest how these models might be improved. The experimental information should in any case contribute to the knowledge of the subject and help understanding of the process.

CHAPTER TWO

REVIEW OF LITERATURE

For brevity this review is restricted to literature on the mechanism of combustion of carbon in air and in beds of inert material fluidized by air.

Combustion of carbon in air has been studied both theoretically and experimentally by a number of investigators to establish the mechanism of combustion and to determine what the primary product of combustion at the carbon surface is at different temperatures. Study of combustion of a wide variety of pulverized coal, 100μm and less in size has also been made during the late 1960's and the early 1970's.[55] Before considering the combustion of carbon in fluidized beds, it is necessary to review combustion of carbon and pulverized coal in air because this combustion process is to some extent related to combustion of carbon in fluidized beds.

2.1 Combustion of Carbon in Air

During the earlier part of this century a number of general mathematical analyses were presented by *Nusselt*[47], *Burke & Schuman*[48,49], *Lewis*[50] and *Wentzel*[51] for the combustion of carbon in air. All of these models used the concept of stagnant gas around the burning carbon particle and assumed that diffusion of oxygen through this film controls the rate of combustion. These models concluded that it was mathematically

justifiable to assume that carbon dioxide was the sole primary product at the carbon surface[52]. But at the time (1934) this assertion was made, no experimental evidence to establish the physical reality had been reported. Later *Arthur*[53] demonstrated experimentally that this assumption was not true and that a significant quantity of carbon monoxide was formed at the carbon surface. These earlier models thus failed to explain all the experimental results which later became available.

Smith & Gudmundsen[54] first reported experimental measurements of burning rate of electrode carbon spheres, of 2-5mm in diameter, in stream of air heated to 900-1000 ^{o}C. The particle temperatures ranged from about 1150-1450 ^{o}C. These results although of limited range, showed that combustion was dominated by the rate of diffusion of oxygen towards the carbon surface[55].

Tu, Davis & Hottel[52] measured burning rates of brush carbon spheres, 25mm diameter, in a mixture of oxygen and nitrogen in an electrically heated furnace over a range of surface temperature, 950-1700 K. These results showed that above 1100 K the combustion was dominated by the rate at which oxygen diffuses towards the carbon surface. Comparing the burning rates of brush carbon in air from their experiments with those of *Dubinsky*[56] in carbon dioxide, they also argued against the hypothesis that combustion of carbon in air involves the transport of oxygen to the carbon surface in the form of carbon dioxide alone.

Parker & Hottel[57] measured the burning rate of brush carbon cylinders with hemispherical end, 25mm diameter, in an electrically heated furnace over a range of carbon surface temperature, 950 - 1400 K, in air stream. They also analysed gas samples withdrawn from the carbon surface by microsampling technique. They detected some oxygen at the carbon surface and concluded that the concentration was too high to be neglected. They also detected practically no carbon monoxide at the carbon surface. The presence of water vapour in the combustion air seems to have catalysed the oxidation of carbon monoxide with available oxygen to give such a result[58].

Hougen & Watson[59] presented a spherical reaction zone model of combustion of carbon particles in air which was based on the experimental results of burning coke on grates by *Kreisinger, Ovitz & Augustine*[60]. This model assumed that above 1000 ^{o}C the combustion of carbon is very fast and oxygen fails to reach the surface, as the carbon monoxide diffusing out from the burning carbon surface consumes oxygen completely in a spherical reaction zone around the burning carbon particle to form carbon dioxide according to the exothermic homogeneous gas-phase reaction:

$$2CO + O_2 \rightarrow 2CO_2 \qquad \ldots (2.1)$$

Part of this carbon dioxide diffuses to the carbon surface where it is reduced to carbon monoxide by the endothermic gasification reaction:

$$CO_2(gas) + C(solid) \rightarrow 2CO \qquad \ldots (2.2)$$

Heat flows from the reaction zone to support this reaction. This model was later widely accepted.

Arthur[53] conducted experiments with two types of carbons of different reactivity - coal char and artificial graphite, to study the primary product of combustion at the surface over the temperature range 460 - 900 ^{o}C. He used phosphorous oxychloride ($POCl_3$) to suppress the oxidation reaction between carbon monoxide and oxygen. His results showed that the proportion of carbon monoxide increased exponentially with temperature and the ratio of carbon monoxide to carbon dioxide formed at the surface could be expressed as follows:

$$\frac{CO}{CO_2} = 10^{3.4} \; e^{-\frac{12,400}{RT_s}} \qquad \ldots (2.3)$$

Spalding[61] suggested that above 1500 K the chemical reaction rate at the carbon surface is very high and oxygen, carbon dioxide and steam may be assumed to be absent near the burning carbon surface. He also reported that *Vulis*[62] found better agreement between his predicted burning times and *Nikolayev's* experimental data on the basis of formation of carbon monoxide at the surface.

Van de Held[63] reported experimental work of *Van Loon*[64] from which it can be concluded that at very high gasification rates carbon monoxide is the primary product at the carbon surface which burns in a thin reaction zone around the burning carbon particle. This reaction zone is at a higher temperature than that of the surface and supplies the heat for gasification reaction between carbon and carbon dioxide at the surface. He also worked out heat and mass transfer

balance at a plane carbon surface assuming the reaction zone model to be valid above 1100 ^{o}C. But he suggested that at a surface temperature of about 800 ^{o}C, oxygen reaches the surface and concentration of carbon-dioxide is also not negligible there. He also referred to the experiments of *Mulder & De Graff*[65] to support the existence of reaction zone which is at a higher temperature than that of the carbon surface.

Wicke & Wurzbacher[58] used capillary suction probes to take gas samples at different distances from a spectreographically pure carbon tube burning in an electrically heated furnace in streams of dry oxygen, a mixture of oxygen-water vapour and a mixture of oxygen - carbon tetrachloride and analysed the samples for concentrations of oxygen, carbon monoxide and carbon dioxide. The carbon surface temperature was in the range 1000 - 1230 ^{o}C. Their results showed that at and above 1100 ^{o}C oxygen concentration approached zero at the carbon surface. They also found that the presence of water vapour accelerated the oxidation reaction between carbon monoxide and oxygen catalytically. They suggested that above 1100 ^{o}C the gasification reaction between carbon and carbon dioxide at the carbon surface would be important.

Golovina & Khaustovich[66] measured burning rates of electrode carbon spheres, 15mm in diameter in cold streams of air (oxygen nitrogen mixture having the oxygen concentration equal to that of air) and carbon dioxide over carbon surface temperature range 1000 - 2800 K. They found that the primary product at the carbon surface was carbon dioxide at about 1200 K and carbon monoxide at about 1700 K, when combustion occurred

in air. They also reported that increase in temperature had little effect on the rate of combustion in air above 1400 ^{o}C.

Khitrin[67] discussed about the combustion of carbon in air and suggested that when Reynolds Number is less than 100 and the carbon surface temperature is in the range of 900 - 1300 ^{o}C oxygen would reach the surface producing both carbon monoxide and carbon dioxide there. But at still higher temperature the reaction zone model will be relevant.

Field et al[55] reviewed the existing literature on combustion of carbon in air in detail and suggested that at carbon combustion temperatures (above 1000 K) carbon monoxide would be the primary product at the surface and for carbon particles larger than 1mm it would burn very close to the surface, the combustion process under such conditions being controlled by the rate of diffusion of oxygen towards the surface.

Roberts & Smith[68] measured the burning rates and temperatures of large carbon spheres, 6 - 6.8mm in diameter, in a stream of cold and dry oxygen over the surface temperature, 1845 - 1893 K to investigate indirectly whether carbon monoxide was the primary product of the carbon surface and if so, whether subsequent combustion of this carbon monoxide around the burning particle has any affect on the particle temperature. His experimentally measured burning rates and carbon surface temperatures agreed well with calculated values when it was assumed that carbon monoxide was the primary product at the surface and combustion was controlled by the rate of diffusion of oxygen towards the carbon surface. However, the use of dry oxygen in their experiments neglected the established

catalytic effect of water vapour on the oxidation of carbon monoxide[55,58] which would have affected their results significantly.

2.2 Combustion of Pulverized Coal in Air

Field[69,70] measured the burning rates of a wide variety of pulverized British Coals in the size range about 20 - 105 μm, over the particle temperature range, 1200 - 2000 K in hot streams of oxygen-nitrogen mixtures. His experiments showed that at gas temperatures above 1500 K the burning rates of coal particles larger than 100 μm was controlled by the rate of diffusion of oxygen towards the surface.

Mulcahy & Smith[71] made an extensive review of literature on the kinetics of combustion of carbon particles and concluded that over the particle temperatures range of about 1200 - 2300 K, the rate of combustion of carbon particles above 100 μm in size will be controlled by the rate of diffusion of oxygen towards the surface.

Mulcahy & Smith[72] also measured combustion rates of four pulverised carbonaceous fuels, in the size range 4 - 77 μm, over the particle temperature range of 1000 - 2300 K in hot gas streams having different oxygen concentrations. They found that the measured combustion rates were less than the limiting rate of diffusion of oxygen to the particles showing that the combustion was controlled by chemical kinetics. Their results thus supported earlier works[69-71].

Smith[73,74] also reported experimental measurements of combustion rates of pulverised fuels of various types and sizes (4 - 78 μm) over

the temperature range of 1200 - 2270 K, but the results were similar to those reported earlier[71,72].

Sergeant & Smith[75] extended burning rate experiments with bituminous coal char particles, 18 - 70 μm in size, to lower temperature range, 800 - 1700 K, to include the temperatures encountered in fluidized bed combustion. Their results were best interpreted by assuming that between 800 -1250 K the combustion occurred under rate control intermediate between that due to chemical reaction alone and that due to the combined effects of pure diffusion and chemical reaction on the pore wall.

2.3 Conclusions on Review of Literature on Combustion of Carbon and Pulverised Coal in Air

The above review suggests that above 1000 ^{o}C the combustion of carbon particles larger than 1mm will be controlled by the rate of diffusion of oxygen towards the burning particle surface. Also above 1000 K the primary product of combustion at the carbon surface is expected to be carbon monoxide. But below 1000 ^{o}C there is some uncertainty about the extent to which chemical kinetics and diffusion rates of oxygen toward the carbon surface controls the combustion process.

2.4 Combustion of Carbon in Fluidized Beds

The conditions of combustion of carbon in fluidized beds are somewhat different from those in air. In a fluidized bed the burning carbon particles constituting about 1-4% of the bed material remain well

dispersed in a bed of refractory inert particles[19].

The burning carbon particles are in a state of random movement in an agitating bed because of bubbling action in the bed. Hence the resistance to diffusion of oxygen to the burning particles will be less than that in stagnant conditions. Also the heat transfer coefficient between the burning carbon particles and the inert particles in the bed are in general about five times greater than normal convective heat transfer coefficient between a gas stream and an immersed body[76]. Hence the burning carbon particle temperature should be less than that expected when burning in a slow stream of air. Hence the mechanism of combustion, the burning rate and the temperature reached by carbon particles in a fluidized bed needs investigation. A review of literature on the study of combustion of carbon in fluidized beds is given below.

Avedesian & Davidson[77] first reported theoretical and experimental study of the mechanism of combustion of carbon in fluidized beds. They presented a model of combustion of carbon particles in fluidized beds based on the model of combustion of carbon in air proposed by *Hougen & Watson*[59]. This model[59] has already been discussed in Section 2.1. *Avedesian & Davidson's* model[77] assumed that in fluidized beds the burning carbon particles burn in the relatively stagnant particulate phase and hence the rate of diffusion of oxygen towards burning carbon particles under such conditions would be less than that expected for combustion of carbon in stagnant air because of the resistance offered by the inert particles surrounding the burning particles. They also

assumed that the burning carbon particles in a fluidized bed remain at temperatures some hundred degrees K higher than that of the bed. Neglecting the finite concentration of carbon dioxide in the particulate phase of the fluidized bed, they showed that the radius of the carbon monoxide reaction zone around a burning carbon particle was equal to the diameter of the burning particle. They presented an expression for the burning rate of a single carbon particle in a fluidized bed as shown by equation 2.4 below:

$$\dot{m} = 24\ \pi\ Sh\ D_G\ d\ c_p \qquad \ldots\ (2.4)$$

Avedesian & Davidson[77] also conducted combustion experiments with batch charges of char and coke particles, 0.23 - 2.61mm in size, in a fluidized bed of ash at 900 ^{o}C. They found good agreement between their theoretical and experimental results and concluded that the combustion of carbon particles in their experiments was controlled by two diffusional resistances in series, namely:

(i) Interphase transfer of oxygen from bubbles of air to the surrounding ash particles;

(ii) Diffusion of oxygen through the ash phase towards each burning carbon particle.

From their experimental data *Avedesian & Davidson*[77] also showed that the Sherwood Number of the burning carbon particles (which characterizes the mass transfer of oxygen towards the burning carbon particles) in a fluidized bed was about 1.4 and it was nearly constant

over the range of variables explored by them. From this they suggested that the value of Sherwood Number of the carbon particles for fluidized bed combustion would be less than that for combustion of carbon in stagnant air, which is two in the latter case.

But *Avedesian & Davidson*[77] neglected the effect of finite concentration of carbon dioxide in the particulate phase on the carbon dioxide reaction zone. They also did not consider the effect of inert particle size, superficial fluidizing velocity and agitation within the fluidized bed created by bubbling action on the burning rate of the carbon particles.

Campbell & Davidson[78] showed that the model of *Avedesian & Davidson*[77] gave increased radius of carbon monoxide reaction zone with increased oxygen concentration in the particulate phase, when finite concentration of carbon dioxide in the particulate phase of the fluidized bed was considered. In reality, carbon dioxide concentration in the particulate phase will be finite in fluidized beds burning carbon particles and if *Avedesian & Davidson's*[77] model is valid, with increased radius of reaction zone, the inert particles will pick up much of the heat from the reaction zone and less energy will be available at the carbon surface to support the endothermic gassification reaction between carbon and carbon dioxide there. *Campbell & Davidson*[78] modified the model of *Avedesian & Davidson*[77] by suggesting that the radius of the carbon monoxide reaction zone around a burning carbon particle would be limited by a heat transfer balance so that sufficient heat is transferred to the burning carbon particle from the reaction

zone to maintain the surface at above 1100 ^{o}C to support the gasification reaction there. Their modified expression for a single carbon particle burning rate in fluidized bed combustion was as follows:

$$\dot{m} = b \quad 24 \pi \, Sh \, D_G \, d \, c_p \qquad \ldots (2.5)$$

where b defines the radius of the carbon monoxide reaction zone, non-dimensionally:

$$b = \frac{r}{(d/2)} \qquad \ldots (2.6)$$

and its value lies between 1 and 2.

Campbell & Davidson[78] also conducted combustion experiments with coal, char and coke particles, 1.3-3.08 mm in size, in a fluidized bed combuster under different bed operating conditions as shown in Table 2.1, feeding both batch charges and continuous charges, but supported the earlier conclusions of *Avedesian & Davidson*[77].

Sergeant & Smith[79] examined the relative roles of mass transfer and chemical reactions on the combustion rates of coal chars in fluidized beds in the light of char particle combustion kinetics and existing correlated data on gas particle mass transfer in fluidized beds. They suggested that in fluidized beds operating between 1000 - 1200 K the combustion rate of materials having reactivity equal to or higher than that of swelling bituminous coal char would be mainly

controlled by mass transfer of oxygen towards the particles. But lack of reliable quatitative data on gas particle mass transfer in fluidized beds made their results unreliable.

Basu, Broughton & Elliott[80] studied the mechanism of combustion of carbon in fluidized bed further by burning carbon particles, 1 - 6mm in size, in a fluidized bed of sand at 850 ^{o}C. They used phosphorous oxychloride to suppress the oxidation reaction between oxygen and carbon monoxide formed at the surface and recorded distinct concentrations of carbon monoxide and carbon dioxide in the products of combustion. Their results suggested that oxygen reaches the burning carbon surface to produce both carbon monoxide and carbon dioxide as primary products there. Thence the carbon monoxide diffuses away and burns in a spherical diffusion flame around the burning carbon particle. They also presented a heat balance calculation around a burning carbon sphere from experimentally measured surface temperature, reaction zone temperature and burning rate in order to demonstrate whether sufficient heat is transferred from the reaction zone to the carbon surface to sustain the endothermic gasification reaction between carbon and carbon dioxide there. Their calculation showed that more heat was radiated away from the burning carbon particle surface than was conducted back from the reaction zone. Thus, the results of this calculation did not support the combustion model presented by *Avedesian & Davidson*[77] and supported by *Campbell & Davidson*[78]. *Basu, Broughton & Elliott*[80] also presented a model for burning rate of a single carbon particle in fluidized beds as shown by equation 2.7 below:

$$\dot{m} = 48 \pi D_G \varepsilon_m d c_p \left(1 + \frac{12 c_p}{\rho_f}\right) \quad \ldots (2.7)$$

The burning rates predicted by this model were about 25% lower than those predicted by the model of *Avedesian & Davidson*[77]. Also *Basu, Broughton & Elliott's* model indicated that the radius of the carbon monoxide reaction zone was negative[81], which is physically inadmissable. They[80] also showed that when radial variation of voidage around a particle in fluidized bed was considered, the value of Sherwood Number changed to some extent from the value obtained by considering uniform voidage. *Basu, Broughton & Elliott's* model[80], like that of *Avedesian & Davidson*[77] neglected any effect of superficial fluidizing velocity, inert particle size and agitation within the bed created by bubbling action on the burning rate of single carbon particles.

Waters[82] discussed in detail about the mechanism of combustion of carbon in fluidized beds. He showed that at bed temperature about 1000 K and with allowance made for the burning carbon particle temperatures to be some 100 K higher, the reaction of carbon with oxygen is $10^{4.5}$ times faster than that with carbon dioxide. He discussed that at bed temperature of 1200 K, with increase of particle temperature the burning rate of carbon particles larger than 1mm will be dominated by diffusion and the gasification reaction between carbon and carbon dioxide will be important at 1500 K. But he suggested that the heat requirements for gasification would tend to depress temperature and reaction rate at the carbon surface. He also suggested that the reaction rate at any instant will be influenced by the particle temperature, the size of the carbon partcle, the surrounding gas flow, and

the thickness and permeability of ash layers, as these factors determine whether chemical or diffusional resistance controls the combustion. Furthermore, these factors change during combustion.

Basu[81,83] measured burning rates of electrode carbon spheres, 3 - 15mm in diameter, in a fluidized bed of sand at 750 - 900 ^{o}C. His results suggested that combustion was controlled by combined effect of chemical kinetics and diffusion of oxygen towards the burning particles. He also measured burning carbon particle temperature by embedding the bead of a thermocouple at its centre and recording the outputs of the thermocouple on a chart recorder. The temperature of the particle was about 50 - 200 K higher than that of the bed and increased as the combustion continued.

Beer et al[84] developed a model to evaluate the effect of mean bed temperature, coal and acceptor particle size and physical properties, superficial fluidizing velocity, excess air and bed height on carbon combustion efficiency. As a part of this model they developed a detailed model for single coal particle combustion for use in developing kinetic parameters to account for difference in reactivity of various types of coals. They also presented an equation for energy balance of a burning carbon particle. The prediction of their model showed that in a fluidized bed allowance for kinetic resistance to combustion must be made to predict burning rates, carbon loading and combustion efficiencies. The predicted burning coal particle temperature showed that except during the volatile evolution period, the

magnitude of difference between the temperatures of the carbon particle and the beds is small and could be neglected.

Yates & Walker[85] measured the burning rates of resin bonded spherical char particles, 2 - 10mm in diameter, in a fluidized bed of sand at 760 - 960 ^{o}C. They found that the burning rate was maximum at a bed temperature of 800 ^{o}C and decreased with further rise in bed temperature and suggested that increased resistance of ash layer to diffusion of oxygen to the carbon surface caused such reduction in burning rates. The burning rates, on the other hand, increased with increase in superficial fluidizing velocity. They also estimated the temperatures of burning char particles by following the history of heat fusible alloy wire rings embedded inside them. Their results showed that in general smaller char particles were at higher temperature than the larger ones and the difference of temperature between the bed and the burning particle ranged from 60 - 140 K.

Leung & Smith[86] studied the effect of fuel reactivity on fluidized bed combustion by extending the two-phase bubbling fluidized-bed model of *Davidson & Harrison*[87]. Their calculation showed that at 1200 K fuel reactivity had little effect on oxygen utilisation, however, at 800 - 1000 K fuel reactivity had showed notable effect. They found that exchange of gas between bubble and particulate phase was rapid with 1mm size inerts and had no controlling effect on burning rate. They also suggested that carbon concentration in the bed, the bubble size and the size of the inert particles are important parameters to affect the fluidized bed combustion and should be taken into account

when studying burning rates in fluidized beds.

Andrei[88] and *Andrei, Sarofim & Beér*[89] studied the mechaism of combustion of coal particles, 1.85 - 3 mm in size, in an electrically heated fluidized bed of fine sand (200 μm) fluidized with mixtures of air and nitrogen having three different oxygen concentrations. They used lower fluidizing velocities (about 7 cm/s) at bed temperatures, 750 ^{o}C and 900 ^{o}C. Their[88], [89] results showed that, although diffusion controlled the combustion at 900 ^{o}C, the effect of chemical kinetics was significant at 750 ^{o}C. Their[88], [89] work also suggested that the ash layer on the coal particles did not offer any resistance to the diffusion of oxygen to the burning coal particles. Their[88], [89] experimental burnout histories of the coal particles agreed closely with the predictions of the model of *Beer et al*[84] at 750 ^{o}C, but at 900 ^{o}C the model[84] predicted higher burning rates than obtained experimentally [88], [89].

2.5 Conclusion on Review of Literature on Fluidized Bed Combustion of Carbon

The above review of combustion of carbon in fluidized beds clearly shows that the actual mechanism of combustion has not yet been firmly established. Also the burning rates and temperatures of carbon particles under different fluidized bed design and operating conditions have not been fully explored. The present trend of fluidized bed combustor design, has been to use larger sizes of coal, particularly in the U.K. [90, 91] to reduce elutriation and cost of fuel preparation and larger sizes of inert particles and higher superficial fluidizing velocities,

particularly in the U.S.A. [92, 93] so as to increase power density of the plant and reduce its size for a given thermal output. But existing published experimental works have not been reported for these wider ranges of bed design and operating conditions. Also existing models of combustion of carbon in fluidized beds have not considered the effects of larger sizes of carbon and inert particles and the higher superficial fluidizing velocities. Hence further investigation in these areas over wider ranges of fluidized bed design and operating conditions is needed to design and control fluidized bed boilers for optimum performance. The present work involves experimental investigation of conditions much nearer to those found in present day fluidized bed combustion systems.

CHAPTER THREE

CARBON COMBUSTION MODELS AND BURNING RATES IN FLUIDIZED BEDS

3.1 Introduction

Combustion of carbon particles in air at different surface temperatures and externally imposed conditions of combustion can be represented by three distinct models of combustion as shown in Figure 3.1. These are the only possible models for combustion of carbon. These models have been developed through theoretical and experimental investigations by earlier research workers[81]. The conditions of combustion of carbon in fluidized beds are somewhat different from those in air as was discussed in Section 2.4 of previous chapter. So these three distinct models of combustion of carbon and their applicability in fluidized bed combustion has been discussed in this chapter in the light of published literature on combustion of carbon in fluidized beds.

Following the approach of *Field et al*[55] and *Avedesian*[94] the burning rate of a single carbon particle and its burnout time has been presented in terms of its diameter for both kinetically controlled as well as diffusion controlled combustion processes.

3.2 Models of Combustion

3.2.1 Model I

This was the earliest model proposed by investigators during the early part of this century[47-52]. This model with concentration distributions of oxygen and carbon dioxide around the carbon particle is shown in Figure 3.1(a). According to this model, oxygen reaches the burning carbon particle surface diffusing through a stagnant film of gas around the particle and forms only carbon dioxide at the surface. But experimental works by other workers later did not support this model[53]. And it is now well established[53,55,58,80] that at temperatures encountered in fluidized bed combustors, this model is physically inadmissible.

3.2.2 Model II

This model originally proposed by *Hougen & Watson*[59] for carbon surface temperatures above 1000 °C and has been discussed in detail in Section 2.2 of the previous chapter. This model, with concentration distributions of carbon monoxide, carbon dioxide and oxygen around the burning carbon particle is shown in Figure 3.1(b). This model was also accepted by *Avedesian & Davidson*[77] and *Campbell & Davidson*[78] for fluidized bed combustion of carbon at a bed temperature of 900 °C because they assumed that the burning carbon surface temperature is of the order of 200 K higher than that of the bed. But experiments by *Basu, Broughton & Elliott*[80] argued against the applicability of this model to fluidized bed combustion (see Section 2.4). *Golovina & Khaustovich*[66] experimentally found that at about 1000 °C, the rate of oxidation of carbon in air was several orders of magnitude higher than that in carbon dioxide. *Mulcahy & Smith*[71] from their review of

literature on combustion of carbon also concluded that the oxidation of carbon by carbon dioxide is not comparable with that of the reaction with oxygen. Moreover, *Beér*[95] recently reported that *Song & Sarofim*[96] estimated burning rates of millimetre-sized carbon particles from the data of *Avedesian & Davidson*[77] and found these to be much higher than those obtained by *Wu*[97] in his study on the kinetics of the carbon-carbon dioxide reaction. From this *Song & Sarofim*[96] concluded that oxidation of carbon by oxygen was the primary process of combustion in *Avedesian & Davidson's*[77] experiments.

It may be commented here that the movement of the burning carbon particles in a fluidized bed agitated by bubbling action would reduce the resistance to diffusion of oxygen to the particle surface. Secondly the higher rates of heat transfer from the burning carbon particles to the bed inert particles will reduce the heat available at the carbon surface to support the gasification reaction between carbon and carbon dioxide. Thus the applicability of this model to fluidized bed combustion situations seems to be unlikely.

3.2.3 Model III

This model is accepted for moderate temperature at the carbon surface (below 1000 °C). It has been supported by a number of investigators through experimental evidence of combustion of carbon in air. A sketch of this model, showing concentration gradients of carbon monoxide, carbon dioxide and oxygen around the burning carbon particle is shown in Figure 3.1(c). According to this, the combustion rate of carbon is not so fast at moderate surface temperature (below 1000 °C) for Model II to apply. Hence, Model III assumes that oxygen

reaches the surface to form both carbon monoxide and carbon dioxide there. A number of investigators[53,98-102] tried to settle the issue as to what the primary product(s) of combustion at the surface is. Their work showed that, depending on the molecular arrangement of the carbon and oxygen molecules when combining, both carbon monoxide and carbon dioxide may be formed at the surface. But *Arthur*[53] showed that with rise in the surface temperature, the amount of carbon monoxide formed at the surface increases. Experiments by *Basu, Broughton & Elliott*[80] in fluidized bed supported this model. *Beér et al's*[84] model suggested that the temperature of burning carbon particles in a fluidized bed was not significantly higher than that of the bed, except during the initial period of volatile evolution. Measurement of particle temperatures by *Yates & Walker*[85] also showed that the temperature of large carbon particles was not much more than that of the bed. The above suggests that Model III is more likely to be applicable to fluidized bed combustion situations than the other models.

The present work is concerned with experiments designed to establish the relative importance of each of these models over the range of operating conditions found in fluidized beds.

3.3 Burning Rate of a Carbon Particle

Consider a spherical carbon particle of mass 'm' and diameter 'd' burning in stagnant air. In steady state combustion condition, the burning rate of the particle will be controlled by the rate of diffusion of oxygen to the surface and the rate of chemical reaction there at given surface temperature. The combustion rate can be expressed by equation (3.1) which is due to *Field et al*[55] and *Avedesian*[94]. It

should be noted that equation (3.1) assumes that there is no relative motion between the burning carbon particle and the medium; this is not true for combustion in a fluidized bed.

$$-\frac{dm}{dt} = 12\ \phi\ k_g\ \pi\ d^2\ (c_p - c_s) = 12\ \phi\ k_s\ \pi\ d^2\ c_s \qquad \ldots(3.1)$$

where ϕ is a mechanism factor which takes the value $\phi = 1$ or $= 2$ according as carbon dioxide or carbon monoxide is transported away from the burning carbon particle surface respectively.

Elimination of c_s from equation (3.1) gives:

$$-\frac{dm}{dt} = 12\ \phi\ \pi\ d^2 \left(\frac{1}{\frac{1}{k_g} + \frac{1}{k_s}} \right)\ c_p \qquad \ldots(3.2)$$

and the assumption that air is stagnant without any relative motion between the burning carbon particle and the air suggests[71]

$$k_g\ \alpha\ \frac{D_G}{d} \qquad \ldots(3.3)$$

where D_G is the molecular diffusion coefficient of oxygen in the gas phase.

The surface reaction rate constant k_s depends on the chemical activity at the carbon surface at a given surface temperature, T_s. It is usual to express k_s in the form suggested by *Arrhenius*[103] as:

$$k_s\ \alpha\ e^{-\frac{E}{RT_s}} \qquad \ldots(3.4)$$

At high temperatures and for larger particles, $k_s >> k_g$ and $c_s \to 0$, the combustion of the particle tends to be dominated by the rate of

diffusion of oxygen from the bulk of the air towards the surface[55]. Under such conditions:

$$-\frac{dm}{dt} = 12\ \phi\ \pi\ d^2\ k_g\ c_p \qquad \ldots(3.5)$$

According to equation (3.3), $k_g \alpha \frac{D_G}{d}$, and for a particular fluidized bed operating condition ϕ, c_p and D_G may be assumed to be constant. Under such conditions equation (3.5) reduces to the form as follows:

$$-\frac{dm}{dt} \alpha\ d \qquad \ldots(3.6)$$

At low temperatures and for small carbon particles or highly unreactive fuels, $k_s << k_g$ and $c_s \rightarrow c_p$ so that combustion tends to be dominated by chemical kinetics[55]. Now the rate of change of k_s with rise in temperature (dk_s/dT) is much higher than that of $k_g(dk_g/dT)$, so that the surface temperature affects the reaction rate more than it affects the mass transfer coefficient of oxygen[94]. Hence from equation (3.2), the burning rate under kinetically controlled combustion conditions is:

$$-\frac{dm}{dt} = 12\ \phi\ \pi\ d^2\ k_s\ c_p \qquad \ldots(3.7)$$

Since for a particular fluidized bed operating condition ϕ, k_s and c_p may be assumed to be constant, equation (3.7) may be expressed as follows:

$$-\frac{dm}{dt} \alpha\ d^2 \qquad \ldots(3.8)$$

3.4 Burn Out Time of a Carbon Particle

3.4.1 Diffusion Controlled Combustion

The burning rate of a carbon particle controlled by the rate of diffusion of oxygen towards the surface was shown to be proportional to its diameter, in the previous Section by equation (3.6) as follows:

$$-\frac{dm}{dt} \propto d \qquad \ldots (3.6)$$

The mass of a carbon particle of diameter 'd' and density 'ρ_c' is given by

$$m = \frac{\pi}{6} d^3 \rho_c \qquad \ldots (3.9)$$

Hence, the rate of change of mass with time at constant density is

$$\frac{dm}{dt} = \frac{\pi}{2} d^2 \rho_c \frac{d}{dt}(d) \qquad \ldots (3.10)$$

Equating equations (3.6) and (3.10), equation (3.11) is obtained, as follows:

$$dt \propto -d \cdot d(d) \qquad \ldots (3.11)$$

The burn out time of a carbon particle, $t_{b_{Diffusion}}$ is thus obtained by integrating R.H.S. of equation (3.11) between the limits $d = d_i$ to $d = 0$ as follows:

$$\int_{0}^{t_{b_{Diffusion}}} \propto - \int_{d=d_i}^{d=0} d.d(d)$$

or

$$t_{b_{Diffusion}} \propto d_i^{\,2} \qquad \ldots (3.12)$$

3.4.2 Kinetically Controlled Combustion

The burning rate of a carbon particle controlled by the rate of chemical reactivity of the surface was shown to be proportional to the square of its diameter by equation (3.8) as follows:

$$-\frac{dm}{dt} \propto d^2 \qquad \ldots (3.8)$$

Equating equations (3.8) and (3.10), the following equation is obtained

$$dt \propto - d(d) \qquad \ldots (3.13)$$

The burn out time of a carbon particle $t_{b_{Kinetic}}$, under kinetically controlled combusion is thus obtained, by integrating the R.H.S. of equation (3.13) between the limits $d = d_i$ to $d = 0$, as follows:

$$\int_{0}^{t_{b_{Kinetic}}} dt \propto \int_{d=d_i}^{d=0} -d(d)$$

or $$t_{b_{Kinetic}} \propto d_i \qquad \ldots (3.14)$$

CHAPTER FOUR

BURNING RATES OF SINGLE CARBON PARTICLES AND BURNING CARBON PARTICLE TEMPERATURES IN SHALLOW FLUIDIZED BEDS

PART A

4.1 Introduction

Experiments to determine burning rates and temperatures of electrode carbon spheres of different diameters in a small experimental fluidized bed combustor under various operating conditions and design parameters are described in this Chapter. The relationship between the burning rate and the diameter of the carbon spheres obtained from experimental results is used to suggest which particular mechanism of combustion is operating. The measured burning rates and temperatures of carbon particles were compared with experimentally measured and predicted values reported earlier.

The influence of the following variables on burning rate and temperatures of electrode carbon particles was explored:

(i) Bed temperature; 800 °C and 900 °C

(ii) Inert particle size; 327.5 μm, 550 μm and 780 μm

(iii) Static bed depth; 12.5 mm, 30 mm and 50 mm

(iv) Superficial fluidizing velocity; 27 cm/s and 71 cm/s (at 900 °C)

(v) Presence of a large number of coal particles in the bed;

(vi) Oxygen concentration in the particulate phase.

2.16×10^{-3}; 1.517×10^{-3}; 1.062×10^{-3} and 0.532×10^{-3} k mol of oxygen/m^3

4.2 Experimental Equipment

4.2.1 Experimental Fluidized Bed Combustor

The fluidized bed combustor shown in Figure 4.1 was made from a quartz glass tube of 71.5mm inside diameter and 2.5mm wall thickness and 300mm length. A porous ceramic distributor plate was fitted to the bottom of the combustor. About 35 turns of 'Kanthal' electrical heating wire (manufactured by Butlen-Kanthal AB, Kathanl Divison, Hellstahammer, Sweden) of 0.8mm diameter were wound round the bottom part of the quartz glass tube at about 3mm pitch. The whole assembly was surrounded with ceramic fibre insulation to reduce heat loss from the heating element to the surroundings. The electrical heater input to the bed could be controlled by a variable output transformer connected to the heater windings to keep the bed at any particular temperature desired. A mineral insulated chromel-alumel thermocouple (manufactured by BICC Pyrotenax Ltd., Prescot, Merseyside, England) was used to measure the bed temperature, the output being displayed as the bed temperature on a digital thermometer (Series 3000, manufactured by Comark Electronics Limited, Brookside Avenue, Rustington, Sussex, England).

4.2.2 Carbon Spheres

The spherical carbon particles used for the experiments were made from electrode carbon rods (manufactured by Le Carbone - Lorraine, France with the specification 'Quality - Ellor 10') by turning in a lathe in sizes 6mm, 9mm and 12mm. Smaller size spheres were obtained by burning them partially down to size. Some typical spheres are shown in Figure 4.2.

A 1mm hole was drilled in several of the 6mm and 12mm carbon spheres so that the junction of a chromel-alumel thermocouple made from fine wire (about 0.3mm diameter) could be placed at the centre, as shown in Figure 4.2. The thermocouple was sealed into the hole by high temperature insulating cement. The output of the thermocuple was displayed continuously on a chart recorder.

4.2.3 Bed Inert Material

Silica sand particles were used as the bed inert materials in every case as they do not sinter at temperatures lower than 1150 ^{o}C. The particles used in the experiments were sized into narrow ranges using British Standard sieves. Details of the sand particles are given in Appendix A. Some samples of inert particles are shown in Figure 4.3.

4.2.4 Fluidizing Gas

Air was used as the fluidizing gas during combustion experiments, but nitrogen was used to fluidize the bed when the carbon particles were being heated to the bed temperature prior to combustion in air. Nitrogen was also used to cool the bed after combustion in air for a specific time, 100s. Two separate solenoid valves were fitted in air and nitrogen flow lines and were operated through a common switch to direct either air or nitrogen to fluidize the bed (see Figure 4.1)..

In one set of experiments a mixture of air and nitrogen was also used during burning rate tests so that reduced concentration of oxygen in the fluidizing gas could be achieved. Rotameters (manufactured by

Rotameter Manufacturing Company Limited, Croydon, England) were used for measuring flow rates of air and nitrogen.

4.3 Burning Rate Experiments - Test Procedure

Burning rates of electrode carbon spheres were measured

(i) In an electrically heated bed fluidized with air without the presence of any other active carbon particles in the bed;

(ii) In a coal fired bed fluidized with air and having a large number of active coal particles burning in the bed so as to maintain the bed temperature without any electrical heating. Thus the oxygen concentration within the bed is lower than in (i) above.

(iii) In an electrically heated bed fluidized with mixtures of air and nitrogen to give reduced oxygen concentration in the particulate phase, without presence of any other active carbon particles in the bed. Thus simulating (ii) above but inferring what the magnitude of oxygen concentration in the bed must have been.

4.3.1 Electrically Heated Bed

A weighed amount of sand was placed into the combustor and the bed was fluidized with air. The electrical heat input was switched on and gradually increased until the bed reached the required temperature. The air flow rate was then adjusted for a particular superficial fluidizing velocity and the bed was allowed to reach a steady state by adjusting the electrical input. The air was then quickly replaced by nitrogen by operating the common switch of the two separate solenoid valves placed in air and nitrogen lines (see Figure 4.1). The nitrogen flow was adjusted to

to keep the bed at the same temperature. About 3 to 6 carbon spheres of different known diameter and mass were then dropped into the nitrogen fluidized bed and were heated for about 1 minute to reach the bed temperature. Preliminary experiments with electrode carbon spheres having a thermocouple bead embedded at its centre showed that they reached the bed temperature in about 30-40s. Also it was found that use of 3 to 6 carbon spheres, instead of one at a time, did not affect individual burning rates by interaction. Hence 3 to 6 carbon spheres were allowed to burn in the bed to save time and cost. When the spheres reached the bed temperature, air was switched on by operating the common switch of the solenoid valves again, so that combustion could commence. A stop watch was also started simultaneously. After a specified time of 100s (50s also in some cases) the air was again replaced by nitrogen and the electrical heating was switched off so that the bed could cool down. The times of combustion, 50s and 100s, were chosen to keep the reduction in diameter of the spheres within 5% of the initial diameter. When the bed cooled down, the carbon spheres were sieved out of the bed and their mass and diameter were measured. The loss in mass was used to calculate the burning rate. The size of the carbon spheres used, in the range of about 2 - 12mm, was limited by difficulites to sieve it out and measure its weight and diameter of the smallest size and by its tendency to remain at the bottom of the bed without having movements for the largest size.

Attrition of the spheres in the fluidized bed was also measured in a separate set of experiments by placing 6 spheres of different known

mass and diameter in a nitrogen fluidized bed heated electrically to 900 ^{o}C. They were allowed to remain in the nitrogen fluidized bed at the bed temperature for 300s and then allowed to cool down by switching off the heater. When the bed cooled down, the spheres were sieved out of the bed and weighed again. The difference in mass was less than one milligram for all the spheres. The attrition of the spheres in the bed was, therefore, considered to be negligible.

Test procedures for burning rate tests in the electrically heated bed under reduced oxygen concentrations in the particulate phase was similar to those described above except that a mixture of air and nitrogen was used during combustion instead of air as described above.

4.3.2 Coal Fired Bed - Effect of Presence of Other Active Particles in the Bed

The burning rate experiments discussed in the previous Section were performed in an electrically heated fluidized bed having a large amount of excess air and only a few (about 3 to 6) active carbon particles. But generally in fluidized bed combustors a large number of coal particles will reside in the bed simultaneously. These burning carbon particles will affect the burning rate of neighbouring individual particles. When a single particle is burned in an electrically heated fluidized bed the oxygen concentration in the particulate phase of the bed is the same as that in the fluidizing gas. But when a large number of carbon particles are burning in the bed simultaneously this is not the case. Under such conditions local oxygen concentration in the particulate phase will be

less than that in the fluidizing gas. As a result the burning rate of the individual carbon particles will be reduced. Alteration of the bed operating conditions change this reduction of burning rate. To have quantitative information about the reduction of burning rate of electrode carbon spheres brought about by the presence of a large number of active coal particles in the bed, burning rate tests on the spheres were performed in fluidized beds where the bed was maintained at the desired temperature by burning coal in it. Anthracite coal particles of the size range -2.4 to 1.4mm were fed to the bed continuously from a vibratory feeder after the bed was preheated electrically. The feed rate of coal was adjusted to keep the bed at the desired temperature without electrical heating. When the bed temperature was steady at the desired value, the air was replaced by nitrogen by operating the common switch of the solenoid valves on air and nitrogen flow lines. The coal feeding was stopped and electrical heating was switched on. After some time the temperature of nitrogen fluidized bed became steady with electrical heating. Then about 3 to 6 electrode carbon spheres of known different size and mass were dropped into the bed and was heated for about one minute in the electrically heated bed fluidized with nitrogen. When the electrode carbon spheres reached the bed temperature, air flow was restored by operating the common switch of the solenoid valves on air and nitrogen flow lines, the coal feeding was restarted and the electrical heating was switched off. A stop watch also started simultaneously with restoration of air flow. The combustion of the electrode carbon particles were allowed to go on in air fluidized bed in presence of other burning coal particles in the bed for 100s. After this period air flow was stopped and nitrogen flow was switched on by operating the common switch of the solenoid valves, the coal feeding was stopped and the bed was

allowed to cool down. When the bed cooled down, the electrode carbon particles were sieved out of the bed and their size and mass were measured. The difference in mass was used to calculate the burning rate.

Burning rate measurements were conducted in this coal fired bed using similar inert particle sizes, superficial fluidizing velocities, bed temperature and static bed depth (only 30mm) as were used when the bed was electrically heated.

4.4 Burning Rate Experiments: Results and Discussion

The burning rates of electrode carbon spheres computed from the loss of mass after combustion in the fluidized bed were plotted against their initial diameters on logarithmic plots, (see Figures 4.4 - 4.16) The experimental data in all these plots fitted straight lines by least squares method. The relationship between the burning rate and the diameter of the carbon sphere can thus be expressed by the relationship

$$\dot{m} = kd^n \qquad \ldots (4.1)$$

where k is a constant for a particular bed design and operating condition and will change with change in inert particle size, bed temperature, superficial fluidizing velocity, oxygen concentration in the particulate phase and bed carbon concentration. The value of the exponent 'n' in equation (4.1) was calculated from the plots. The results obtained for different bed design and operating conditions are discussed below.

4.4.1 Results and Discussion - Electrically Heated Bed Fluidized with Air

4.4.1.1 Variation of Bed Temperature

The variation of burning rate of the electrode carbon particles at bed temperatures of 800 ^{o}C and 900 ^{o}C is shown in Figure 4.4. The bed inert particle size, the static bed depth and the superficial fluidizing velocity for these experiments were 327.5 μm, 30mm and 27cm/s (at 900 ^{o}C) respectively. The results show that the burning rate increases substantially with bed temperature. The single carbon particle burning rates obtained from predictions of the models of *Avedesian & Davidson*[77] and *Basu, Broughton & Elliott*[80] are also shown in this figure. It is found that for larger carbon particles (> 3mm) the burning rates found in present experimental work is significantly higher than those predicted by these models. The models of above workers assumed that the carbon particles burn in a relatively stagnant particulate phase under diffusion controlled rate of combustion. Visual observation of the bed during the experiments using a stainless steel mirror showed that the burning particles were in random movement, occasionally appearing at the top of the bubbling surface. The movement of the carbon particles during combustion could be expected to reduce the resistance to flow of oxygen towards the burning particles, otherwise such higher burning rates would not be observed. Hence the above models do not explain the actual experimental results obtained. The value of exponent 'n' in equation (4.1) was found to be 1.95 at 800 ^{o}C and 1.83 at 900 ^{o}C. For diffusion controlled combustion the value of n = 1, (see equation (3.6)) and for kinetically controlled combustion n = 2, (see equation (3.8)). Thus

the value of 'n' suggests that combustion was mainly controlled by chemical kinetics. Single carbon particle burning rate experiments were also reported by *Basu*[81, 83], *Yates & Walker*[85], *Andrei*[88] and *Andrei, Sarofim & Beer*[89]. *Basu*[81,83] measured burning rate of electrode carbon spheres in a fluidized bed of sand at 750 - 900 ^{o}C and found that the value of 'n' was in the range 1.22 - 1.52 suggesting that the combustion was controlled by the combined effect of diffusion and chemical kinetics. The size of the inert particle (100 μm) and the superficial fluidizing velocity (8 cm/s) used by *Basu*[81, 83] were much less than those used in the present experiments. Moreover the carbon particles in *Basu's*[81,83] experiment did not have complete freedom in the bed as they were suspended by wire from the top. *Yates & Walker*[85] burning 2 - 10mm char particles in a fluidized bed of sand at 760 - 960 ^{o}C reported that maximum burning rate occurred at about 800 ^{o}C and it decreased with rise of temperature thereafter. They attributed this to the increased resistance to diffusion of ash layers at higher temperature, but did not report whether or not ash was observed as a coating on the carbon surface. *Andrei*[88] and *Andrei, Sarofim & Beer*[89] from their combustion experiments with coal particles, 1.85 - 3 mm in size, in an electrically heated fluidized bed of sand at low fluidizing velocities (about 7cm/s) found that chemical kinetics played a significant role on the burning rate at 750 ^{o}C; however, at 900 ^{o}C, combustion was completely controlled by the rate of diffusion of oxygen to the coal surface. Burning rate was also higher at higher bed temperature during their work. In addition, their[88,89] results suggested that the ash layer on the coal particle did not offer any resistance to the diffusion of oxygen to the

surface and thus contradicted earlier reported results of *Yates & Walker*[85].

4.4.1.2 Variation of Inert Particle Size

Figure 4.5 shows the effect of bed inert particle size on the burning rate of single particles. The inert particle mean sizes were 327.5 μm, 550 μm and 780 μm. Bed temperature, superficial fluidizing velocity and static bed depth were 900 ^{o}C, 71 cm/s (at 900 ^{o}C) and 30 mm respectively. The results suggests that significant increase in burning rate is achieved by increasing the size of the bed inert material. The predicted burning rates from models of *Avedesian & Davidson*[77] and *Basu, Broughton & Elliott*[80] are also shown in this figure. Neither of these models considered any affect of bed inert particle size on the burning rates of single carbon particles. But present experiments results suggest that the effect is significant. The value of the exponent 'n' was about 1.81 for all the three sizes of inert particles used, thus suggesting that combustion was controlled mainly by chemical kinetics.

The higher burning rates obtained in beds of larger inert particles can be explained as follows:

(1) It is well established that in fluidized beds operating within bubbling regimes, the rate of heat transfer between an immersed object and the bed inert materials decreases significantly with increase in inert particle size up to about 1mm as shown in Figure 4.17 [104]. Under equilibrium combustion conditions, the heat released by combustion may be related to the heat transferred to bed by the equation (4.2) as follows:

$$(\dot{m}).(\text{Calorific value of Fuel}) = h\pi d^2(T_s - T_b) \qquad \ldots (4.2)$$

It may be noted that the heat transfer coefficient, 'h' is a function of both inert particle size and superficial fluidizing velocity and consists of three components as given by equation (4.3) below[104].

$$h = \underbrace{h_{pc}}_{\substack{\text{Particle}\\ \text{Convective}\\ \text{Component}}} + \underbrace{h_{gc}}_{\substack{\text{Gas Convective}\\ \text{Component}}} + \underbrace{h_r}_{\substack{\text{Radiative}\\ \text{Component}}} \qquad \ldots (4.3)$$

Increase in inert particle size during the present work resulted in decrease in 'h_{pc}' and hence 'h'. As a result the burning particle temperature would increase as is evident from equation (4.2). Burning carbon particle temperatures measured during the present work, as shown in Table 4.1, supported this. However, if the burning rate is influenced by chemical kinetics, the increase in particle temperature will be accompanied by an increase in surface reaction rate coefficient k_s (see equation (3.4)) and hence the burning rate (see equation (3.7)). On the otherhand, if the burning rate is solely controlled by the rate of diffusion of oxygen towards the burning particle surface, then no such increase in burning rate would result from increase in surface temperature of the particle. In practical situations mixed mode burning, under combined effect of diffusion and chemical kinetics is possible.

(2) The voidage around the burning carbon particles increased to some extent with larger sizes of inert particles, which offered less resistance to the flow of oxygen to the burning carbon particle and thus supported the higher burning rates observed at the higher burning particle temperatures under such conditions.

4.4.1.3 Variation of Superficial Fluidizing Velocity

The effect of variation of superficial fluidizing velocity from 27 cm/s to 71 cm/s (at bed temperature, 900 ^{o}C) on the burning rate of single carbon particles is shown in Figure 4.6. The bed temperature, the inert particle size and the static bed depth were 900 ^{o}C, 327.5 μm and 30mm respectively. It was found that the burning rates were increased significantly by increasing the superficial fluidizing velocity from 27 cm/s to 71 cm/s. The predicted burning ratio from models of *Avedesian & Davidson*[77] and *Basu, Broughton & Elliott*[80] are also shown in this Figure.

The burning rates of larger carbon particles (> 3mm) are substantially higher than those predicted by these models[77, 80]. The present results can be explained as follows:

(1) It has been reported[76] that in general the maximum rate of heat transfer from an immersed object to the fluidized bed occurs when the fluidization index (the ratio of superficial fluidizing velocity to the minimum fluidizing velocity of the bed inert particles, both calculated at bed temperatures) is about 1 - 2

(lower for larger sizes of inert particles) and decreases with further increase of superficial fluidizing velocity as shown in Figure 4.18. During the present experiments the value of fluidization index was 7.4 and 19.4 for superficial fluidizing velocities of 27 cm/s and 71 cm/s respectively. So at the higher fluidizing velocity used the particle temperature was higher because of reduced amount of heat transferred to the bed and this resulted in higher burning rates under such conditions.

(2) At the higher superficial fluidizing velocity used (71 cm/s at 900 ^{o}C), the agitation within the bed was observed to be considerable and the bed appeared to be turbulent. The bed expanded to a great extent, from 30mm (static bed depth) to about 90mm at this higher superficial fluidizing velocity. *Lanneu*[105] also reported that at higher superficial fluidizing velocities, almost uniform or "particulate" fluidization is approached. The effect of forced convection on oxygen transfer to the burning carbon particle was present under such operating conditions and so higher burning rates were supported by increased rate of transfer of oxygen to the carbon particle burning at the higher temperature (see Table 4.1).

4.4.1.4 Variation of Static Bed Depth

Figure 4.7 shows the effect of variation of static bed depth on the burning rate of the carbon particles. The bed depths used were 12.5mm, 30mm and 50mm while the bed temperature, the superficial fluidizing velocity and the bed inert particle size were 900 ^{o}C, 27 cm/s

(at 900 ^{o}C) and 327.5 μm respectively. The results show that in very shallow fluidized beds (static depth of 12.5mm) higher burning rates could be achieved than with deeper beds. Visual observation of the bed at very shallow static bed depth of 12.5mm, during combustion showed that a large number of bubbles of small sizes were dispersed uniformly throughout the bed. In such shallow beds the small size bubbles do not have the opportunity to coalesce into bigger sizes and as a result the exchange of gas between the bubble phase and the particulate phase is faster than that in deeper beds[87]. Also, the burning carbon particles were in the bubble phase most of the time in such a shallow bed containing a large number of small bubbles. As a result, the heat transferred from the burning carbon particles to the bed was less, and the burning particle temperatures were higher than those in deeper beds (static depths, 30mm and 50mm) as is found in Table 4.1. The faster interphase transfer of oxygen and higher particle temperature resulted in significantly higher burning rates in the very shallow bed used (static bed depth 12.5mm). However, no significant improvement was achieved by reducing the static bed depth from 50mm to 30mm suggesting that except in very shallow beds, the bed depth does not affect burning rate significantly. *Campbell & Davidson*[78], from their combustion experiments over a range of static bed depth, 40 - 140mm, also found that no significant variation in bed combustion rate was achieved. The value of exponent 'n' (equation (4.1)) for all the three bed depths was in the range, 1.75 - 1.83mm, thus suggesting that the combustion was mainly controlled by chemical kinetics and the static bed depth did not affect the mechanism of combustion. The predicted burning rates from the

models of *Avedesian & Davidson*[77] and *Basu, Broughton & Elliott*[80] are also shown in Figure 4.7. The present burning rates for larger carbon particles (> 3mm) are substantially higher than the predictions of these models[77, 80].

4.4.1.5 Mechanisms of Combustion

The value of the exponent 'n' in equation (4.1) obtained from present experimental plots ranged from 1.75 to 1.95 . For pure diffusion controlled combustion process the value of n is 1 (see equation (3.6)) and for pure kinetically controlled combustion the value of n is 2 (see equation (3.8)). Thus the results clearly suggested that within the present experimental conditions, combustion was mainly controlled by chemical kinetics; *Basu*[83] also measured burnings rates of single electrode carbon particles using small sizes of inerts (100 μm) and lower superficial fluidizing velocities (8 cm/s) at temperatures 750 - 900 ^{o}C and found the value of n in the range, 1.22 - 1.55. His results thus showed combined effect of diffusion and chemical kinetics. *Andrei*[88] and *Andrei, Sarofim and Beer*[89] also conducted combustion experiments with smaller coal particles (1.85mm - 3 mm in size) at lower fluidizing velocities (about 7 cm/s) and found the influence of chemical kinotics at 750 ^{o}C. It should be noted that the present experiments were conducted in shallower beds compared to earlier workers and covered a much wider range of operating parameters than investigated by previous workers[77, 83, 88, 89] and the results clearly suggests that in shallow fluidized beds operating within the limits of present experimental conditions, the combustion of the carbon particles are mainly controlled by chemical kinetics.

Andrei[88] discussed that oxygen is able to penetrate deep into the solid matrix of the carbon for pure kinetically controlled combustion and the surface becomes rough with fine pores, whereas the pure diffusion controlled combustion, the oxidant molecules are consumed immediately on reaching the outer surface and penetration will be negligible. *Mulcahy & Smith*[71] also discussed 'rough sphere' burning under influence of chemical kinetics. Visual observation of the surface of the partially burnt electrode carbon spheres used for the work described in this thesis, showed that the surface of these burnt spheres appeared rough with fine pores throughout, whereas the surface of the fresh spheres were fairly smooth without any such pores. The observation of the surface of the spheres used for determining the attrition in the nitrogen fluidized hot bed without combustion (see Section 4.3.1) also showed that such fine pores were not produced by attrition with bed inert particles when they were not burning in the bed. This observation clearly supported that oxygen reached the carbon surface to cause such an effect on the surface and combustion was controlled mainly by chemical kinetics (see Fig. 4.19).

4.4.1.6 Significance of Sherwood Number in Shallow Fluidized Bed Combustors

Sherwood Number ($Sh = \frac{k_g d}{D_G}$) of a burning carbon particle is a dimensionless group which characterises the rate of mass (oxygen for combustion) transfer towards its surface. From a stationary carbon particle burning in stagnant air, the numerical value of Sherwood Number is two[55]. It should be noted that the only way in which oxygen can reach the surface under such conditions is by diffusion of oxygen

molecules through the space between the nitrogen molecules and the molecules in the air. If there is any relative motion between the carbon particle and the oxidizing medium the value of Sherwood Number increases because of the effect of forced convection on the rate mass transfer. *Avedesian & Davidson*[77] developed their diffusion controlled model of combustion of carbon particles in fluidized beds on the assumption that during combustion these particles remain in the relatively stagnant particular phase of the bed. They suggested that under such conditions Sherwood Number would be less than two because of the additional resistance to diffusion offered by the surrounding inert particles.

On the basis of the above model their[77] experimental data (obtained by burning batch charges of char and coke particles, 0.23 - 2.61mm in size, in a fluidized bed of ash at 900 ^{o}C over the range of superficial fluidizing velocity, 21.4 - 38.3 cm/s), suggested an average value of Sherwood Number of about 1.42. This value of Sherwood Number was found to be independent of the carbon particle sizes and the superficial fluidizing velocities used by them. However, *Avedesian & Davidson*[77] did not suggest how the Sherwood Number would be affected if the bed design and operating parameters were extended beyond the ranges explored by them. In the work described in this thesis the design and operating parameters are significantly beyond the ranges explored in reference *(77)*. Burning rates for larger carbon particles (> 3mm) were found to be substantially higher than those predicted by the model of *Avedesian & Davidson*[77]. From the present data the values of Sherwood Number for three different sizes of carbon particles

(3,6 and 12mm) were calculated by using equation (2.4) as shown below, which was presented by *Avedesian & Davidson*[77]

$$\dot{m} = 24\ \pi\ Sh\ D_G\ d\ c_p \qquad \ldots\ (2.4)$$

The calculated values of Sherwood Number for different bed design and operating conditions used during the present work is shown in Table 4.2. It was found that the value of Sherwood Number lies between 0.65 - 5.5 and it increased not only with carbon particle size, but with bed temperature, inert particle size and superficial fluidizing velocity. It should be noted that the values of Sherwood Number shown in Table 4.2 are the limiting values obtained assuming, (a) that combustion was controlled by the rate of diffusion of oxygen and (b) that carbon monoxide was the only product at the surface. *Ross*[106] reported from his recent work that for larger carbon particles (> 3mm) the carbon monoxide reaction zone is very thin and the conversion of carbon to carbon dioxide may be considered to take place essentially at the carbon surface. Under such conditions the values of Sherwood Number shown in Table 4.2 would be doubled. Moreover, the present burning rate data were related to the carbon particle diameter by equation (4.1) as shown below

$$\dot{m} = kd^n \qquad \ldots\ (4.1)$$

with $1.75 < n < 1.95$

The values of 'n' suggested that under the present experimental conditions combustion was mainly controlled by chemical kinetics and hence the actual

values of Sherwood Number must be higher than the limiting values shown in Table 4.2 which were calculated on the basis of diffusion controlled rate of combustion. However, it was difficult to predict the values of Sherwood Number accurately under present experimental conditions because of the uncertainty of the velocity of the burning carbon particles relative to the local air velocity.

Avedesian[94] used the minimum fluidizing velocity of the bed inert particles to calculate the value of Reynolds Number of the largest char particle (2.61mm) used by him and found it to be less than one and suggested that the effect of forced convection would be negligible in fluidized beds. However, visual observation of the top of the bubbling fluidized bed during the combustion experiments described in this thesis showed that the burning carbon particles were moving freely and randomly in the agitated bed, occasionally appearing at the top of the bubbling surface. This observation demonstrated clearly that the carbon particles were not always burning in the relatively stagnant particulate phase, but were changing their position from the particulate phase to the bubble phase and vice-versa, at random. It was not possible to determine the fraction of total burning time that a carbon particle remained in each phase of the bed. From visual observation it was also clear that the velocity with which the carbon particles were moving, within the bed was definitely higher than the minimum superficial fluidizing velocity of the inert particles. At times they seemed to have approached the bubble rising velocity as they were carried upwards by the bubbles. The present results thus suggested that the burning particles were getting oxygen by the effect of forced convection because of their random motion within the bed.

Andrei[88] and *Andrei, Sarofim & Beer*[89] also estimated burning coal particle Sherwood Number using data from their combustion experiments with coal particles, 1.85mm and 3mm in size, in a fluidized bed of sand at 750 - 950 ^{o}C at low superficial fluidizing velocities (about 7 cm/s). They [88,89] assumed that carbon is oxidized to carbon dioxide at the surface and used the equation (4.4) shown below to estimate the Sherwood Number from experimental data:

$$t_b = \frac{di^2 \rho_{char}}{48\ Sh\ D_G\ c_p} \qquad \ldots (4.4)$$

where ρ_{char} is the density of the char obtained after devolatalization of coal. They found the value of Sherwood Number to be about 1.75 for both sizes of coal particles.

They also used the *Ranz & Marshall* correlation[107], (see below) for mass transfer for flow past a single sphere

$$Sh = 2 + 0.6\ Re^{\frac{1}{2}}\ S_c^{\frac{1}{3}} \qquad \ldots (4.5)$$

to predict the value of Sherwood Number and found the value to be 2.3. They attributed the lower value of Sherwood Number, 1.75, obtained from their experimental data to the errors involved in the estimation of D_G and ρ_{char} and in the burn out data due to the experimental apparatus and the non homogeneous nature of individual coal particles and suggested that the experimental value of Sherwood Number should be approximately two. They further discussed the possible influence of chemical kinetics and resistance offered by the ash layers on the coal particle and the

surrounding inert particles to the diffusion of oxygen on the value of Sherwood Number estimated from their experimental data and suggested that the smaller inert particles surrounding the char particle restricted the free diffusion of oxygen to the carbon surface and hence the predicted value of 2.3 from *Ranz & Marshall*[107] correlation could not be obtained from experimental data.

Ross[106] recently analysed some of the present burning rate data reported elsewhere[108] which were substantially higher than the predictions of the model of *Avedesian & Davidson*[77] and that of *Basu, Broughton & Elliott*[80]. He suggested that in the shallow fluidized beds used during the present work, the burning carbon particles approached the superficial fluidizing velocity of the bed and thus mass transfer rates were higher than those predicted by these models[77, 80]. He showed that if the Sherwood Number was estimated from the *Ranz & Marshall*[107] correlation (see equation (4.5)) using the superficial fluidizing velocity as the velocity of burning carbon particles, then the burning rates obtained under present operating conditons would be predicted from equation (4.6) as shown below

$$\dot{m} = 12 \pi \, Sh \, D_G \, d \, c_p \qquad \ldots (4.6)$$

Equation (4.6) is thus only a slight modification of equation (2.4) originally presented by *Avedesian & Davidson*[77].

Recent work by *Ross*[106] indicated that for larger carbon particles (> 3mm), the carbon monoxide reaction zone thickness was negligible and carbon might be considered to be converted to carbon dioxide by oxygen essentially at the surface and he suggested the modified equation (4.6) on this basis. The predictions of his[106] modified model, of course, could not explain all the experimental data of the present work as evident from Figure 4.20. The actual burning rate data obtained during the present work were higher with large inert particles (780 μm) and lower with smaller inert particles (327.5 μm) when compared with the predictions of *Ross's*[106] suggested model. The matter is still unresolved.

4.4.2 Coal Fired Bed Fluidized with Air : Effect of Presence of Other Active Particles in the Bed

Figures 4.8 to 4.11 shows the logarithmic plots of burning rates of electrode carbon particles against their diameters in the coal fired fluidized bed under bed design and operating conditions identical to those used for burning rate experiments in the electrically heated bed already described. The bed was fed with anthracite coal particles, in the size range of -2.4 to 1.4mm, from a vibratory feeder to maintain it at the required temperature. Burning rates obtained in an electrically heated bed are also shown in these figures for comparison. It was found that the burning rates of electrode carbon particles were significantly less in the presence of other active anthracite coal particles burning simultaneously in the bed when compared to those obtained in the electrically heated bed in the absence of other active coal particles. Table 4.3

shows some burning rate data of three different sizes of electrode carbon particles (3, 6 and 12mm) obtained in a coal fired bed and in an eletrically heated bed. The values of the exponent 'n' in equation (4.1), calculated from the burning rate data obtained in a coal fired bed were found to be about the same as were found for electrically heated beds under identical bed design and operating conditions, thus suggesting the mechanism of combustion did not change when the bed was coal fired. The value of 'n' in coal fired bed suggested that the combustion was controlled mainly by chemical kinetics as was the case with electrically heated beds. It should be noted that the burning rate of a carbon particle, under kinetically controlled combustion conditions depend on the oxygen concentration in the particulate phase of the bed as was shown by equation (3.7) in Section 3.3. The reduction in burning rate of a single electrode carbon particle in the presence of a large number of other active anthracite coal particles in the coal fired bed thus suggested that the local oxygen concentration in the partiuclate phase was reduced under such conditions. This reduction of oxygen concentration in the particulate phase resulted in lower burning rates in coal fired beds.

The amount of carbon residing in the bed to maintain the required bed temperature when the bed was fired with anthracite coal particles, ranging in size, 1.4 - 2.4mm, was also measured in a separate set of experiments. When the bed was running steady with a continuous feed of coal, the common switch to the two separate solenoid

valves in the air and nitrogen flow lines was operated to fluidize the bed with nitrogen by replacing air, and the coal feed was stopped simultaneously. The bed cooled down slowly with coal particles remaining in the bed. When the bed cooled down, the coal particles were sieved out of the bed inert particles (sand). Some black carbon particles either equal to or less than the size of bed inert particles, were mixed with the inert particles. These appeared at the top of the inert particles when the pan was shaken and were separated from the top with some bed inert particles with them. These separated carbon particles were then placed in a shallow crucible and were burnt completely in air in an electrically heated furnace at 900 ^{o}C. The loss in mass of the crucible with contents, weighted before and after placing in the furnace thus gave an estimation of the amount of fixed carbon residue in the fluidized bed under steady condition. It was found that at 900 ^{o}C and 71 cm/s of superficial fluidizing, the amount of fixed carbon in the bed was about 2.4g and 4.3gm for the bed inert particle sizes of 780 μm and 327.5 μm respectively. The above experiment showed that a large number of carbon particles, ranging in size from zero to the top size fed to the bed resided in the coal fired bed and the amount depended on the bed design and operating conditions. It was not possible to count the number of these carbon particles physically, but their presence definitely reduced oxygen concentration in the particulate phase and thus reduced the burning rate of single electrode carbon spheres in a coal fired bed by interaction. The present results thus suggested that in an actual coal fired fluidized bed boiler, a large number of coal particles of a wide size range would burn simultaneously causing reduced local oxygen concentration in the bed and hence allowance

must be made for this reduced oxygen concentration on the burning rate of individual coal particles in designing a combustor for a required thermal output.

4.4.3 Electrically Heated Bed at Reduced Oxygen Concentrations (Fluidized with Mixtures of Air and Nitrogen)

In the previous Section it has been shown qualitatively that when a large number of active carbon particles reside in the fluidized bed, the burning rates of single electrode carbon particles reduced significantly. The effect of the reduced burning rate was such that as if the oxygen concentration in the particulate phase of the bed was reduced. To obtain quantitative information of the reduction in oxygen concentration in the bed for reduced burning rates obtained in coal fired beds, burning rates of electrode carbon particles were also measured experimentally in the electrically heated fluidized bed already described, where the concentration of oxygen in the fluidizing gas was altered to obtain reduced oxygen concentration in the particulate phase of the bed. Nitrogen was mixed with air in definite proportions to obtain reduced oxygen concentrations in the fluidizing gas. Design and operating conditions were otherwise similar to those used during burning rate experiments in the coal fired bed. The results are discussed below.

Figure 4.12 to 4.16 shows the logarithmic plots of burning rates of electrode carbon particles against their diameter for different oxygen concentration in the fluidizing gas and hence different oxygen concentrations in the particulate phase of the bed. These figures show that burning rate increased significantly with increase in oxygen concentration

in the particulate phase. But the slopes of these lines for different particulate phase oxygen concentrations were almost the same, thus suggesting that the mechanism of combustion was the same under such conditions. Burning rates obtained in coal fired beds for similar bed operating conditions were also shown in these figures. Using different oxygen concentration plots in these figures, the oxygen concentration in the particulate phase when the bed was coal fired was found by interpolation and was shown in each figure. Table 4.4 also showed burning rates for three different sizes of carbon particles (3, 6 and 12mm) at different oxygen concentrations for each particular bed design and operating condition.

The value of 'n' obtained (see equation (4.1)) at different oxygen concentrations once again suggested that combustion was mainly controlled by chemical kinetics. In the coal fired bed described in the previous section, the molar feed rate of carbon in the some cases was nearly equal to the molar feed rate of oxygen and thus represented the actual operating conditions of a coal fired fluidized bed boiler. The interpolated values of oxygen concentration in the particulate phase, found in Figures 4.13 to 4.16 thus presented some quantitative as well as qualitative information of oxygen concentrations when a large number of coal particles of a wide size range would burn in an actual fluidized bed boiler.

This information may be helpful to designers in determining the feed rate of coal particles and the amount residing in the bed to sustain the required output.

4.4.4 Order of Reaction

Figures 4.21 to 4.25 shows the burning rates of electrode carbon particles, 3mm and 12mm in diameter, plotted against the oxygen concentration in the fluidizing gas. The experimental data fitted straight lines passing close to the origin. This suggests that the order of reaction[103] was unity with respect to oxygen concentration in the fluidizing gas. Published values for the order of reaction between carbon and oxygen lay in the range, 0 to 1, depending on the type of carbon, the surface temperature and the oxygen concentration used. *Parker & Hottel*[57], studied the combustion of brush carbon in air over the temperature range of 950 - 1400 K and found that the order of reaction was unity. *Mulcahy & Smith*[71], from their review of literature on kinetics of combustion of carbon, suggested a value of 0.5. *Smith & Tyler*[109], from experiments with porous brown coal char, 22 μm in size, over 630 - 1812 K, found the order of reaction to be zero. *Basu's*[81] burning rate data in fluidized beds showed a nonlinear relationship with oxygen concentration which agreed qualitatively with their model of combustion shown in equation (2.7) below -

$$\dot{m} = 48\pi \varepsilon_m D_G d c_p \left(1 + \frac{12 c_p}{\rho_f}\right) \quad \ldots (2.7)$$

But the predicted burning rate using *Basu's*[80,81] model was found to be

substantially lower than the burning rates obtained experimentally during the present work. *Andrei*[88], from his combustion experiments with coal particles, 1.85 - 3mm in size, in a fluidized bed found the value of apparent order of reaction to be 1 at 900 °C and 0.87 at 750 °C. From this he suggested that combustion is controlled mainly by diffusion. But *Kanury*[103] showed that, in general, the burning rate under kinetically controlled combustion depends on the concentration of the reactants. Hence the value of 'n' does not necessarily indicate the influence of diffusion on the combustion rate. The present results suggests the order of reaction to be unity. This has important implications for the control of combustion in fluidized beds. For example, recycling part of the products of combustion through the bed, reduces the oxygen concentration in the fluidizing gas; thus the burning rate could be reduced to meet a lower thermal demand.

Pritchard & Caplin[110] have already reported the use of this technique to control the temperature of an industrial fluidized bed boiler in the United Kingdom.

4.5 Burning Carbon Particle Temperature Measurements : Results and Discussion

Temperatures of burning electrode carbon particles, 6 and 12mm in diameter, were measured in fluidized beds operating under design and operating conditions similar to those used for burning rate experiments described earlier. A carbon particle with a chromel-alumel thermocouple junction embedded at its centre was dropped into the fluidized bed and its temperature was recorded continuously on a chart recorder for as long as the bead remained inside the particle. A typical temperature history of a burning carbon particle is shown in Figure 4.26 Table 4.1 lists burning carbon particle temperatures measured experimentally under different bed design and operating conditions. From Table 4.1 it was found that the burning carbon particle temperatures were higher than that of the bed and the temperature difference varied over a wide range, namely 15 - 215 K. This temperature difference depended on the bed design and operating conditions used. Also, the temperatures of the smaller carbon particles (6mm) were in general, higher than those of the larger ones (12mm). Figure 4.26 shows that during the period of measurement, the burning particle temperature did not vary much. Carbon particle temperature measurement experiments in fluidized beds have also been reported by *Whellock*[111], *Basu*[81,83] and *Yates & Walker*[85]. *Whellock*[111] measured temperatures of coal particles of various shapes and sizes, with overall linear dimensions, ranging from $\frac{1}{8}$ to $\frac{1}{2}$ inch (3 - 12mm), by using a special calliper with a sheathed chromel-alumel thermocouple as one of its arms. He reported that in a fluidized bed of lime stone at 630 ^{o}C, fluidized with products of combustion of propane in air, the burning coal particles attained a maximum

temperatures which were about 200 K higher than that of the bed. But the burning particles used by *Whellock*[111] did not have any freedom to move in the bed. *Whellock*[111] did not state the inert particle size or the superficial fluidizing velocity. *Basu*[81,83] measured the temperature of an electrode carbon sphere, about 7mm in diameter in a fludized bed of fine sand (100 μm) at 800 ^{o}C using low superficial fluidizing velocity (8 cm/s) and found that the temperature difference was initially about 45 K and finally reached about 200 K as combustion proceeded. *Yates & Walker*[85] also measured char particle temperatures indirectly by following the history of fusible alloy wire rings embedded in the burning particles in a fluidized bed of sand (225 μm) at about 850 - 950 ^{o}C using low superficial fluidizing velocities (12.4 - 16.4 cm/s). They found that the temperatures of the burning char particles were about 60 - 140 K higher than that of the bed, the smaller char particles (2.5mm) being at higher temperatures than the larger ones (7.5mm). The above, however, did not cover a wide range of bed design and operating conditions. The work reported in this thesis was carried out over an extended range of conditions.

It was evident from Table 4.1 that in general, the temperatures of the burning carbon particles were higher under the conditions where burning rates were higher. The oxygen concentration, inert particle size, superficial fluidizing velocity and presence of a large number of carbon particles in the bed, all affected the particle temperature significantly.

Zabrodsky & Parnas[112] estimated tentatively the difference in temperature between burning carbon particles (about 2mm in size) and the fluidized beds by using the model of *Avedesian & Davidson*[77] and found it to be small (about 10 K) for continuous combustion at 10% excess air level. They further suggested that this temperature difference would be still smaller when the carbon particles are considerably larger than the bed inert particles. This was attributed to increased heat transfer rate from carbon particle arising from increased relative motion between the carbon particles and the bed inerts. However, their calculations showed large temperature differences, ranging from 30 K (initially) to 130 K (at the end of the run) for a carbon particle, 1.44mm in size, under the same experimental conditions used by *Avedesian & Davidson*[77]. The authors[112] commented that *Avedesian & Davidson*[77] used small charges of carbon particles in batches and under such conditions, as the carbon particle diameter approached zero at the end of the run, the oxygen concentration in the particulate phase approached that in the fluidizing gas. This naturally resulted in an increase of both the burning rate and the burning particle temperature. *Zabrodsky & Parnas*[112] also did not agree with the idea of *Avedesian & Davidson*[77] that the temperature of burning carbon particles above the bed would be lower than that inside the bed due to radiation, because their[112] estimation showed that heat removed by radiation and gas conduction when fine particles were used, could be smaller than the cooling of such particles inside the fluidized bed.

The model of *Beér et al*[84] also indicated that the burning coal particles should not be much hotter than the bed except during the period when volatile matters are evolved. *Andrei*[88] and *Andrei, Sarofim & Beér*[89] during their combustion experiment with coal particles, 1.85 - 3mm in size, in a fluidized bed at 750 - 900 ^{o}C also observed visually that the glowing intensity of the coal particles were less at reduced oxygen concentration and in general particles appeared more luminous as they burnt down to smaller size.

The present work suggests that the burning particle temperatures would be affected significantly by the inert particle size, superficial fluidizing velocity, the carbon concentration in the bed, oxygen concentration in the fluidizing gas. In general larger carbon particles would be at a lower temperature than the smaller ones. Measured particle temperatures shown in Table 4.1 suggest that the assumption made by *Avedesian & Davidson*[77] that in fluidized beds, burning carbon particles would be at temperatures some 200 K higher than that of the bed could not be generalised.

The present results also suggest that in a continuously operated fluidized bed fed with large coal particles, the particle temperature would not be much higher than that of the bed. Thus it would be advantageous if a small number of large carbon particles are fed to the bed per unit time than the converse. Also lower particle temperature would reduce (a) evolution of oxides of nitrogen and (b) problem of fusion of ash in the bed.

PART B

4.6 Introduction

In Part A of this Chapter experimental measurements of burning rates and temperatures of single electrode carbon particles in a shallow fluidized bed of sand have been described. Bed design and operating conditions for the above work covered a wider range of variables than covered by previous workers. Thus the ranges explored were

(i) static bed depth, 12.5 - 50 mm

(ii) superficial fluidizing velocity, 27 - 71 cm/s

(iii) inert sand particle size, 327.5 - 780 μm

(iv) carbon particle size, 2 - 12 mm

However, the present trends in fluidized bed coal combustor designs are -

(i) to use larger sizes of inert particles and higher superficial fluidizing velocities to increase the throughput of air so that the size of the combustion could be reduced[5, 92, 93];

(ii) to use larger sizes of coal particles to reduce the cost of crushing coal and minimize the effect of elutriation of carbon on combustion efficiency[90, 91]. Also, use of larger sizes of coal increase the intensity of combustion within the bed[91] (MW/m^3)

The use of a relatively shallow bed for the work described in Part A limited the amount of electrial heat input to the bed and hence the superficial fluidizing velocity to 71 cm/s; this, in turn, limited the size of the carbon particle to 12mm.

In this part (Part B) experimental measurements of burning rates and temperatures of electrode carbon particles in relatively deeper beds of high specific gravity alumina are described. The ranges of variables explored are as shown below:

(i) static bed depth, 100 - 150mm

(ii) superficial fluidizing velocity, 1.37 - 2.5 m/s

(iii) inert alumina particle mean size, 1008 μm
(size range 850 - 1180 μm)

(iv) carbon particle size, 3 - 20mm

Experimentally measured burning rates were compared with predictions of the existing models and the limitations of these models were discussed. The Effect of forced convection on burning rates were examined and discussed.

4.7 Experimental Equipment

4.7.1 Experimental Fluidized Bed Combustor

The combustor already described in Section 4.2.1 and shown in figure 4.1 was also used for Part B experiments with some necessary modification. Since the superficial fluidizing velocities for Part B experiments were considerably higher than those used for Part A work, two separate Kanthal heating coils were wound on the outside of the

quartz glass tube - one at the bottom and the other at the top of it. The terminals of the lower and the upper heating coils were connected to two separate variable output transformers so that independent adjustment of electrical input could be made. In addition to these two heating coils, an air heater (Model 571, manufactured by Secomak Electric Co. Limited, Secomak Works, Honeypot Lane, Stanmore, Middlesex, England) was used to preheat the air to about 350 ^{o}C before it entered the plenum chamber. The heater terminals were also connected to a third variable output transformer for adjusting the electrical input to the air heater.

4.7.2 Carbon Particles

Carbon particles used for Part B experiment were similar to those described in Section 4.2.2. However, for Part B work the largest size was about 20mm. In some of the spheres a 1.5mm hole was drilled to the centre so that the bead of a stainless steel sheathed Chromel-Alumel thermocouple could be sealed to measure burning particle temperatures.

4.7.3 Bed Inert Material

Brown fused alumina (commercial name: Brown Bauxilite Abrasive - Type AS; supplied by Universal Abrasives Limited, Stoney, Stafford, England) was used as the bed inert material. The properties of this aluminium are given in Appendix B. The particles were sieved out in the size range of 850 to 1180 μm by using B.S. Standard Sieves (supplied by Endecotts Limited, London, England) with a mean size of 1008 μm. Figure 4.27 shows some alumina particles used.

Butler[28] reported that Northern Engineering Industries, Derby, U.K. were using this type of alumina particles as bed inert materials in their demonstration fluidized bed shell boilers because of its high density (3930 kg/m^3) which requires higher fluidizing velocity. Because of this, the throughput of air to the bed is increased and hence the opportunity arises for increasing the intensity of combustion to a level comparable with that found in oil-fired and gas-fired combustion chambers.

4.7.4 Fluidizing Gas

Air was used as the fluidizing gas during the period of combustion of the carbon particles. A calibrated rotameter (Metric Series Rotameter, Tube Size 18, Float type Korannite; manufactured by Rotameter Manufacturing Co. Limited, Croydon, England) was used to measure the air flow rate.

Nitrogen was also used to fluidize the bed during the periods of heating the carbon particles to the bed temperature and cooling the bed after the particles burnt in air for a specific time so that the atmosphere remains inert. Two separate solenoid valves were fitted in the air and nitrogen flow lines and operated through a common switch so that instant changes to either nitrogen and air flow could be made.

4.8 Burning Rate Experiments; Test Procedure

Test procedure was similar to that described in Section 4.3.1 except that the time allowed for heating the carbon particles in the nitrogen fluidized bed was increased to about two minutes. This was needed to heat the largest carbon particle (about 20mm) to the bed temperature.

4.8.1 Attrition of the Carbon Particles in High Density Alumina Bed

Attrition of the carbon particles in the alumina bed was also measured separately through the same procedure described in Section 4.3.1. It was found that the loss of mass of carbon spheres by attrition ranged from 0.0005 to 0.008 g and was found to be higher for larger sizes of carbon particles. However, the percentage of loss of mass by attrition was found to be not more than 2% of the total loss of mass during combustion in the bed fluidized with air for all sizes of carbon particles and thus it was neglected.

The period of combustion of the carbon particles in the alumina bed fluidized with air was limited to 50s in all cases to keep the reduction in size within 5% of the initial diameter. It was found that the reduction in diameter was within this limit for larger sizes of carbon particles. However, for carbon particles smaller than 6mm in diameter, reduction in size during combustion exceeded 5% of the initial diameter. Hence, the mean diameter of the carbon particles during their combustion in the fluidized bed was used for plots.

Burning rates of the carbon particles were computed from loss of mass observed by weighing them before and after combustion.

4.9 Burning Rates of Carbon Particles in Fluidized Beds of High Density Alumina: Results and Discussion

Burning rates of carbon particles are shown plotted against their mean diameters in logarithmic plots in Figures 4.28 to 4.30 for

different design and operating conditions of the bed. The data points lie close to straight lines fitted by the least squares method. Burning rates of carbon particles are thus related to their mean diameters by equation (4.1) ($\dot{m} = kd^n$) which has already been discussed in Section 4.4. Values of the exponent 'n' obtained from these plots are found to lie in the range, 1.41 to 1.44 . Equations (3.6) and (3.8) suggested that value of 'n' would be either 1 or 2 according as the combustion process was controlled by the rate of diffusion of oxygen towards the surface or the rate of chemical reactivity at the burning carbon surface.

Avedesian[94] and *Basu*[81, 83] also supported the above viewpoint. Moreover, *Basu*[83] found the value of n in the range, 1.22 - 1.55 from similar single carbon particle burning rate experiments at lower superficial fluidizing velocities (8 cm/s) in a bed of finer inert particles (100 μm sand) and therefore suggested that combustion was controlled by the combined effect of chemical kinetics and diffusion. The values of 'n' obtained under present experimental conditions shows that *Basu's*[113] contention holds over a much wider range of variables than those covered by his experiments. The arguments about mixed mode burning explained in Section 4.4.1.2 are still valid for combustion in high density alumina fluidized beds.

When the burning rate data obtained when burning in the fluidized bed of high density alumina is compared with the predictions of *Avedesian & Davidson's*[77] diffusion controlled model of combustion of carbon in fluidized beds as shown in Figures 4.28 to 4.30. it is evident that for all the sizes of carbon particles used, the burning rates are higher

than the predictions of this model. Furthermore the discrepancy between the experimental and predicted burning rates increased with carbon particle size. It will be recalled that *Avedesian & Davidson*[77] postulated that the burning carbon particles remain in the relatively stagnant particulate phase of the bed and therefore, the Sherwood Number is constant and less than 2 because of added diffusional resistance of the inert particles around it. Their experimental burning rate data supported this model and suggested that a suitable value for Sherwood Number would be 1.42.

On the other hand combustion experiments by *Andrei*[88] using coal particles, 1.85 - 3mm in size in a fluidized bed (static bed depth of 120mm) at low superficial fluidizing velocity suggested a value of Sherwood Number to be nearer to 2. Burning rate experiments at Aston described in Part A in relatively shallow fluidized beds yielded values of Sherwood Number in the range, 0.65 to 5.5, thus indicating that forced convection plays an important part in transferring oxygen to the burning carbon particle surface. *Avedesian & Davidson's*[77] postulation of constant Sherwood Number thus seems to have limited applicability. They did not however, comment on whether or not their quoted value of Sherwood Number would be applicable to other situations.

In private communication, *Ross*[106] suggested another explanation for some of the higher burning rates reported in Part A of this Chapter. It was suggested that with such shallow beds the local velocity of the burning carbon particles within the bed probably approached the superficial fluidizing velocity so that the mass transfer rate of oxygen to

the burning surfaces was very much higher than that assumed by *Avedesian & Davidson's*[77] model. But this did not necessarily mean that the kinetic limit had been reached. By using the *Ranz & Marshall*[107] correlation for Sherwood Number (see equation (4.5) below) and

$$Sh = 2 + 0.6\ Re^{\frac{1}{2}}\ S_c^{\frac{1}{3}} \qquad \ldots (4.5)$$

(Note : To calculate Reynolds Number (Re) in above equation, the superficial fluidizing velocity was used.)

modifying *Avedesian & Davidson's*[77] model as shown by equation (4.6), below

$$\dot{m} = 12\ \pi\ Sh\ D_G\ d\ C_p \qquad \ldots (4.6)$$

Ross[106] showed that the burning rate predicted by this method were in better agreement with the experimental data reported in Part A of this Chapter. However, as mentioned in Section 4.4.1.6, *Ross's*[106] explanation was not sufficient to describe all the results over the whole range of variables explored. The matter is therefore not completely resolved.

Ross[106] further suggested that in a deep bed the burning carbon particles would be in an essentially quiescent particulate phase of the bed and hence a constant Sherwood Number could be postulated. In such a deep bed, in the absence of forced convection Sherwood Number of burning carbon particles would approach the lower limit of 2. This latter point is not borne out by the burning rate data shown in Figures 4.28 to 4.30 which were obtained in deeper beds (static bed depth of 100 - 150 mm)

than those used by *Avedesian & Davidson*[77] (static bed depth of 82mm). *Avedesian & Davidson's*[77] model could not explain these results on the basis of a constant Sherwood Number. The higher burning rates shown in Figures 4.28 to 4.30 could not be achieved if the forced convection effect was absent.

Visual observation of the bed during combustion experiments showed that agitation and mixing within the bed due to bubbling action caused the burning carbon particles to appear occasionally at the top of the bubbling surface. Moreover, bed expansion was observed to be much greater than with a bed of sand (the bed height was about twice the static bed depth). The expanded bed level was also observed to fluctuate considerably, as large bubbles burst at the surface. In such an expanded bed the bubble phase occupies a substantial part of the bed volume. Agitation within the bed causes the carbon particles to exchange positions between bubble and particulate phase frequently[113]. The proportion of the burning time that the burning carbon particle would remain in the bubble phase is uncertain, but the fact that the burning rates were high suggests that this proportion is significant.

Thus, it appears that in shallow fluidized bed combustors (static bed depth of the order of 150mm) with operating conditions similar to those met in industrial designs, the effect of forced convection on the rate of mass transfer of oxygen to the burning carbon particles is significant and the model of *Avedesian & Davidson*[77] needs to be modified if it is to be used for production of burning rates under such conditions.

4.10 Burning Carbon Particle Temperature in Fluidized Beds of High Density Alumina : Results and Discussion

Carbon particles, about 19-20mm in diameter, were used for this test. A 1.5mm hole was drilled up to the centre of the particles and a mineral insulated chromel-alumel thermocouple probe with a stainless steel sheath over it (outside diameter of sheath, 1.5mm) was sealed into the hole with high temperature insulating cement (commercial name : Fortafix, manufactured by Fortafix Limited, Fengate, Peterborough, England). The output of the thermocouple was recorded continuously on a chart recorder. It should be noted that attempts to use chromel-alumel thermocouples of smaller size wires, as were used for Part A work, were not successful in relatively deeper beds of high density alumina operated at higher superficial fluidizing velocities (Part B work). It was found that soon after the carbon particles with embedded thermocouples made from smaller sized (0.3mm wire diameter) wires were dropped into the bed, the wires broke and it was not possible to measure temperature of the carbon particles with these thermocouples. So mineral insulated stainless steel sheathed thermocouples had to be used. This restricted the movement of the burning carbon particles to some extent, but visual observation showed that they moved within the bed and occasionally came out of the bubbling bed with rise and bursting of bubbles. The recorded temperatures were also reproducible within ± 10 K.

Burning particle temperature data obtained in fluidized beds of alumina are shown in Table 4.5. The table shows that the difference between the particle temperature and the bed temperature was over 200 K when the bed temperature was 800 ^{o}C, whereas at a bed temperature of

of 900 ^{o}C, this difference was less than 200 K in magnitude. These may be attributed to the higher rates of heat transfer by radiation of higher carbon particle temperature and control of combustion by rate of mass transfer at 900 ^{o}C. Also it was found that particle temperatures in Table 4.5 (Part B work) were in general higher than those shown in Table 4.1 (Part A work). This may be attributed to the fact that the size of inert particles for Part B work was larger than those used for Part A work and so rate of heat transfer from the burning carbon particles to the inert particles would be significantly less under such conditions because of the lower heat transfer coefficient with larger inerts[76]. This has already been discussed in Section 4.4.1.2. However, the burning carbon particle temperatures would be significantly less than those shown in Table 4.5 in a continuously fed fluidized bed coal combustor under steady state combustion, because of the reduction in local oxygen concentration within the bed due to the presence of a large number of other burning carbon particles under such conditions. Estimation of burning carbon particle temperatures by *Zabrodsky & Parnas*[112] for continuous fluidized combustion at low excess air also showed such results. This has already been discussed in Section 4.5 .

CHAPTER FIVE

COMBUSTION EXPERIMENTS WITH BATCH CHARGES OF CHAR PARTICLES IN SHALLOW FLUIDIZED BEDS

5.1 Introduction

In Section 3.4 of Chapter 3, the burn out time of a carbon particle was expressed in terms of the initial diameter assuming the combustion process to be controlled either (i) by the rate of diffusion of oxygen towards the surface of the particle or (ii) by the chemical kinetics. In this Chapter combustion experiments with batch charges of char particles of different size ranges and mass are described. Burn out time data of the charge was obtained from

(i) visual observation

(ii) continuous record of bed temperature against time

(iii) continuous record of oxygen concentration in the off gas against time.

Experience showed that in most of the cases, all three measurements were in good agreement with each other. However, the burn out time estimated from oxygen concentration-time record was found to be better reproducibile and consistent throughout and hence it was used to analyse the mechanism of combustion. The following variables were explored:

(i) Char particle size : 1.84 - 4.375 mm

(ii) Char particle charge mass : 0.75 - 3.75 g of char

(iii) Bed temperature : 800 - 900 °C

(iv) Inert particle size : 327.5 - 780 μm

(v) Superficial fluidizing velocity : 27 - 71 cm/s at 900 °C

The results were compared with those reported by previous workers and discussed.

5.2 Experimental Equipment

5.2.1 Experimental Fluidized Bed Combustor

This has already been described in Section 4.2.1 of previous Chapter. During the batch burn out experiments, the bed temperature was recorded continuously on a chart recorder running at a speed of 1 cm/m since this record was used to estimate the burn out time of the charge.

5.2.2 Char Particles

Char particles used for the work reported in this thesis was supplied by Coventry Homefire Works, Coventry, U.K. and was reported to have been prepared from a blend of high volatile coals by carbonizing in a fluidized bed carbonizer at about 420 ^{o}C. Blending data are given in Appendix C. The char particles were sieved into six different size ranges using B.S.S. standard sieves with the minimum size of 1.84mm and the maximum size of 4.375mm. The minimum size of the char particles was limited to 1.84mm so as to minimize elutriation; the maximum size was

limited to 4.375mm as it was not possible to get any size larger than this in sufficient quantity from the bulk of the char supplied. Proximate analysis, size ranges, mean sizes and charge masses of char particles used are shown in Appendix C. Also, Figure 5.1 shows a photograph of two size ranges of char particles, 1.68-2.0mm and 4.0-4.75mm, in order to indicate the shape of the particles.

5.2.3 Bed Inert Material

Silica sand particles (supplied by British Industrial Sand Limited, Foundry Division, Church Bridge Industrial Estate, Oldbury, Warley, West Midlands, U.K. under specifications (i) Chelford 50 (for mean sizes of 327.5 μm and 550 μm and (ii) Levenseat (for mean size of 780 μm)) were used as bed inert materials. Their size ranges, mean sizes and minimum superficial fluidizing velocity is shown in Appendix A.

5.2.4 Fluidizing Gas

Air was used as fluidizing gas. A calibrated rotameter (metric series tube, size 14, Duralumin float; supplied by Rotameter Manufacturing Company Limited, Croydon, England) was used to measure the airflow rate.

5.2.5 Analysis of the Products of Combustion

During the burn out time of the batch charges of char particles the products of combustion was sampled continuously by using a water cooled probe placed about 50 mm away from the bubbling surface of the fluidized bed and the sample was analysed continuously for carbon

monoxide, carbon dioxide and oxygen. An infra red analyser (MEXA - 310 infrared analyser, manufactured by Horiba Limited, Kyoto, Japan) was used to analyse the concentrations of carbon monoxide and carbon dioxide, while a paramagnetic oxygen analyser (oxygen analyser : Type OA.272, manufactured by Taylor Servomex Limited, Crowborough, Sussex, England) was used to analyse the concentration of oxygen. The concentrations of carbon monoxide, carbon dioxide and oxygen were continuously recorded on chart recorders.

Figure 5.2 shows a photograph of the experimental set up.

5.3 Batch Burn Out Experiments: Test Procedure

At the beginning of each experimental run, about 210 g of sand particles of a particular size range was placed into the bed to obtain a static bed depth of 30mm. The bed was fluidized with air, the electrical heating was switched on and the input was gradually increased to heat the bed to the required temperature (800 ^{o}C or 900 ^{o}C). When the bed approached this temperature, the air flow rate was adjusted to obtain a particular superficial fluidizing velocity and the electrical heat input was finally adjusted to keep the bed steady at the required bed temperature. The bed reached a steady state in about two hours. When the bed was running steadily, a weighed amount of char particles of a particular size range was dropped into the bed from the top and a stop watch was started simultaneously. Before dropping the batch charge the recorders for recording the bed temperature, concentrations of carbon monoxide, carbon dioxide and oxygen were started. All these recorders were set to the same speed of 1cm/s.

Immediately after the charge was dropped into the bed, smoky yellow flame appeared at the top of the bubbling bed. This lasted for about 5 to 20 seconds depending on the carbon particle size, charge mass, bed temperature, bed inert particle size and superficial fluidizing velocity used. After the volatile evolution was complete bright glowing char particles were observed through the mirror which was placed at an inclined position and some distance away from the top of the combustor (see Figure 4.1).

A colour cine film of the process was made and is available for display from Dr. J. R. Howard of the Department of Mechanical Engineering, University of Aston, Birmingham.

The burning char particles were found to be moving at random in the agitated bed and occasionally appeared at the top of the bubbling surface. As combustion proceeded, the particles appeared to be reducing in size and number. They also appeared to be brighter as they burnt down to smaller sizes and eventually disappeared as burn out was completed. The watch was stopped at the instant no further glowing char particles were seen. In some cases, some glowing char particles were found to be elutriated from the bed as they burnt down to small enough size. Also, in some cases some of the char particles shattered during the periods of volatile evolution and combustion and elutriation of smaller fragments occurred. But visual observation suggested that the portion of the batch charge which was elutriated was not significant. The elutriated fines were not recollected or recycled and no allowance was made for the lost elutriated fines on the initial charge mass or the burn out time of

the batch charge. These elutriated fine particles would have burnt out with main part of the batch charge had they not been elutriated and so they did not affect the burn out time significantly. During combustion of char particles, temperature of the bed and concentrations of oxygen, carbon monoxide and carbon dioxide in the products of combustion were continuously recored on chart papers. Figure 5.3 shows a typical record of all these.

5.3.1 Burn out time measurements

The burn out time of the batch charges of the char particles, the most important data collected during the experiment, was used for analysis of the mechanism of combustion.

The visually observed burn out time obtained with the help of a stop watch was found to be reproducible with good accuracy (within 2 to 5 s) for the smaller sizes of char particles having a narrower size range. But for the larger sizes of char particles having a wider size range, the visually observed burn out time was found to give a rough value because they could not be reproduced with sufficient accuracy.

5.3.1.1 Comparison of the above experience with that of other workers

Avedesian & Davidson[77] performed similar batch burn out experiments with char and coke particles, 0.23 - 2.61 mm in size and reported that visual observation gave reproducibility within ± 5%. They confirmed these visual observed burn out times from bed temperature-time continuous

records. Their visually observed end of the burn out period corresponded to a time instant on the bed temperature time recorded which was slightly later than the time at which the bed temperature was a maximum as shown in figure 5.4.

Campbell & Davidson[78] used carbon particles, 1.3 - 3.08 mm in size, for similar batch burn out experiments. *Campbell*[114] reported that the visually observed burn out times were of rather limited value for larger particles with broader size range. However, he[114] reported that a point of inflection which occurred much later than the maximum temperature point in bed temperature-time record was found to indicate the end of burn out of the charge. This point is shown in figure 5.5.

Campbell[114] found this method could give burn out time with consistency within an error of ±5 s.

Because the char particles used in the present work were generally larger (1.68 - 4.75mm) than those of *Campbell & Davidson*[78], visually observed burn out times were found to have reproducibility varying within 20s in some cases, which was not very accurate. Bed temperature-time curve, of course, gave good estimation of burn out times in most cases, except for smaller charge masses. However, oxygen concentration in the off gases-time record was found to give a better reproducibility (within ± 5s) and consistency of batch burn out time throughout. In view of this better reproducibility, burn out time estimated from oxygen concentration-time record was used for analysing the results.

5.4 Burn out of batch charges of char particles : Results and Discussion

5.4.1 Variation of initial mean diameter of char particles in the charge

The burn out times of the batch charges of char particles, for a charge mass of 3g of char (2.025g of fixed carbon) are shown plotted against their initial mean diameters in figures 5.6 - 5.8, for different fluidized bed design and operating conditions. The plotted data points lie on straight lines fitted by least squares method. These plots, therefore, indicates that combustion of the char particles under present conditions were controlled mainly by chemical kinetics as was suggested by equation 3.14 in Chapter 3 and also by previous workers[77, 88]. Although the assumptions which led to equation 3.14 were not strictly applicable to the present fluidized bed combustion situations, the linear variation of burn out time with initial mean diameter of the char particles in the charge suggested that like combustion of single carbon particles described in Chapter 4, the combustion process for batch charges, is influenced by chemical kinetics[77, 88]. If the combustion process was entirely diffusion controlled, the data points plotted in figures 5.6 - 5.8 would lie on a parabola[77, 88], but this is not so. *Avedesian & Davidson's*[77] burn out experiments, using smaller sizes of char particles (0.23 - 2.61mm), in a deeper fluidized bed of ash (static bed depth 82mm), operating at lower fluidizing velocities (21.4 - 38.3 cm/s) showed that their data fitted straight lines against the square of the initial mean diameter of the char particles (di^2), as shown in Figure 5.9b. From this they[77] suggested that under their experimental

conditions combustion was controlled entirely by the rate of diffusion of oxygen towards burning char particles.

However, it is interesting to note that their published data could also be fitted closely to straight lines when burn out times were plotted against initial mean diameter of char particles (di), as shown in figure 5.9a. Thus fitting data points to a predetermined law can be inconclusive.

The present burn out data, however, is not directly comparable with those of *Avedesian & Davidson*[77], because the bed operating parameters were by no means identical as shown in Table 2.1.

The present burn out time data were also found to be substantially affected by bed temperature, inert particle size and superficial fluidizing velocity which are discussed below:

(a) Effect of bed temperature : Figure 5.6 shows the decrease in burn out time with increase in bed temperature from 800 ^{o}C to 900 ^{o}C. *Yates & Walker*[85] from their burning rate experiments with resin bonded coal dust particles found that burning rate was maximum when the bed temperature was about 800 ^{o}C , decreasing with further rise in bed temperature. They attributed this to the increased resistance to diffusion of oxygen offered by ash layers formed on the burning carbon particles at high temperature. Char particles used during the present work had also ash layers formed on them as they burnt in the bed. However, no such reduction in burning rates was observed as temperature was increased from 800 ^{o}C to 900 ^{o}C.

Andrei[88] and *Andrei, Sarofim & Beér*[89] also found that burning rates of coal particles, 1.85 - 3mm in size, increased with increase in bed temperature from 750 °C to 900 °C. Their[88, 89] experimental results also strongly suggested that ash layer on the coal particles did not impose any additional diffusional resistance. The explanation for *Yates & Walker's*[85] lower burning rates at high temperature may arise from the fact that their carbon particles were made from a mixture of anthracite coal dust and pheolic resin by compressing in a mould to a pressure of 20 bar at 413 K. This method of preparation could have affected the active surface area of the carbon particles and thus leading to different behaviour. *Laine, Vastola & Walker*[115] suggested that, depending on the carbon type, structure and impurities in it, the active surface area of the carbon available for the reaction with oxygen varies widely and demonstrated the importance of active surface area in carbon oxygen reactions experimentally. The present results, thus, clearly suggest that higher burning rates could be achieved by increasing the temperature of the fluidized bed.

(b) Effect of bed inert particle size : Figure 5.7 shows the effect of bed inert particle size on the burn out time. The bed temperature, the static bed depth and the superficial fluidizing velocity were 900 °C, 30mm and 71 cm/s (at bed temperature) respectively. Three different sizes of sand particles of mean sizes 327.5 μm, 550 μm and 780 μm were used. It was found that the burn out times were substantially lower in beds of larger inert particles. As with single carbon particle combustion, (Section 4.4.1.2), the most likely explanation for this faster burning is that the rate of heat transfer from the burning particles to bed is

lower with larger inerts, resulting in a higher char particle temperature and thus a higher burning rate. In addition to this, gas transport from the bubble phase to the dense phase of the bed is bound to be faster with larger inert particles. These results tend to support the model recently proposed by *Leung & Smith*[86], (Section 2.4). Thus to increase the intensity of combustion (MW/m^3 of bed) larger sized inert particles should be used subject to satisfactory heat removal from the bed.

(c) Effect of superficial fluidizing velocity : Figure 5.8 shows the effect of superficial fluidizing velocity on the burn out time of the batch charge. It was found that burn out time was reduced significantly (typically 30%) by increasing the superficial fluidizing velocity from 27 cm/s to 71 cm/s. *Avedesian & Davidson*[77] also reported similar results to lower fluidizing velocities. As with single particle combustion (Section 4.4.1.3), the increased agitation in the bed arising from the increase in bubble frequency due to higher superficial fluidizing velocity and also the higher amount of oxygen supplied at the higher superficial fluidizing velocity caused faster burning of the batch charge.

5.4.2 Variation of initial charge mass of fixed carbon in the charge

The burn out times of the batch charges of char particles are shown plotted against the initial charge mass of fixed carbon in figures 5.10 - 5.13 for different bed operating conditions. The plotted data lies close to straight lines fitted by least squares method. The burn out time of the batch charge always increased with the mass of the charge.

Since the number of individual particles in the batch charge was large, the intercept made by the straight line on the burn out time axis gives a close approximation to the burn out time of a single char particle of mean size of the batch, assuming that there is no interaction between the char particles. These estimated single char particle burn out times are listed in Section A of Table 5.1. The estimated single char particle burn out times are also shown plotted against the initial diameter in figure 5.14, which are in reasonably close agreement with equation 3.14, which is also shown below.

$$t_{b_{kinetic}} \propto di \qquad \ldots (3.14)$$

Analysis of the data listed in Section A of Table 5.1 and plotted in figure 5.14 showed that the ratio of the estimated single char particle burn out times for any two particular sizes was very nearly equal to the ratio of these sizes as shown by equation (5.1) below

$$\frac{t_{b_{estimated}}^{(di_1)}}{t_{b_{estimated}}^{(di_2)}} = \left(\frac{di_1}{di_2} \right) \qquad \ldots (5.1)$$

Section B of Table 5.1 shows all such ratios which suggests that chemical kinetics play an important role[77, 88].

Data due to *Avedesian & Davidson*[77] also shows the same characteristics, as shown in Sections C and D of Table 5.1. However, *Avedesian*

& Davidson[77] interpreted their data (Section C, Table 5.1) differently, claiming that the ratio of the estimated single char particle burn times follow the relationship shown by equation (5.2) below

$$\frac{t_{b_{estimated}}^{(di_1)}}{t_{b_{estimated}}^{(di_2)}} = \left(\frac{di_1}{di_2}\right)^2 \qquad \ldots (5.2)$$

and hence that diffusion was controlling the combustion. But, as Section D of Table 5.1 shows, their claim that combustion was diffusion controlled is not fully substantiated when the ratios of estimated single particle burn out times were compared with equations (5.1) and (5.2). The issue is thus unresolved.

An alternative explanation could be that the single particle burning rate under kinetically controlled combustion is also affected by oxygen concentration in the bed according to equation (3.7), which is shown below

$$-\frac{dm}{dt} = 12\,\phi\pi\,d^2 k_s\,c_p \qquad \ldots (3.7)$$

It has already been discussed in Section 4.4.2 that burning rate of a single electrode carbon particle was substantially lower in the presence of a large number of active anthracite coal particles burning simultaneously with it. Large number of active carbon particles, present in the bed,

consumed locally available oxygen readily and thus reduced the local oxygen concentration in the bed. As a result, the burning rate of the single electrode carbon particle, which depended on the local oxygen concentration in the bed was lower.

Results of burning rate experiments performed when the oxygen concentration was reduced by adding nitrogen to the fluidizing air, reported in Section 4.4.3 showed that the slope of log $\dot{m}$ vs log d_i lines (Figures 4.12 to 4.16) did not change with oxygen concentration. However, the burning rate for a given value of 'd' depended strongly on oxygen concentration. Because the slope of these lines lay near to 2, chemical kinetics appeared likely to be the principal controlling mechanism[81,83] what is really a mixed mode, because the char particles moved to and fro between the bubble and particulate phases of the bed during their burn out.

The increase in charge mass of char particles increased the number of char particles in the bed as shown in Table 5.2 below exposing more active surface area and consumes an increasing amount of oxygen locally available. Thus the local oxygen concentration within the bed is lower which leads to a lower burning rate of the individual char particles.

TABLE 5.2

NUMBER OF CHAR PARTICLES OF MEAN SIZE IN THE BATCH CHARGE

Charge Mass of Char Particles (g)	Approximate Number of Char Particles in the Charge for Mean size of		
	1.84mm	2.6mm	4.37mm
0.75	304	108	23
1.50	607	215	45
2.25	911	323	68
3.00	1214	430	90
3.75	1518	538	113

5.4.3 Devolatilization of Char Particles

Char particles used for the present work contained approximately 27% of volatile matter. The process of devolatilisation was studied qualitatively from visual observation. Soon after the batch charge of char particles was fed to the bed, a smoky yellow flame was visible at the top of the bubbling surface indicating the evolution of volatile matter. The period of volatile evolution and combustion was measured with a stop watch by visually observing the flame and was found to last from 5 to 20 s depending on the char particle size, charge mass, bed temperature and superficial fluidizing velocity. The flame was initially tall, but decreased gradually in height as evolution and combustion of volatile matter slowed down, finally disappearing at completion of volatile evolution and combustion. Concentrations of carbon monoxide, carbon dioxide and oxygen in the products of combustion sampled from 50mm above

the bubbling surface were also recorded continuously during the combustion of char particles. Figure 5.3b(i) to 5.3b(iii) shows typical records of oxygen, carbon dioxide and carbon monoxide concentrations. These records show that immediately after the batch change of char particles was fed to the bed, the oxygen concentration in the off gas fell sharply, whereas the concentrations of carbon monoxide and carbon dioxide showed sharp rise. This corresponded to the rapid evolution of volatile matter. Carbon monoxide concentration, however, dropped to zero level after a short period and this period corresponded to the visually observed volatile evolution and combustion. After volatile evolution and combustion was complete, the oxygen concentration gradually increased and the carbon dioxide concentration gradually decreased as the residue carbon combustion went on.

Carbon monoxide concentration in the off gas, was found to vary over a wide range, from 0.10 to 5% (by volume) decreasing with reduction in charge mass and bed temperature, but with increase in char particle size and superficial fluidizing velocity. Thus, the lowest concentration of carbon monoxide was recorded when the smallest batch charge (0.75g of char) of the largest size range 4 to 4.75mm of char was fed to the bed at the highest superficial fluidizing velocity (71cm/s). The qualitative study of volatile evolution, therefore, suggests that the best conditions for burning the maximum proportion of the volatiles within the bed when fuelled at a fixed mass per unit time is to feed with large local particles rather than small because of the slower release of volatiles.

The cine film referred to on page 79 of Section 5.3 also demonstrated the volatile evolution and combustion as described.

As distinct from the char containing about 27% volatile matter used above, experiments with high volatile bituminous coal (about 48% volatile matter) about 25 - 30mm in size showed that volatile evolution and combustion continued for a much longer period (about 3 minutes) even though the large particle shattered into 3 to 5 fragments shortly after being dropped into the bed.

Andrei[88] and *Andrei, Sarofim & Beer*[89] also observed flame with evolution and combustion of volatiles for 4 - 13s while burning coal, 1.85 - 3mm in size in a fluidized bed.

The volatile evolution period for large size, high volatile coals is thus not instanteous and depends on char particle size, the charge mass, the bed temperature and superficial fluidizing velocity (amount of oxygen supplied per unit time). This needs to be considered when designing a fluidized bed combustor in which high volatile coals are to be burnt to avoid excessive free board zone combustion. The designer would have to decide whether to use a deeper bed, under bed feeding, injection of secondary air etc.

5.4.4 Elutriation

It is generally accepted that elutriation of fuel particles of a given size occurs when the local gas velocity exceeds the terminal velocity of such particles. This condition occurs when a large fuel particle has burnt down to a sufficiently small size and/or when the fuel feed contains fine particles. During the present combustion experiments, elutriation was found to be insigificant with all the sizes of char

particles at the lower superficial fluidizing velocity (27 cm/s). However, at a superficial fluidizing velocity of 71 cm/s, some elutriation from the bed occurred with smaller size ranges, but elutriation was again insignificant with larger size ranges. The mass of a char particle is proportional to the cube of its diameter, thus a larger fraction of mass burns before a larger char particle reaches elutriable size and so loss by elutriation becomes insignificant. The present results thus supported the contention of *Highley et al*[90] and *Gibbs & Hedley*[91] that high combustion efficiency could be achieved without much elutriation by feeding large size coal particles to the bed instead of crushed coal. This avoids the need for a carbon burn-up cell or for recycling the relatively small amount of fines elutriated or deep beds with under bed feedings.

5.4.5. Burning Char Particle Temperature

Visual observation of the bed during combustion of the char particles showed that under the same bed design and operating conditions, the char particles of smaller size ranges fed to the bed appeared brighter than those of larger size range ones. Also, the burning char particles appeared brighter as they burnt down to smaller sizes. A colour cine film and colour slides taken during the combustion experiments supported these observations which is available from Dr. J. R. Howard of Mechanical Engineering Department, University of Aston in Birmingham, U.K. The mass of char particle is proportional to the cube of its diameter; thus as it burns to a smaller size, a greater portion of carbon is burnt. Hence use of larger sizes of char particles would help to keep the burning particles temperature to a lower value. This has important effect on

the reduction of problem of ash fusion and evolution of oxides of nitrogen from inherent ash and nitrogen bound in coal particles.

CHAPTER SIX

GENERAL DISCUSSION ON PRESENT EXPERIMENTAL FINDINGS

6.1 The Relevant Model of Combustion of Carbon in Fluidized Beds

In Chapter 3 of this thesis the three possible models of combustion of carbon, developed through investigations of previous research workers were described and their applicability to fluidized bed combustion situations was examined in the light of the published work available on the study of combustion of carbon in fluidized beds. Model III (Section 3.2.3) appeared to be appropriate under fluidized bed combustion conditions. This model is discussed further in the light of the new experimental findings reported in this thesis.

It was discussed in Chapter 3 that Model III is appropriate for moderate carbon particle surface temperature ($< 1000\ ^{o}C$).

Table 4.1 showed that in a fluidized bed combustor fed continuously with anthracite coal particles, the temperature of a burning electrode carbon particle in the bed was less than 1000 ^{o}C and in general not greatly in excess of the bed temperature (see last two columns of Table 4.1). It should be noted that the local oxygen concentration in the bed would be lower due to the presence of a large number of burning anthracite coal particles which would reduce the burning rate and therefore

the rate of heat release from each burning carbon particle. It is expected that the heat transfer coefficient between the burning carbon particle and the bed is not affected significantly by the lowering of the local oxygen concentration. Therefore, the temperature difference between a burning carbon particle and the bed would be lower under such conditions. *Zabrodsky & Parnas*[112] estimated analytically burning carbon particle temperatures assuming continuous fluidized bed combustion condition at low excess air and found that the superheat of the burning carbon particle was small.

Single electrode carbon particle burning rate data reported in Chapter 4 of this thesis showed that forced convection played an important part in transferring oxygen to the burning carbon particle surface.

Thus both particle temperature and burning rate data reported in Chapter 4 of this thesis raises doubt about the applicability of Model II under fluidized bed combustion conditions explored. *Beér*[95] recently reported that *Song & Sarofim's*[96] analysis of *Avedesian & Davidson's*[77] results in the light of reported results of kinetics of carbon-carbon dioxide reactions by *Wu*[97] argued strongly against the applicability of model II to *Avedesian & Davidson's*[77] experimental conditions. *Ross*[106] reported that more recent work at the Department of Chemical Engineering, the University of Cambridge, England indicated that for larger carbon particles (> 3mm) the oxidation of carbon monoxide which is the primary product at the surface, takes place very near to the surface and for all practical purposes it may be assumed that carbon is oxidized to carbon dioxide essentially at the surface.

Andrei[88] reported that experiments by *Ayling, Mulcahy & Smith*[116] and *Smith*[117] suggested that only an exothermic reaction at the carbon surface could provide the sufficient rate of energy release to maintain the particle surface temperature in excess over that of the surrounding medium. *Basu, Brought & Elliott*[80] also reached similar conclusions from the results of their modelling work.

In an attempt to resolve the argument about the existence or otherwise of a high temperature reaction zone surrounding the burning carbon particle, a simple experiment was carred out with an electrode carbon particle, 12mm in diameter, having a mineral insulated stainless steel sheathed chromel-alumel thermocouple junction at the outer surface. The electrode carbon particle was burnt in an alumina bed (static bed depth, 100mm) at 900 ^{o}C, fluidized with air at a superficial fluidizing velocity of 1.5 m/s. The temperature indicated by the thermocouple junction, initially located at the burning carbon particle surface was continuously recorded as shown in Figure 6.1. This record suggests that a high temperature reaction zone surrounding the burning carbon particle does not exist which argues against the premises of *Avedesian & Davidson*[77].

Thus from present experimental finding it is evident that for larger carbon particles and higher superficial fluidizing velocities expected to be met in industrial fluidized bed combustors, Model III is the most appropriate model of combustion of carbon. In addition carbon monoxide, which is the primary product of combustion at the carbon surface, burns very near to the surface so that it may be assumed that the conversion of carbon to carbon dioxide takes place essentially at the surface.

6.2 Proposals for Predicting Single Carbon Particle Burning Rates in Shallow Fluidized Beds

These proposals modify the equation 4.6 due to *Ross*[106] and take into account the effect of forced convection.

Burning rate data reported in Part A and Part B of Chapter 4 in this thesis indicated that for larger carbon particles (> about 3mm) and higher superficial fluidizing velocities, burning rates predicted by the model of *Avedesian & Davidson*[77] and that of *Basu, Broughton & Elliott*[80] were substantially lower. These models were based upon the assumptions that burning carbon particles burn in the relatively stagnant particulate phase of the fluidized bed and mass transfer to the burning particles are limited by molecular diffusion only. These models were tested at conditions where small carbon particles were burnt at low superficial fluidizing velocities. These predictions were in good agreement with experimental results. But these models were inusfficient to explain the present experimental data obtained with large sizes of carbon particles at high superficial fluidizing velocities. Modification of the existing single particle burning rate models, is therefore, necessary to predict burning rates under such conditions.

No general correlation was available which could be applied to calculate mass transfer to burning carbon particles under present experimental conditions[118-120]. However, *Field et al*[55] discussed mass transfer between a gas and a particle in relative motion and suggested the use of *Rowe, Claxton & Lewis's*[121] correlation for

for Sherwood Number which is given by equation (6.1) below,

$$Sh = 2 + 0.69\ Re^{\frac{1}{2}}\ Sc^{\frac{1}{3}} \qquad \ldots (6.1)$$

The above correlation was presented by *Rowe, Claxton & Lewis*[121] from experimental study of mass transfer between air and spherical particles, 12.5 - 37.5mm in size (½ - 1½ inch) covering a range of Reynold's Number, $20 < Re < 2000$.

It was found that the modified single particle burning rate model of *Avedesian & Davidson*[77] (suggested by *Ross*[106]), see equation (4.6)) with Sherwood Number calculated from the correlation of *Rowe, Claxton & Lewis* (see equation (6.1)) using superficial fluidizing velocity for the Reynolds Number predicted burning rates in reasonable agreement with experimental data. These are shown in Figures 6.2 to 6.7. From these figures it is found that experimental burning rates at 800 ^{o}C were lower than the predictions of the proposed model. This suggested that chemical kinetics was limiting the burning rates. However, at 900 ^{o}C, the experimental burning rates were found much closer to the values predicted by the proposed model and thus indicated the mass transfer controlled combustion. However, some of the burning rate data reported in Part A of Chapter 4, were found to be higher than the predictions of the proposed model. This suggested that the burning carbon particles approached velocities higher than the superfical fluidizing velocity under the shallow bed conditions used for Part A experiments. It was not unlikely for the burning carbon particles to approach the bubble velocities (which is higher than the superficial fluidizing velocities) and so explain such results.

6.3 Overall Resistance to Combustion of Single Carbon Particles in Shallow Fluidized Beds: Relative Importance of Kinetic and Mass Transfer Resistances

In Chapter 3 of this thesis (see Section 3.3), burning rate of a single carbon particle was presented by equation (3.2) which was the familiar reciprocal resistance in series expression for burning rate containing resistances due to both chemical kinetics and mass transfer effects as shown below:

$$-\frac{dm}{dt} = 12\ \phi\ \pi\ d^2 \left(\frac{1}{\frac{1}{k_g} + \frac{1}{k_s}} \right) \quad c_p \qquad \ldots (3.2)$$

The overall resistance to combustion, $\frac{1}{K}$, may, therefore, be expressed by equation (6.2) as shown below:

$$\frac{1}{K} = \frac{1}{k_g} + \frac{1}{k_s} \qquad \ldots (6.2)$$

where $\frac{1}{k_g}$ and $\frac{1}{k_s}$ are individual resistances to combustion due to mass transfer and chemical kinetics respectively.

In Section 6.1, it has already been discussed that for larger carbon particles (> about 3 mm), the oxidation of carbon monoxide, which is the primary product of combustion at the carbon surface, takes place very close to the surface and for all practical purposes it may be assumed that carbon is oxidized to carbon dioxide essentially at the surface. Under the above conditions the value of mechanism factor (ϕ) becomes equal to 1 and with the help of equation (6.2) equation (3.2) may be written in the form shown by equation (6.3)

below:

$$-\frac{dm}{dt} = 12\ \pi\ d^2\ K\ c_p \qquad \ldots\ (6.3)$$

where $\frac{1}{K}$ is the overall resistance to combustion. The overall resistance to combustion, $\frac{1}{K}$, is, therefore, given by equation (6.4) as follows:

$$\frac{1}{K} = \frac{12\ \pi\ d^2}{-\frac{dm}{dt}}\ c_p \qquad \ldots\ (6.4)$$

Equation (6.4) could, thus, be used to estimate the overall resistance to the combustion of single carbon particles described in Chapter 4 from the burning rate data reported there.

It is most important to have an idea of the relative influence of chemical kinetics and mass transfer on the overall resistance to combustion of carbon particles in fluidized beds under different bed design and operating conditions. Resistance due to chemical kinetics, $\frac{1}{k_s}$, is difficult to calculate directly with reasonable accuracy because of the uncertainties about the values of kinetic parameters such as activation energy,(E), the true order of reaction and the pre-exponential factors, (A), since all these vary with the type of the carbon particles and the conditions of combustion. In addition to this, the burning carbon particle surface temperature also varies widely under different bed design and operating conditions and makes it difficult to estimate kinetic resistance, $\frac{1}{k_s}$, directly.

On the other hand, it is possible to calculate the mass transfer resistance, $\frac{1}{k_g}$, directly with reasonable accuracy from the definition

of Sherwood Number if the Sherwood Number of a burning carbon particle could be predicted with reasonable accuracy. Sherwood Number of a burning carbon particle is defined by equation (6.5) as shown below:

$$Sh = \frac{k_g d}{D_G} \qquad \ldots (6.5)$$

Therefore, the mass transfer resistance to combustion may be expressed by equation (6.6) as follows:

$$\frac{1}{k_g} = \frac{d}{Sh\ D_G} \qquad \ldots (6.6)$$

Equation (6.6) could be used to estimate the resistance to combustion due to mass transfer. In section 6.2 of this thesis, equation (6.1) has been proposed for the estimation of Sherwood Number of a burning carbon particle where the Reynolds Number is based on the superficial fluidizing velocity at bed temperature. It was already discussed in Section 6.2 that use of Sherwood Number estimated on this basis in equation (4.6) predicted single carbon particle burning rates in good agreement with experimental burning rate data described in Chapter 4 of this thesis. Hence, use of Sherwood Number estimated from equation (6.1) on the above basis would estimate mass transfer resistance from equation (6.6) with reasonable accuracy.

Kinetic resistance to combustion, $\frac{1}{k_s}$, may be estimated from equation (6.7) as shown below when the overall resistance, $\frac{1}{K}$, and the mass transfer resistance, $\frac{1}{k_g}$, are estimated from equations (6.4) and (6.6) respectively. Thus,

$$\frac{1}{k_s} = \frac{1}{K} - \frac{1}{k_g} \qquad \ldots (6.7)$$

Table 6.1 shows the estimated values of overall resistance to combustion, $\frac{1}{K}$, (see equation (6.4)), for three different sizes of carbon particles, together with corresponding estimated values of mass transfer resistance, $\frac{1}{k_g}$, (see equation (6.6)) and kinetic resistance, $\frac{1}{k_s}$, (see equation (6.7)), for different fluidized bed design and operating conditions explored for Part A work of Chapter 4, while Table 6.2 shows values of such resistances for Part B work of Chapter 4.

From Table 6.1 it is found that both the overall resistance, $\frac{1}{K}$, and the mass transfer resistance, $\frac{1}{k_g}$, increase with the carbon particle size. Also the overall resistance varies over a wide range of $4.02 \frac{s}{m}$ to $14.88 \frac{s}{m}$, depending on the bed design and operating conditions. The overall resistance was found to decrease with increase in bed temperature, inert particle size and the superficial fluidizing velocity. In some cases (see Table 6.1), the mass transfer resistance was found to be greater than the overall resistance; this is physically inadmissible. This shows the error which can arise when Sherwood Number is calculated on the basis of superficial fluidizing velocity. Mass transfer rate, and hence burning rate, is sensitive to local gas velocity at the particle rather than the superficial fluidizing velocity which takes no account of voidage or localised disturbances.

Thus actual mass transfer resistance was less than the values calculated on the basis of superficial fluidizing velocity. From Table 6.1 it was found that kinetic resistance was more significant for smaller sizes of carbon particles. Also in some cases the kinetic resistance, $\frac{1}{k_s}$, calculated by this method, turned out to be negative,

due to the use of superficial velocity for calculating mass transfer resistance. However, the estimated values of kinetic resistances shown in Table 6.1 are an under-estimation of the kinetic resistance to combustion because the value of activation energy, E, of the combustion reaction, calculated from values of $\frac{1}{k_s}$ shown in Table 6.1 using equation (6.8) shown below:

$$k_s = A\, e^{-\frac{E}{RT_s}} \qquad \ldots (6.8)$$

together with the particle temperature data reported in Table 4.1 was either negative (for $\frac{1}{k_s}$ at 800 °C), or very low (for $\frac{1}{k_s}$ at 900 °C), both of which are physically inadmissible (see the calculation in Appendix D, Section D1).

On the other hand, if the kinetic resistance is assumed to be equal to the overall resistance, i.e. $\frac{1}{k_s} = \frac{1}{K}$, and activation energy is calculated on this basis (see Appendix D, Section D2), the values agree with commonly found values of activation energy reported by *Spalding*[122], e.g. E = 10,000 to 80,000 cal/mole ($4.2 - 33.5 \times 10^4 \frac{kJ}{k\ mol}$). It would thus appear again that the estimated mass transfer resistance is too high because the local gas velocity past the burning carbon particles is higher than the superficial fluidizing velocity used for calculating mass transfer resistance. Appendix E shows the effect of carbon particle velocity on the mass transfer resistance.

Table 6.2 suggests that the overall resistance to combustion is smaller in relatively deeper alumina beds where larger sizes of inert particles and higher superficial fluidizing velocities were used;

however, as was shown in Table 6.1, both the overall resistance and the mass transfer resistance increased with carbon particle size. Calculation of activation energy using equation (6.8), on the basis of measured particle temperature of data in Table 4.5 and estimated values of kinetic resistance of Table 6.2 again suggested that kinetic resistance was under-estimated (see Appendix D, Section D3).

The above analysis, therefore, clearly suggests that combustion of the single carbon particles under the experimental conditions described in Part A of Chapter 4 was mainly controlled by chemical kinetics. Some effect of mass transfer was, however, observed at 900 °C, especially with the largest size of inert particle used.

On the other hand, under experimental conditions used in Part B work of Chapter 4, at a bed temperature of 800 °C the combustion was mainly controlled by chemical kinetics. However, at a bed temperature of 900 °C, the burning rate data suggested more strongly that mass transfer by forced convection at superficial fluidizing velocity was controlling the combustion.

CHAPTER SEVEN

CONCLUSIONS

1. Combustion of large carbon particles (> 3 mm) in shallow fluidized beds at a bed temperature of 800 °C at high superficial fluidizing velocities is almost entirely controlled by chemical kinetics.

On the other hand, at a bed temperature of 900 °C, the rate of mass transfer of oxygen to the burning carbon particle surface influences the rate of combustion progressively as the size of the inert particles in the bed increases. With large size of inert particles, the burning carbon particle-to-bed heat transfer coefficient will be smaller than when small inert particles are used in the bed, consequently if the burning rate were unchanged, the carbon surface temperature would increase. This higher carbon surface temperature will increase the reaction rate until such time as the rate at which oxygen reaches the carbon surface is insufficient to sustain any further increase in burning rate.

2. In shallow fluidized beds operating at high superficial fluidizing velocities, the agitation within the bed created by bubbling action results in the relative velocity between the individual carbon particles and the fluidizing gas being generally higher although the complexity of particle motion means considerable fluctuation in relative velocity. However, it has been demonstrated that forced convection plays an

important role to transfer oxygen to the burning carbon particle surface and the extent has been quantified approximately by equation (6.1).

3. Oxygen reaches the burning carbon particle surface to oxidize carbon there and carbon monoxide, the primary product of combustion at the surface, is oxidized to carbon dioxide very near to the surface. Therefore, for all practical purposes, it may be assumed that carbon is oxidized to carbon dioxide essentially at the surface. No high temperature carbon monoxide reaction zone exists around burning carbon particles.

4. Proposals have been made to modify the existing models of combustion of a single carbon particle in fluidized beds so as to take into account the effect of forced convection on rate of mass transfer of oxygen and transport of carbon dioxide away from the burning carbon particle surface.

5. The proposals in 4. above have been tested by comparing the predictions of the modified models with experimental observations. Good agreement between predictions and experimental measurements of burning rates has been found.

6. Shallow fluidized bed design and operating conditions affect combustion of carbon particles substantially; burning rate increases with increase in bed temperature, inert particle size and superficial fluidizing velocity.

7. The presence of a large number of burning carbon particles in a continuously fed fluidized bed coal combustor reduces the local oxygen concentration in the bed. Burning rates and temperatures of individual carbon particles are, therefore, reduced significantly.

8. The manner in which burning rate varies with oxygen concentration in the fluidizing gas suggests that the combustion reaction of carbon with oxygen in fluidized beds is of the 'first order'.

9. Recycling a part of the products of combustion through the bed is likely to be a valuable technique for control of combustion within a fluidized bed combustor to meet fluctuating load demands.

10. Combustion of carbon particles in shallow fluidized beds is not affected by altering the static bed depth except for very shallow static bed depth (12.5 mm) in which burning rate increases significantly. Presence of a large number of small bubbles dispersed uniformly in such shallow beds creates good mixing and agitation within the bed and reduces the heat transfer coefficient between carbon particle-to-bed to cause such results.

11. In fluidized beds, in general larger carbon particles remain at lower surface temperatures compared to the smaller ones. The difference of temperature between the burning carbon particle and the bed varied over a wide range of 15-235 K, depending on the fluidized bed design and operating conditions. However, in a fluidized bed combustor fed continuously with coal, the temperature of the large coal particles is not expected to exceed 100 K in excess of bed temperature. This

has implications (a) in reducing the ash fusion problem with coals containing ash having low fusion temperature and (b) in reducing evolution of oxides of nitrogen from the nitrogen bound into the coal.

12. Burn-out times of char particles in shallow fluidized beds has been shown to be directly proportional to the initial size, d_i, of the particles rather than the square of the size, d_i^2, as suggested by previous workers[77].

13. Loss of unburnt carbon particles by elutriation is minimum when large size coal is fed to the bed. Thus with large size coal provisions for recycling the fines through the bed or burning them in a separate carbon burn-up cell may be avoided without affecting the combustion efficiency significantly. The cost of crushing coals would thus be avoided but removal of fines may offset this advantage.

14. Evolution of volatiles from high volatile coals is not instantaneous. In fact, the time of volative evolution increases with increase in size of the coal and it may take over a minute for a coal particle of about 25 mm size to give up all its volatile matter. It seems very difficult to ensure complete combustion of volatile matter within a shallow fluidized bed even if under-bed feeding is employed. Combustion of some volatile matter in the freeboard space is almost inevitable when burning high volatile coals.

Further the level of carbon monoxide in the products of combustion may be unacceptably high if coal is fed as a small number of large batches per unit time.

15. Bed expansion is considerable at high superficial fluidizing velocities and the expanded bed depth approaches about twice the static bed depth. Volumes of bubbles, therefore, occupy a significant portion of bed volumes under such conditions. This reduces the carbon-to-bed heat transfer coefficient and promotes forced convection of air surrounding the burning particle. Consequently the burning rate and carbon temperature are increased under such conditions.

CHAPTER EIGHT

RECOMMENDATIONS FOR FURTHER WORK

1. Detail models of combustion of coal in fluidized beds need to consider the effect of forced convection on the rate of mass transfer of oxygen to large coal particles (> 3 mm), especially in shallow fluidized beds at high superficial fluidizing velocities.

2. The proposals made for predicting burning rates of single carbon particles considering the effect of forced convection needs to be tested in larger and deeper beds.

3. Measurements of large burning coal particle temperatures in continuously fed fluidized bed coal combustors by some suitable techniques will be very helpful to further strengthen the validity of Model III for the mechanism of combustion.

4. Study of evolution of volatiles from high volatile coals and their subsequent combustion needs further work, both theoretically and experimentally to develop a complete model of combustion of coal in fluidized beds.

5. Study of carbon-carbon dioxide combustion kinetics in fluidized beds under different bed design and operating conditions will help to establish the mechanism of combustion firmly.

6. Use of recycled combustion products to control bed temperature should be studied.

7. The data that has been presented in this thesis should be used to develop a system for control of combustion in fluidized beds.

APPENDIX A

DETAILS OF INERT SAND PARTICLES

A1 Particle Density

Density of the inert sand particles used for the work reported in this thesis was experimentally determined with standard specific gravity bottles using n-heptane as the liquid. The following equation was used:

$$\rho_{inert} = \frac{(m_2-m_1)}{(m_2-m_1)-(m_3-m_4)} \rho_{n\text{-heptane}} \quad g/cm^3$$

where

m_1 = Mass of empty bottle, g

m_2 = Mass of bottle with sample of inert particles, g

m_3 = Mass of bottle with sample of inert particles and rest of n-heptane to fill it

m_4 = Mass of bottle with n-heptane to fill it

$\rho_{n\text{-heptane}}$ = Density of n-heptane, 0.683 g/cm^3

Mean density of sand particles = 2.63 g/cm^3

A2 Size Range and Mean Size

Sand particles used for the present work were sieved out into 3 different narrow size ranges using B.S. sieves. The size ranges with corresponding mean sizes are shown below

Size Range (μm)	Mean Size (μm)
-355 to +300	327.5
-600 to +500	550
-850 to +710	780

A3 Minimum Fluidizing Velocity

Minimum fluidizing velocity of the inert particles was calculated by using the equation shown below which was suggested by *Kunii & Levenspiel,* [118]

$$U_{mf} = \frac{d_p^2(\rho_s-\rho_f)g}{1650\mu} \qquad Re_p < 20$$

where

U_{mf} = Minimum fluidizing velocity, m/s

d_p = Mean size of inert particles, m

ρ_s = Density of inert particles, kg/m^3

ρ_f = Density of fluidizing gas, kg/m^3

g = Acceleration due to gravity, m/s

μ = Viscosity of fluidizing gas, kg/m-s

Re_p = Reynolds Number of inert particles, $\left(\frac{U_{mf}\, d_p \rho_f}{\mu}\right)$

At 900 ^oC

$$\rho_{f(air)} = 0.301 \text{ kg/m}^3$$

$$\mu_{(air)} = 4.5639 \times 10^{-5} \text{ kg/m-s}$$

Also

$$\rho_{s(sand)} = 2630 \text{ kg/m}^3$$

$$g = 9.80665 \text{ m/s}^2$$

Hence, the minimum fluidizing velocity (U_{mf}) of inert sand particles of mean size 327.5 μm, at a bed bed temperature of 900 ^oC is

$$U_{mf\ 327.5\ \mu m}\ (\text{at } 900\ ^{o}C) = -\frac{(327.5 \times 10^{-6})^{2}(2630-0.301)(9.80665)}{(1650)(4.5639 \times 10^{-5})}$$

$$= 0.0367\ \text{m/s}$$

Similarly,

$$U_{mf\ 550\ \mu m}\ (\text{at } 900\ ^{o}C) = 0.1036\ \text{m/s}$$

$$U_{mf\ 780\ \mu m}\ (\text{at } 900\ ^{o}C) = 0.2084\ \text{m/s}$$

APPENDIX B

DETAILS OF INERT ALUMINA PARTICLES

B.1 Particle Density

Density of inert alumina particles used for the work described in Part B, Chapter 4 of this thesis was determined in the similar way already described in Section A1 of Appendix A.

Mean density of alumina particles = 3.93 g/cm^3

B2 Size Range and Mean Size

Alumina particles used as the bed inert material were sieved out in the size range -1180 to +850 μm by using B.S. sieves. The mean size of the particles was determined by the procedure suggested by *Kunii & Levenspiel* [118] as shown below:

Size Range (μm)	Mean Size of range d'_p (μm)	Weight of sample in size range (g)	Weight fraction in size range x_i	$\left(\frac{x}{d'_p}\right)_i$
850-1000	925	457.50	0.4575	0.0004945
1000-1180	1090	542.50	0.5425	0.0004977

$$\Sigma \left(\frac{x}{d'_p}\right)_i = 0.0009922$$

$$\text{Mean size, } d_p = \frac{1}{\Sigma\left(\frac{x}{d'_p}\right)_i} = \frac{1}{0.0009922} = 1008 \text{ μm}$$

B3 Minimum Fluidizing Velocity

Minimum fluidizing velocity of the inert alumina particles was calculated by the similar method described in Section A3 of Appendix A.

U_{mf} (at 900 ^{o}C) = 0.51997 m/s
1008 μm

U_{mf} (at 800 ^{o}C) = 0.5483 m/s
1008 μm

APPENDIX C

DETAILS OF CHAR PARTICLES

Char particles used for the work described in Chapter 5 of this thesis was obtained from Coventry Homefire Works of National Smokeless Fuels Limited, Coventry, England. It was reported to have been prepared by carbonizing a blend of coals in the Fluidized Bed Process at about 420 ^{o}C. Typical analyses of coals making up the process blend are shown on the next page.

Coal	% in blend	Rank	Moisture %	Volatile Matter (as received) %	Ash (as received) %	Sulphur (as received) %	Swelling Number
Markham	30	702	13.4	31.5	4.0	1.32	2½
Warsop	30	802	11.0	34.9	4.3	1.64	2½
Gedling	10	902	15.0	33.5	4.0	1.23	1
Blidworth	10	702	9.7	34.8	3.7	0.95	3
Teversal	5	802	11.2	34.5	3.1	1.37	2
Langwirth	5	802	12.3	33.5	4.5	1.79	2½
Recycled char	10	-	25.0	18.0	4.1	1.00	-
Char ex Fluidizer	-	-	nil	23.6	5.5	1.30	-

N.B. The above figures are typical. Both the analysis and % in blend are variable.

C1 Proximate Analysis

Typical proximate analysis of the char sample, performed in the laboratory is shown below

Moisture	:	1.05%
Ash	:	4.37%
Volatile Matter	:	27.09%
Fixed Carbon	:	67.49%

C2 Particle Density

Density of the char particles was determined in the laboratory in the similar way already described in Section A1 of Appendix A.

Mean density of char particles : 0.757 g/cm^3

C3 Size Range and Mean Size

Char particles were sieved into 6 different narrow size ranges by using B.S. sieves. The size ranges and the corresponding mean sizes are shown below

Size Range mm	Mean Size mm
-2.00 to +1.68	1.840
-2.40 to +2.00	2.200
-2.80 to +2.40	2.600
-3.35 to +2.80	3.075
-4.00 to +3.35	3.675
-4.75 to +4.00	4.375

C4 Charge Mass

3g of char for fixed mass-variable size experiments

0.75, 1.5, 2.25, 3 and 3.75 g of char for fixed size - variable mass experiments.

APPENDIX D

CALCULATION OF ACTIVATION ENERGY

In Chapter 6 of this thesis the first order reaction rate constant at the burning carbon particle surface, k_s was expressed by equation (6.8) which is written below

$$k_s = A\, e^{-\frac{E}{RT_s}} \qquad (6.8)$$

The kinetic resistance to combustion, $\frac{1}{k_s}$, is therefore, given by equation (D1) as follows:

$$\frac{1}{k_s} = \frac{e}{A}^{\frac{E}{RT_s}} \qquad (D1)$$

The activation energy of combustion, E, can be calculated from equation (D1) using any two values of $\frac{1}{k_s}$ from Table 6.1 (or Table 6.2) and corresponding values of T_s from Table 4.1 (or Table 4.5). The calculation of activation energy for a number of cases is given below.

SECTION D1

Case 1: Experimental conditions

Bed temperature :	800°C
Inert sand particle size:	327.5 μm
Static bed depth:	30 mm
Superficial gluidizing velocity: (at bed temp.)	25 cm/s

Under the above experimental conditions the values of $1/k_s$ (from Table 6.1) and the values of T_s (from Table 4.1) for 6 mm and 12 mm carbon particles are

1. 6 mm: $\frac{1}{k_{s_1}} = 5.76 \frac{s}{m}$ $T_{s_1} = 1143$ K

2. 12 mm: $\frac{1}{k_{s_2}} = 1.34 \frac{s}{m}$; $T_{s_2} = 1123$ K

Therefore

$$(1/k_{s_1})/(1/k_{s_2}) = e^{(E/R)(1/T_{s_1} - 1/T_{s_2})}$$

or $$5.76/1.34 = e^{(E/R)(1/1143 - 1/1123)}$$

or $$4.2985 = e^{(E/R)(-1.55 \times 10^{-5})}$$

Taking "Ln" on both sides,

$$1.45827 = -(E/R) \times 1.55 \times 10^{-5}$$

or $$(E/R) = -0.94082 \times 10^{5}$$

or $$E = -0.94082 \times 10^{5} \times R$$

$$= -0.94082 \times 10^{5} \times 1.986$$

$$= -186847 \text{ cal/mol.}$$

Case II Experimental conditions

Bed temperature:	900°C
Inert sand particle size:	327.5 μm
Static bed depth:	30 mm
Superficial fluidizing velocity (at bed temp.)	(1) 27 cm/s (2) 71 cm/s

Under the above experimental conditions, the values of $1/k_s$ (from Table 6.1) and T_s (from Table 4.1) for a 6 mm carbon particle are

1. Superficial fluidizing velocity: 27 cm/s

$$1/k_{s_1} = 2.80 \frac{S}{m} ; \qquad T_{s_1} = 1253 \text{ K}$$

2. Superficial fluidizing velocity: 71 cm/s

$$1/k_{s_2} = 2.76 \frac{S}{m} ; \qquad T_{s_2} = 1303 \text{ K}$$

Hence

$$(1/k_{s_1})/(1/k_{s_2}) = e^{(E/R)(1/T_{s_1} - 1/T_{s_2})}$$

or $$2.80/2.76 = e^{(E/R)(1/1253 - 1/1303)}$$

or $$1.01449 = e^{(E/R)(3.06 \times 10^{-5})}$$

Taking "Ln" on both sides

$$0.01439 = (E/R)(3.06 \times 10^{-5})$$

or $$E/R = 0.0047 \times 10^5$$

or $$E = 0.0047 \times 10^5 \times R$$

$$= 0.0047 \times 10^5 \times 1.986$$

$$= 933 \text{ cal/mol}.$$

SECTION D2

In this section, the kinetic resistance to combustion ($1/k_s$) has been assumed to be equal to the overall resistance to combustion ($1/k_s = 1/K$) for calculation of activation energy.

Case I:

Experimental conditions are identical to those in Case I of the previous section (Section D1)

Under the above experimental conditions the values of 1/K (from Table 6.1) and T_s (from Table 4.1) for 6 and 12 mm carbon particles are

1. 6 mm: $1/K_1 = 13.97 \frac{s}{m}$; $T_{s_1} = 1143$
2. 12 mm: $1/K_2 = 14.88 \frac{s}{m}$; $T_{s_2} = 1123$

Assuming the kinetic resistance to be equal to the overall resistance, i.e. $1/k_s = 1/K$

$$(1/K_2)/(1/K_1) = (1/k_{s_2})/(1/k_{s_1}) = e^{(E/R)(1/T_{s_2} - 1/T_{s_1})}$$

or $$14.88/13.97 = e^{(E/R)(1/1123 - 1/1143)}$$

or $$1.06514 = e^{(E/R)(1.55 \times 10^{-5})}$$

Taking "Ln" on both sides

$$0.0631 = (E/R)(1.55 \times 10^{-5})$$

or $$E/R = 0.04071 \times 10^5$$

or $$E = 0.04071 \times 10^5 \times R$$

$$= 0.04071 \times 10^5 \times 1.986$$

$$= 8085 \text{ cal/mol.}$$

Case II:

Experimental conditions are identical to those in Case II of the previous section (Section D1).

Under the above experimental conditions, the values of 1/K (from Table 6.1) and T_s (from Table 4.1) for a 6 mm carbon particle are

1. Superficial fluidizing velocity: 27 cm/s.

$$1/K_1 = 9.96 \frac{s}{m}; \qquad T_{s_1} = 1253 \text{ K}$$

2. Superficial fluidizing velocity: 71 cm/s

$$1/K_2 = 8.21 \frac{s}{m}; \qquad T_{s_2} = 1303 \text{ K}$$

Assuming the kinetic resistance to be equal to the overall resistance, i.e. $1/k_s = 1/K$,

$$(1/K_1)/(1/K_2) = (1/k_{s_1})/(1/k_{s_2}) = e^{(E/R)(1/T_{s_1} - 1/T_{s_2})}$$

$$\text{or} \quad \frac{9.96}{8.21} = e^{(E/R)(3.06 \times 10^{-5})}$$

$$\text{or} \quad 1.21315 = e^{(E/R)(3.06 \times 10^{-5})}$$

Taking "Ln" on both sides,

$$0.19322 = (E/R)(3.06 \times 10^{-5})$$

$$\text{or} \quad E = 0.06314 \times 10^5 \times R$$

$$= 0.6314 \times 10^5 \times 1.986$$

$$= 12540 \text{ cal/mol.}$$

SECTION D3

Experimental conditions:

Bed temperature:	800°C
Inert alumina particle size:	1008 μm
Static bed depth:	100 mm
Superficial fluidizing velocity (at bed temp.):	(1) 1.37 m/s (2) 2.50 m/s

Under the above experimental conditions, the values of $1/k_s$ (from Table 6.2) and T_s (from Table 4.5) for 18 mm carbon particles are

1. Superficial velocity: 1.37 m/s

$$1/k_{s_1} = 1.53 \frac{s}{m}; \qquad T_{s_1} = 1293 \text{ K}$$

2. Superficial fluidizing velocity: 2.5 ,/s

$$1/k_{s_2} = 3.35 \frac{s}{m}; \qquad T_{s_2} = 1308\text{K}$$

Hence

$$(1/k_{s_2})/(1/k_{s_1}) = e^{(E/R)(1/T_{s_2} - 1/T_{s_1})}$$

$$\text{or} \quad 3.35/1.53 = e^{(E/R)(1/1308 - 1/1293)}$$

$$\text{or} \quad 2.18954 = e^{(E/R)(-8.8 \times 10^{-6})}$$

Taking "Ln" on both sides,

$$0.78369 = -(E/R)(8.8 \times 10^{-6})$$

$$\text{or} \quad E/R = -0.08906 \times 10^{6}$$

$$\text{or} \quad E = -0.08906 \times 10^{6} \times R$$

$$= -0.08906 \times 10^{6} \times 1.986$$

$$E = -176864 \text{ cal/mol.}$$

APPENDIX E

EFFECT OF CARBON PARTICLE VELOCITY ON MASS TRANSFER RESISTANCE

In Chapter 6 of this thesis, the mass transfer resistance, $1/k_g$ was expressed by equation (6.6) as shown below:

$$\frac{1}{k_g} = \frac{d}{Sh\ D_G} \qquad (6.6)$$

Table 6.1 listed values of mass transfer resistance estimated from equation (6.6) in which the Sherwood Number of burning carbon particles was calculated from the *Rowe, Claxton & Lewis*[121] correlation as shown below by equation (6.1)

$$Sh = 2 + 0.69\ R_e^{1/2}\ S_c^{1/3} \qquad (6.1)$$

N.B.

Superficial fluidizing velocity was used as the carbon particle velocity to estimate Reynolds Number in the above equation.

The effect of increase in carbon particle velocity to 1.5 and 2 times the superficial fluidizing velocity on mass transfer resistance at a bed temperature of 900°C is shown in the table below:

Carbon Particle

Size d (mm)	Velocity U (cm/s)	Reynolds Number $Re = \frac{Ud\rho_f}{\mu}$	Sherwood Number $Sh = 2 + 0.69\ Re^{1/2}\ Sc^{1/3}$	Estimated mass transfer resistance, $\frac{1}{k_g} = \frac{d}{Sh\ D_G}$ $(\frac{s}{m})$
3	71	14.048	4.328	3.333
	1.5 x 71	21.072	4.851	2.973
	2 x 71	28.096	5.292	2.726
6	71	28.096	5.292	5.451
	1.5 x 71	42.143	6.031	4.783
	2 x 71	56.191	6.655	4.334
12	71	56.191	6.655	8.669
	1.5 x 71	84.287	7.701	7.491
	2 x 71	112.382	8.583	6.721

APPENDIX F

ESTIMATION OF THE BINARY MOLECULAR DIFFUSION COEFFICIENT

Kanury[103] suggested the following equation for estimating the binary molecular diffusion coefficient D_G, which was based on Lennard and Jones force potential and Chapman and Enskog correction

$$D_G = D_{AB} = D_{BA} = 0.2628 \frac{\sqrt{\frac{T^3}{2}\left(\frac{1}{M_A} + \frac{1}{M_B}\right)}}{P\ \sigma_{AB}^2\ \Omega_D} \quad \frac{mm^2}{s} \qquad \ldots (F1)$$

where T is the temperature in degrees Kelvin, K

M_A and M_B are the molecular weights of the gas species A and B

P is the pressure in atmospheres, atm

σ_{AB} is the Lennard and Jones potential force constant

Ω_D is the collision integral

$$\sigma_{AB} = \frac{\sigma_A + \sigma_B}{2} \qquad \ldots (F2)$$

where σ_A and σ_B are molecular diameters of gases A and B in Angstrom units (1 $\mathring{A}$ = 10^{-8} cm).

The collision integral Ω_D is a tabulated function of $K'T/\varepsilon_{AB}$ where K' is Boltzman's constant. ε_A/K' and ε_B/K' are molecular constants of gases A and B and ε_{AB} is given by:

$$\varepsilon_{AB} = (\varepsilon_A\ \varepsilon_B)^{\frac{1}{2}} \qquad \ldots (F3)$$

Let us consider oxygen diffuses through air at 900 °C and one atmosphere pressure.

From Table 3.3 on page 53 of Kanury's book:[103]

For oxygen: $\sigma_A = 3.433$ Å ; $\frac{\varepsilon_A}{K'} = 113$ K

For air: $\sigma_B = 3.617$ Å ; $\frac{\varepsilon_B}{K'} = 97$ K

From equations (B2) and (B3):

$$\sigma_{AB} = \frac{3.433 + 3.617}{2} = 3.525 \text{ Å}$$

$$\frac{\varepsilon_{AB}}{K'} = \sqrt{(113)(97)} = 104.7 \text{ K}$$

$$\frac{K'T}{\varepsilon_{AB}} = \frac{1173}{104.7} = 11.2$$

For $\frac{K'T}{\varepsilon_{AB}} = 11.2$, $\Omega_D = 0.733$ from Table 3.2 on page 52 of Kanury's[103] book. Substituting these values into equation (F1):

$$D_G = \frac{0.2628\sqrt{\left(\frac{1173}{2}\right)^3 \left(\frac{1}{32} + \frac{1}{28.97}\right)}}{(1)(3.535)^2(0.733)}$$

$$= 208 \text{ mm}^2/\text{s}$$

This value of D_G was used for calculating predicted burning rates in Chapter 4.

At any other temperature, T:

$$D_G = 208\left(\frac{T}{1173}\right)^{3/2} \times \frac{0.733}{\Omega_D \text{ at } T} \quad \frac{\text{mm}^2}{\text{s}} \qquad \ldots \text{(F4)}$$

Thus for oxygen diffusing through air at 800 °C,

$$D_G = 178 \frac{mm^2}{s}$$

REFERENCES

1. Hawthorne, Sir W., Energy : a renewed challenge for engineers. Proceedings of the Institution of Mechanical Engineers, 1975 Paper 52/75.

2. Ezra, Sir D., Coal Research 2000, Robens Coal Science Lecture, Institution of Electrical Engineers, London, U.K., October, 1978.

3. Elliott, D.E., Preliminary work on fluid bed boilers. Proceedings of a symposium on 'Combustion of coal in fluidized beds', Coal Research Establishment, Stoke Orchard, Cheltenham, Gloucester, England, May 23, 1968.

4. Skinner, DG., The fluidized combustion of coal, M & B Monograph CE/3, Mills & Boon Limited, London, U.K., 1971.

5. Ehrlich, S., History of the development of fluidized-bed boiler, Proceedings of the Fourth International Conference on Fluidized Bed Combustion, McLean, Virginia, U.S.A., December 9-11, 1975, pp.15-20.

6. Gibson, J., Present status of fluidized bed combustion, Applied Energy, Vol.3, No.2., April, 1977, pp.87-99.

7. Wright, S.J., Combustion of coal in fluidized beds. Physics in Technology, November, 1977 pp. 244-248.

8. Thurlow, G.G., The combustion of coal in fluidized beds, Proceedings of The Institution of Mechanical Engineers, Vol.192, No.15, 1978 pp. 145-156.

9. Howard, J.R., Fluidized-bed combustion and heat treatment, Engineering, December, 1978.

10. Kaye, W.G., New developments in coal burning equipment, Solid Fuel, January 28, 1976, pp.13-20.

11. Anson, D., Fluidized bed combustion of coal for power generation. Progress of Energy Combustion Science, Vol. 2, 1976 pp.61-82.

12. Highley, J., Fluidized bed combustion, Lecture presented to Northern Ireland Branch of the District Heating Association, May 5, 1977.

13. Finlayson, P. & Ballantyne, J., Fluidized bed combustion for steam raising and power generation, Eurochem Conference - Chemical Engineering in a Hostile World, National Exhibition Centre, Birmingham, U.K., June 20 - 24, 1977, paper 12.

14. Highley, J., Fluidized bed combustion, Lecture presented to Sheffield University, Sheffield, U.K., April 14, 1978.

15. Mesko, J.E., Coal combustion in a limestone bed, Chemical Engineering Progress, August, 1978, pp.99-102.

16. McKenzie, E.C., Burning coal in fluidized beds, Chemical Engineering, Vol. 85, No.18, August 14, 1978, pp.116-127.

17. Cooke, M.J. & Rogers, E.A., Investigation of fireside corrosion in fluidized combustion systems, Proceedings of the Institute of Fuel Symposium Series No.1 : Fluidized Combustion, Imperial College, London, U.K., September 16-17, 1975, paper B6.

18. Caplin, P.B., A fluid bed boiler, Proceedings of Conference on Energy Utilisation Today and Tommorrow, Combustion Engineering Association, 1977.

19. Rao, C.S.R., Fluidized-bed combustion technology - a review, Combustion Science and Technology, Vol.16, 1977, pp.215-227.

20. Proceedings of the First International Conference on Fluidized-Bed Combustion, Hueston Woods, Ohio, U.S.A., 1968.

21. Proceedings of the Second International Conference on Fluidized-Bed Combustion, Houston Woods, Ohio, U.S.A., 1970

22. Proceedings of the Third Internatational Conference on Fluidized-Bed Combustion, Hueston Woods, Ohio, U.S.A., October 29 - November 1, 1973.

23. Proceedings of the Fourth International Conference on Fluidized-Bed Combustion, McLean, Virginia, U.S.A., December 9-11, 1975.

24. Proceedings of the Fifth International Conference on Fluidized-Bed Combustion, Washington D.C., U.S.A., December 12-14, 1977.

25. Proceedings of the Institute of Fuel Symposium Series No 1.: Fluidized Combustion, Imperial College, London, U.K., September 16-17, 1975.

26. Fluidization : Proceedings of the Second Engineering Foundation Conference, Trinity College, Cambridge, England, April 2-6, 1978, Cambridge University Press, Cambridge, England, 1978.

27. Virr, M.J., Industrial coal fired fluidized bed boilers and waste heat boilers. Proceedings of the Fifth International Conference on Fluidized-Bed Combustion, Washington D.C., U.S.A., December 12-14, 1977.

28. Butler, P., Shell boilers will burn cheap and nasty fuels on a fluid bed. The Engineer, July 13, 1978 pp. 53-54.

29. Butler, P., A firm outlook for fluid beds aimed at the U.S. market. The Engineer, December 14/21 , 1978 pp. 32-37.

30. Gibson, J. & Highley, J., Fluidized bed combustion for industrial applications, Paper presented at VDI Fluidized Combustion Conference, Dusseldorf, Federal German Republic, November, 1978.

31 McKenzie, E.C., Fluidized bed firing in boilers, Space Heating and Air Conditioning Journal, March 1977, pp.28-32.

32. Butler, P., Fluid bed is proving a hot number at 80% efficiency. The Engineer, September 7, 1978, pp.56-57,106.

33. Pritchard, A.B. & Caplin, P.B., Private Communication, Energy Equipment Limited, England.

34. Grainger, L., The International Energy Agency, Colliery Guardian, Vol.224, August 1976, pp.405-408.

35. Nutkis, M.S., Operation and performance of the pressurized FBC miniplant. Proceedings of the Fourth International Conference on Fluidized Bed Combustion, McLean, Virginia, U.S.A., December 9-11, 1975, pp.221-238.

36. Roberts, A.G., Stanton, J.E., Wilkins, D.M., Beacham, B. & Hoy, H.R., Fluidized combustion of coal and oil under pressure, Proceedings of the Institute of Fuel Symposium Series No. 1 : Fluidized Combustion, Imperial College, London, U.K., September 16-17, 1975, Paper D4.

37. Keairns, D.L., Hamm, J.R. & Archer, D.H., Design of a pressurised fluidized bed boiler plant. American Institute of Chemical Engineers Symposium Series, Vol.68, No.126, 1972 pp.267-275.

38. Chalchal, S., Sheehan, T.V. & Steinberg, M., Coal combustion and desulpherization in a rotating fluidized bed reactor. Brookhaven National Laboratory, U.S.A., Report 19308, October, 1974.

39. Broughton, J. & Elliott, D.E., Heat transfer and combustion in centrifugal fluidized beds. Institution of Chemical Engineers Symposium Series No. 43, Harrogate, England, June 1975.

40. Levy, E.K., Dodge, C. & Chen, J., Parametric analysis of a centrifugal fluidized bed coal combustor, Paper presented at the American Society of Mechanical Engineers - American Institute of Chemical Engineers Heat Transfer Conference, St. Louis, Mo., August 9-11, 1976.

41. Metcalfe, C.I. & Howard, J. R., Fluidization and gas combustion in a rotating fluidized bed, Applied energy, Vol.3, No.2, April 1977, pp.65-73.

42. Shakespeare, W.J., Levy, E.K., Chen, J.C. & Kadambi, V. Analysis of power cycles with centrifugal fluidized bed coal combustion, Paper presented at the Intersociety Energy Conversion Engineering Conference, Washington D.C., August 28, 1977.

43. Metcalfe, C. I., & Howard, J.R., Combustion experiments within a rotating fluidized bed, Proceedings of the Fifth International Conference on Fluidized Bed Combustion, Washington D.C., December 12-14, 1977.

44. Levy, E.K., Martin, N.W. & Chen, J.C., Centrifugal fluidized bed combustion., Proceedings of the Fifth International Conference on Fluidized-Bed Combustion, Washington D.C., December 12-14, 1977.

45. Metcalfe, C.I. & Howard, J.R., Towards higher intensity combustion rotating fluidized beds, Fluidization : Proceedings of the Second Engineering Foundation Conference, Trinity College, Cambridge, England, April 2-6, 1978, Cambridge University Press, Cambridge, England, 1978, pp.276-279.

46. Demircan, N., Gibbs, B.M., Swithenbank, J. & Taylor, D.S., Rotating fluidized bed combustor, Fluidization : Proceedings of the Second Engineering Foundation Conference, Trinity College, Cambridge, England April 2-6, 1978, Cambridge University Press, Cambridge, England, 1978, pp.270-275.

47. Nusselt, W., Z. Ver. deut.Ing., Vol.68, 1924, pp.124-128.

48. Burke, S.P. & Schuman, T.E.W., Industrial and Engineering Chemistry, Vol.23, 1931, p.406.

49. Burke, S.P. & Schuman, T.E.W., Proceedings of the Third International Conference on Bituminous Coal, Vol.2, 1931 pp.485-509.

50. Lewis, W.K., Industrial and Engineering Chemistry, Vol.15, 1923, p.502.

51. Wentzel, Fuel, Vol.11, 1932, pp.177-196 and 222-228.

52. Tu., C.M., Davis, H. & Hottel, H.C., Combustion rate of carbon, Industrial and Engineering Chemistry, Vol.26, No.7, 1934 pp.749-757.

53. Arthur, J.R, Reactions between carbon and oxygen, Transaction of the Faraday Society, Vol.47, 1951, pp.164-178.

54. Smith, D.F. & Gudmundsen, A., Industrial and Engineering Chemistry, Vol.23, 1931, pp.277-285.

55. Field, M.A., Gill, D.W., Morgan, B.B. & Hawksley, P.G.W., Combustion of pulverized coal, The British Coal Utilization Research Association, Leatherhead, Surrey, England, 1967.

56. Dubinsky, M.S., Thesis, Massachusetts Institute of Technology, 1932.

57. Parker, A.S. & Hottel, H.C., Combustion rate of carbon, Industrial and Engineering Chemistry, Vol.28, No.11, 1936, pp.1334-1341.

58. Wicke, E. & Wurzbacher G., Concentration distributions in front of a carbon surface burning in a stream of oxygen, International Journal of Heat and Mass Transfer, Vol.5, 1962, pp.277-289.

59. Hougen, O.A. & Watson, K.M., Chemical Process Principles, Kinetic and Catalysis, Part 3, John Wiley & Sons, New York, 1947.

60. Kreisinger, H., Ovitz, F.K. & Augustine, C.E., Combustion in the fuel bed of hand fired furnaces, U.S. Bureau of Mines : Technical Paper, No. 137, 1916.

61. Spalding, D.B., The calculation of mass transfer rates in absorption, vaporization, condensation and combustion processes, Proceedings of the Insitution of Mechanical Engineers, Vol.168, 1954, pp. 545-570.

62. Vulis, L.A., Journal of Technical Physics, U.S.S.R., Vol.16, No. 1, 1946, pp.95-100.

63. Van Der Held, E.F.M., The reaction between a surface of solid carbon and oxygen. Chemical Engineering Science, Vol.14, 1961, pp.300-313.

64. Loon Van, W., De vergassing van koolstof met zuurstof en stoom, Thesis, Delft, 1952.

65. Mulder, L. L. & Graaf, J. G. A., De Central Technical Institute T.N.O., Delft., Private communication to Van der Held, E.F.M.

66. Golovina, E.S. & Khaustovich, G.P., The interaction of carbon with carbon dioxide and oxygen at temperatures up to 3000 K, Proceedings of the Eight International Symposium on Combustion, 1962, pp.784-792.

67. Khitrin, L.N., The Physics of Combustion and Explosion, IPST, Jerusalem, 1962.

68. Roberts, O. C. & Smith, I. W., Measured and calculated burning histories of large carbon spheres in oxygen, Combustion and Flame, Vol.21, 1973, pp.123-127.

69. Field, M.A., Rate of combustion of size-graded fractions of char from a low-rank coal between 1200 K and 2000 K, Combustion and Flame, Vol.13, 1969, pp.237-252.

70. Field, M.A., Measurements of the effect of rank on combustion rates of pulverized coal, Combustion and Flame, Vol.14, 1970 pp.237-248.

71. Mulcahy, M.F.R. & Smith, I. W., Kinetics of combustion of pulverized fuel : A review of theory and experiment, Review of Pure and Applied Chemistry, Vol.19, 1969, pp.81-108.

72. Mulcahy, M.F.R. & Smith, I. W., The kinetics of combustion of pulverized coke, anthracite and coal chars, Chemeca '70' : Proceedings of a conference convened by the Australian National Committee of the Institution of Chemical Engineers and the Australian Academy of Science, Melbourne and Sydney, Australia, August 19-26, 1970, pp.101-117.

73. Smith, I.W., Kinetics of combustion of size-graded pulverized fuel in the temperature range 1200 -2270 K., Combustion and Flame, Vol.17, 1971, pp.303-314.

74. Smith, I.W., The kinetics of combustion of pulverized semi-anthracite in the temperature range 1400 - 2200 K. Combustion and Flame, Vol. 17, 1971, pp.421-428.

75. Sergeant, G. D. & Smith, I. W., Combustion rate of bituminous coal char in the temperature range 800 - 1700 K, Fuel, Vol.52, January 1973, pp.52-57.

76. Botterill, J. S. M., Fluid-bed heat transfer, Academic Press, London, 1975.

77. Avedesian, M. M. & Davidson, J. F., Combustion of carbon particles in a fluidized bed, Transactions of the Institution of Chemical Engineers, Vol.51, 1973, pp. 121-131.

78. Campbell, E. K. & Davidson, J. F., The combustion of coal in fluidized beds, Proceedings of the Institute of Fuel Symposium Series No. 1 : Fluidized Combustion, Imperial College, London, U.K., September 16-17, 1975, Paper A2.

79. Sergeant, G. D. & Smith, I. W., Relative rates of chemical and mass transfer rate control in fluidized-bed combustion of coal chars, Fuel, Vol.52, January 1973, pp.58-60.

80. Basu, P., Broughton, J. & Elliott, D. E., Combustion of single coal particles in fluidized beds., Proceedings of the Institute of Fuel Symposium Series No. 1 : Fluidized Combustion, Imperial College, London, U.K., September 16-17, 1975, Paper A3.

81. Basu, P., Combustion of coal in shallow fluidized beds, PhD Thesis, Department of Mechanical Engineering, The University of Aston in Birmingham, U.K., 1976.

82. Waters, P. L., Factors influencing the fluidized combustion of low grade liquid and solid fuels, Proceedings of the Institute of Fuel Symposium Series No. 1 : Fluidized Combustion, Imperial College, London, U.K., September 16-17, 1975, Paper C6.

83. Basu, P., Burning rate of carbon in fluidized beds, Fuel, Vol. 56, October, 1977, pp.390-392.

84. Beer, J. M., Baron, R.E., Boreghi, G., Hodges, J. L. & Sarofim, A. F., A model of coal combustion in fluidized bed combustors, Proceedings of the Fifth International Conference on Fluidized-Bed Combustion, Washington D.C., December 12-14, 1977.

85. Yates, J. G. & Walker, P.R., Particle temperatures in a fluidized bed combustor, Fluidization : Proceedings of the Second Engineering Foundation Conference, Trinity College, Cambridge, England, April 2-6, 1978. Cambridge University Press, Cambridge, England, 1978. pp.241-245.

86. Leung, L. S. & Smith, I. W., The role of fuel reactivity in fluidized bed combustion, Fuel, Vol.58, May 1979, pp.354-360.

87. Davidson, J. F. & Harrison, D., Fluidized Particles, Cambridge University Press, Cambridge, England, 1963.

88. Andrei, M. A., Time resolved burnout in the combustion of coal particles in a fluidized bed, Master of Science and Chemical Engineer Thesis, Massachusetts Institute of Technology, 1978.

89. Andrei, M. A., Sarofim, A. F. & Beer, J. M., Time resolved burnout in the combustion of coal particles in a fluidized bed, Paper presented at the 86th National Meeting of the American Institute of Chemical Engineers, Houston, Texas, U.S.A., April 1-5, 1979.

90. Highley, J., Kaye, W. G. Chiba, T., Nienow, A. W. & Rowe, P.N., The application of fluidized combustion to industrial boilers and furnaces, Proceedings of the Institute of Fuel Symposium Series No.1 : Fluidized Combustion, Imperial College, London, U.K., September 16-17, 1975, Paper B3.

91. Gibbs, B. M. & Hedley, A. B., Combustion of large coal particles in a fluidized bed, Fluidization : Proceedings of the Second Engineering Foundation Conference, Trinity College, Cambridge, England, April 2-6, 1978, Cambridge University Press, Cambridge, England, 1978, pp.235-240.

92. Anderson, J. B. & Norcross, Wm. R., Fluidized bed industrial boiler, Combustion, Vol.50, No.8, February 1979, pp.9-14.

93. Walker, D. J., McIlroy, R. A. Lange, H. B., Fluidized bed combustion technology for industrial boilers of the future - a progress report, Combustion, Vol.50, No. 8, February, 1979, pp.26-32.

94. Avedesian, M. M., Combustion of char in fluidized beds, PhD Thesis, Department of Chemical Engineering, University of Cambridge, Cambridge, England, 1972.

95. Beér, J. M., The fluidized combustion of coal, Proceedings of the Sixteenth (International) Symposium on Combustion, Massachusetts Institute of Technology, Cambridge, Massachusetts, USA, August 15-20 1976, Organised by The Combustion Institute, Pittsburgh, Pennsylvania, USA.

96. Song, Y. H. & Sarofim, A. F., Fluidized bed head start programme, phase 1, Massachusetts Institute of Technology, Cambridge, Massachusetts, USA, September 1975.

97. Wu, P. C., Sc D Thesis, Massachusetts Institute of Technology, Cambridge, Massachusetts, USA, 1949.

98. Shah, M. S., The combustion of charcoal in oxygen, nitric oxide and nitrous oxide, Part 2, The effect of temperature, Journal of Chemical Society, Vol.132, No.11, 1929, pp.2676-2692.

99. Meyer, R., Der mechanisms der primarreaktion zwischen sauaerstoff und graphit, Physikal Chemistry, Vol.17, 1932, pp.384-404.

100. Sihvonen, V., Uber primarvogfange bei der graphitoxydation, Zeitschr Electrochemis, Vol.40, No.76, 1934, pp.456-460.

101. Strickland-Constable, R. F., Part played by surface oxides in the oxidation of carbon, Transactions of the Faraday Society, 1938, pp.1074-1080.

102. Laine, N. R., Vastola,F.J.& Walker, P. R. (Jr.), Proceedings of the Fifth Carbon Conference, Vol.II, Pergamon Press, New York, 1963, pp.211-217.

103. Kanury, A. M., Introduction to combustion phenomena, Gordon and Breach Science Publishers, New York, 1977.

104. Botterill, J. S. M., Fluid-bed heat transfer, Notes on a short course "Fluidized Bed Combustion and Heat Transfer for Beginners", Department of Mechanical Engineering, The University of Aston in Birmingham, UK, March 27-28, 1979.

105. Lanneu, K. P., Gas-solids contacting in fluidized beds, Transactions of the Institution of Chemical Engineers, Vol.38, 1960, pp.125-145.

106. Ross, I. Private communication, Department of Chemical Engineering, University of Cambridge, Cambridge, England.

107. Ranz, W. E. & Marshall, W. R. (Jr.), Evaporation from drops, Part I and Part II, Chemical Engineering Progress, Vol.48, No.4, April 1952, pp.141-146 and 173-180.

108. Chakraborty, R. K. & Howard, J. R., Burning rates and temperatures of carbon particles in a shallow fluidized bed combustor, Journal of the Institute of Fuel, December 1978, pp.220-224.

109. Smith, I. W. & Tyler, R. J., The reactivity of a porous brown coal char to oxygen between 630 and 1812 K, Combustion Science and Technology, Vol.9, 1974, pp.87-94.

110. Pritchard, A. B. & Caplin, P. B., Fluid bed combustion systems, Energy World, Bulletin of the Institute of Energy, No.51, August/September 1978, pp.16-18.

111. Whellock, J. G., Birmingham University Chemical Engineer, Vol.23, No.1, 1972, pp.18-20.

112. Zabrodsky, S. S. & Parnas, A. L., On the temperature condition of coal fluidized combustion, Proceedings of the Institute of Fuel Symposium Series No.1: Fluidized Combustion, Imperial College, London, UK, September 16-17 1975, Paper B5.

113. Basu, P., Private communication, Central Mechanical Engineering Research Institute, Durgapur, India.

114. Campbell, E. K., The combustion of coal in fluidized beds, PhD Thesis, Department of Chemical Engineering, University of Cambridge, Cambridge, England, 1975.

115. Laine, N. R., Vastola, F. J. & Walker, P. L. (Jr.), The importance of active surface area in the carbon-oxygen reaction, Journal of the Physical Chemistry, Vol.67, October 1963, pp.2030-2034.

116. Ayling, A. B., Mulcahy, M. F. R. & Smith I. W., The temperature of burning pulverized fuel particles, Proceedings of the Second Members' Conference, International Flame Research Foundation, Ch.1, 1971.

117. Smith, I. W., Commonwealth Scientific and Industrial Research Organisation, Sydney, Australia, Division of Mineral Chemistry Investigation Report No.86, December 1970.

118. Kunii, D. & Levenspiel, O., Fluidization Engineering, John Wiley & Sons, New York, USA, 1968.

119. Davidson, J. F. & Harrison, D., Fluidization, Academic Press, London, UK, 1971.

120. Dwivedi P. N. & Upadhyay, S. N., Particle-fluid mass transfer in fixed and fluidized beds, Industrial and Engineering Chemistry, Process Design and Development, Vol.16, No.2, 1977, pp.157-165.

121. Rowe, P. N., Claxton, K. T. & Lewis, J. B., Heat and mass transfer from a single sphere in an extensive flowing fluid, Transactions of the Institution of Chemical Engineers, Vol.43, 1965, pp.T14-T31.

122. Spalding, D. B., Some fundamentals of combustion, Butterworths Scientific Publications, London, UK, 1955, p.151.

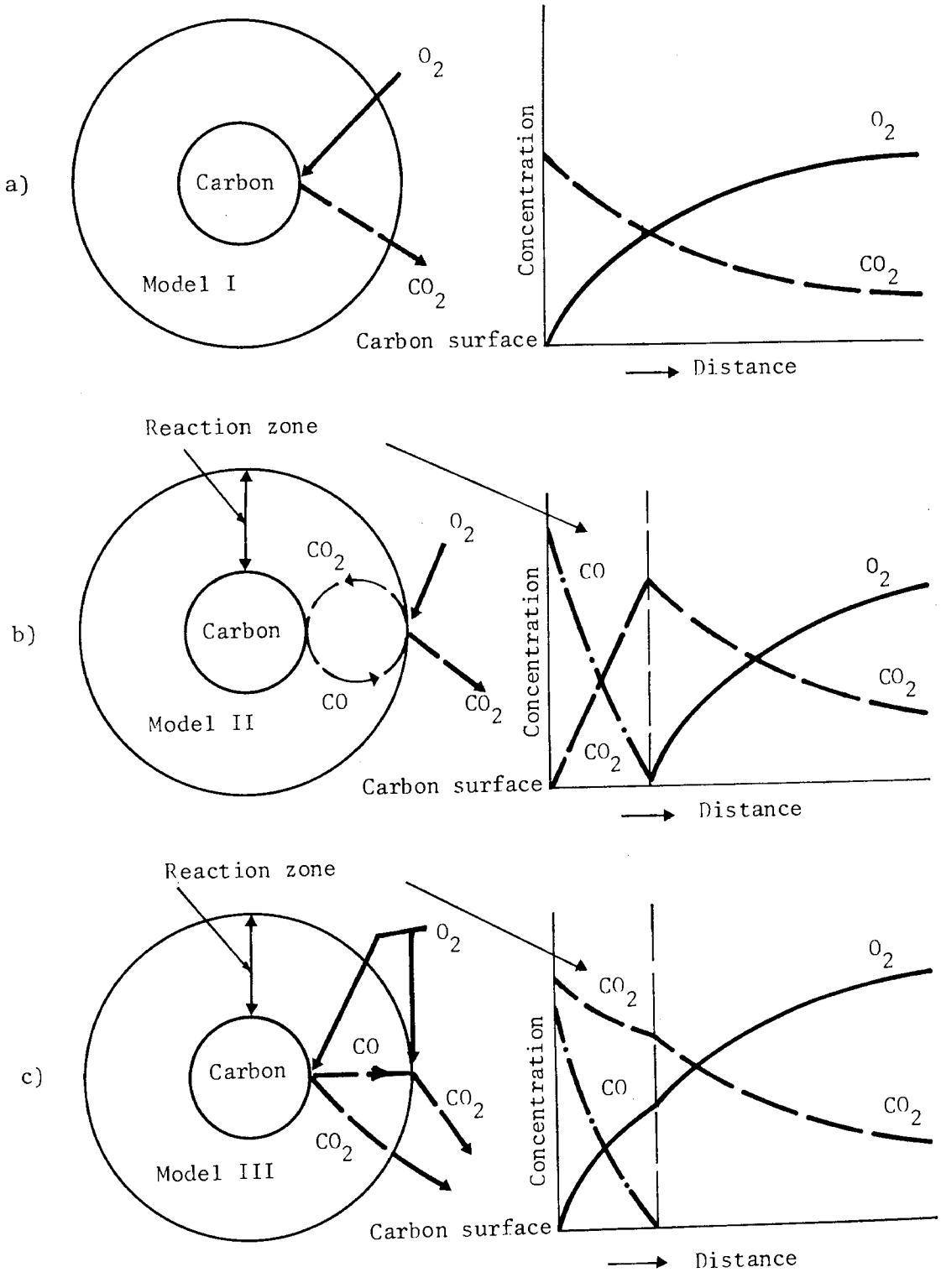

Figure 3.1 Different models of combustion mechanism on the carbon surface with concentration distributions of CO, CO_2 and O_2 on and around it

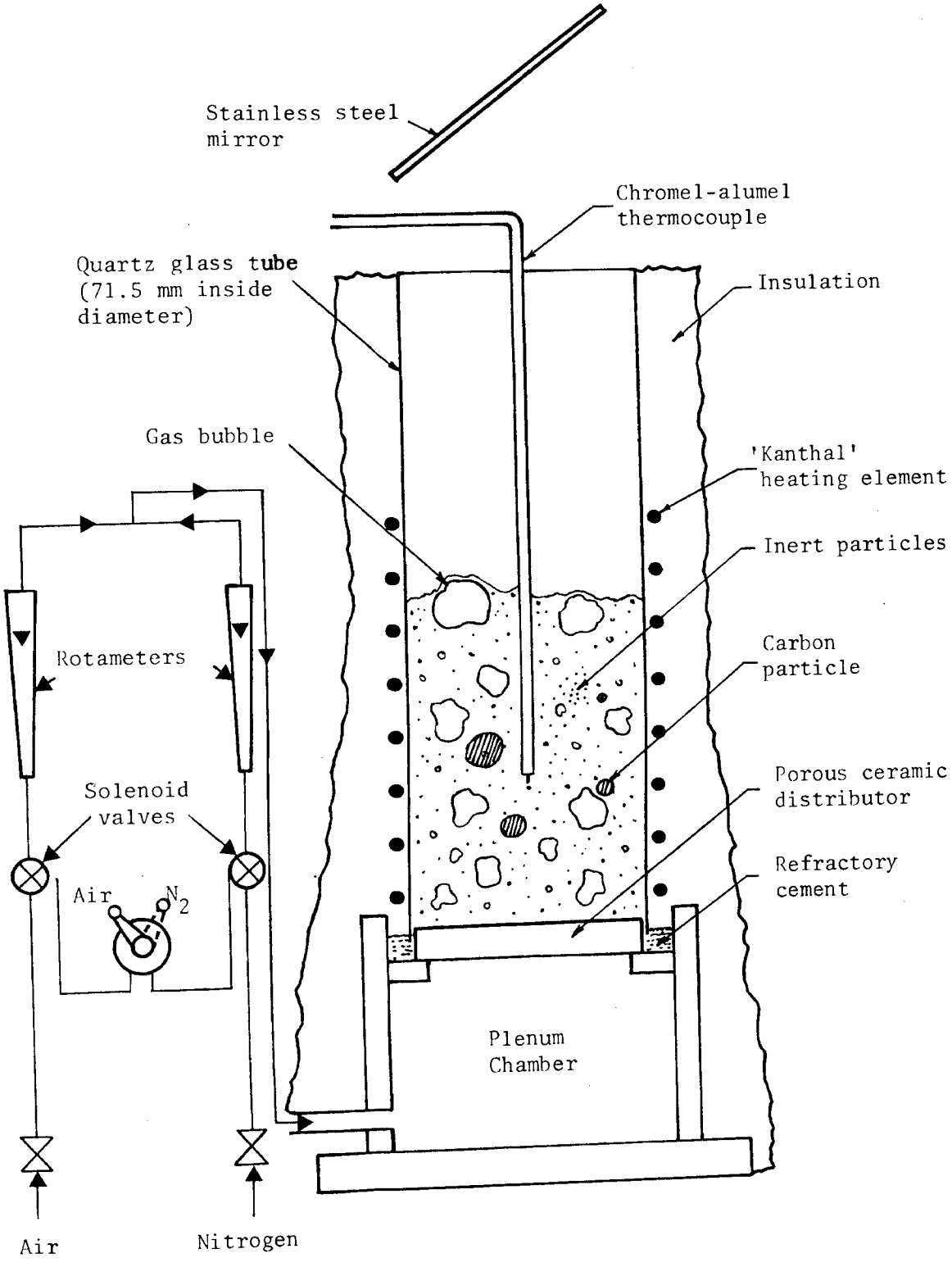

Figure 4.1 Experimental fluidized bed combustor

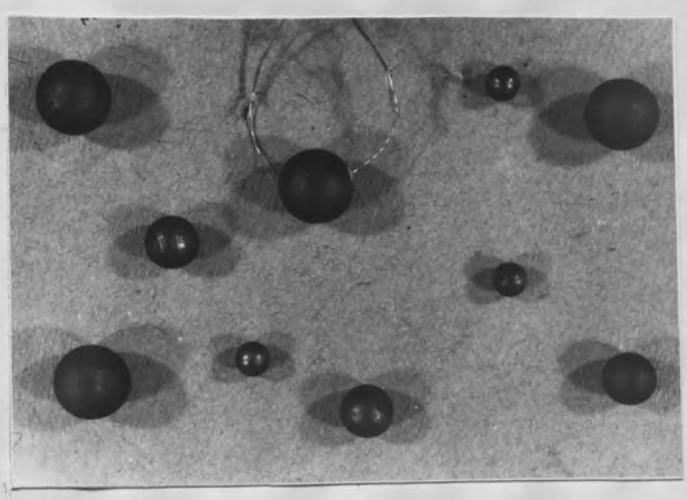

FIGURE 4.2: Photograph of some electrode carbon particles

Mean size: 327.5 µm Mean size: 780 µm

FIGURE 4.3: Photograph of some inert sand particles

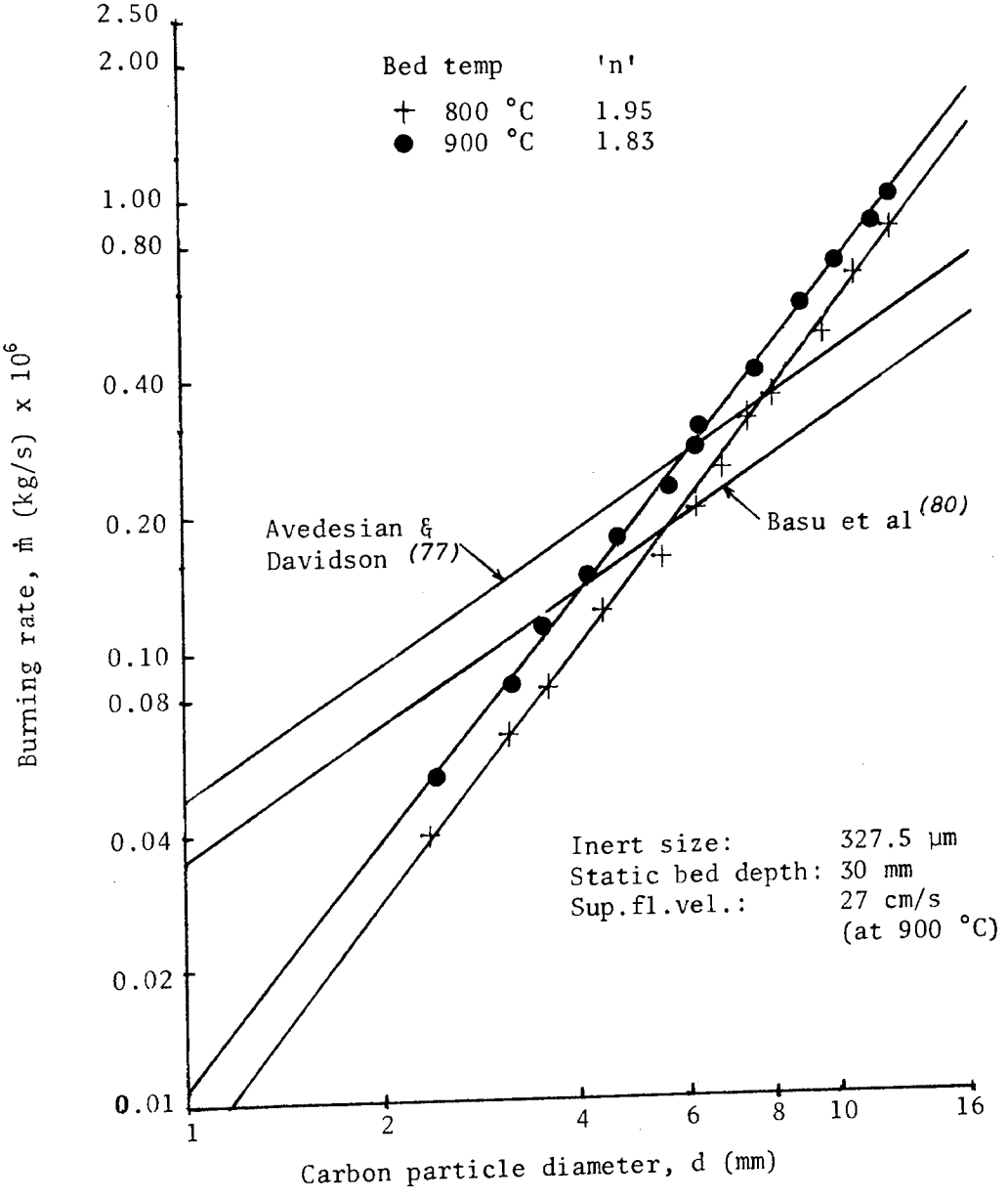

FIGURE 4.4: Variation of burning rate of carbon particles with diameter at different bed temperatures

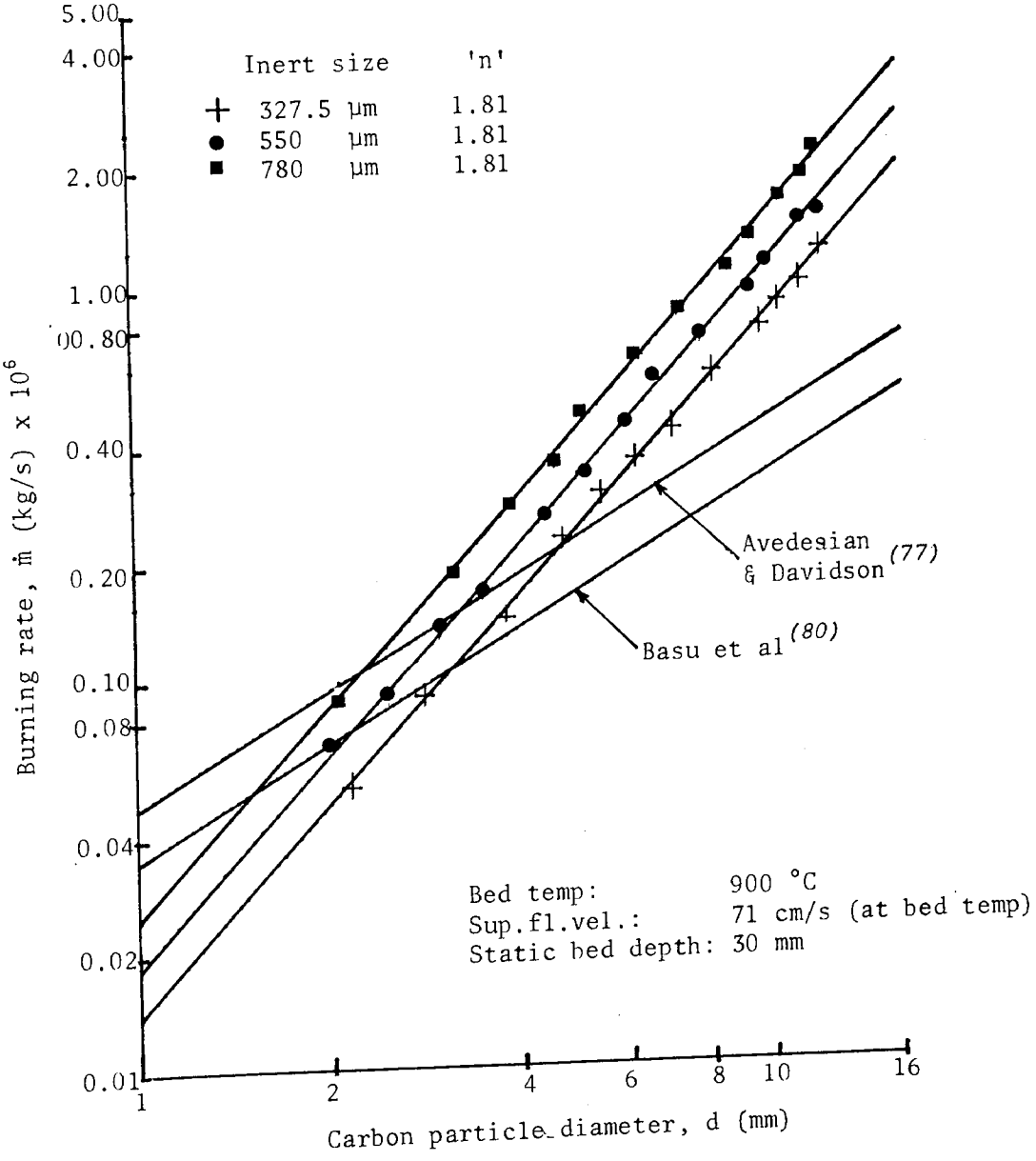

FIGURE 4.5: Variation of burning rate of carbon particles with diameter showing the effect of different sizes of inert particles in the bed

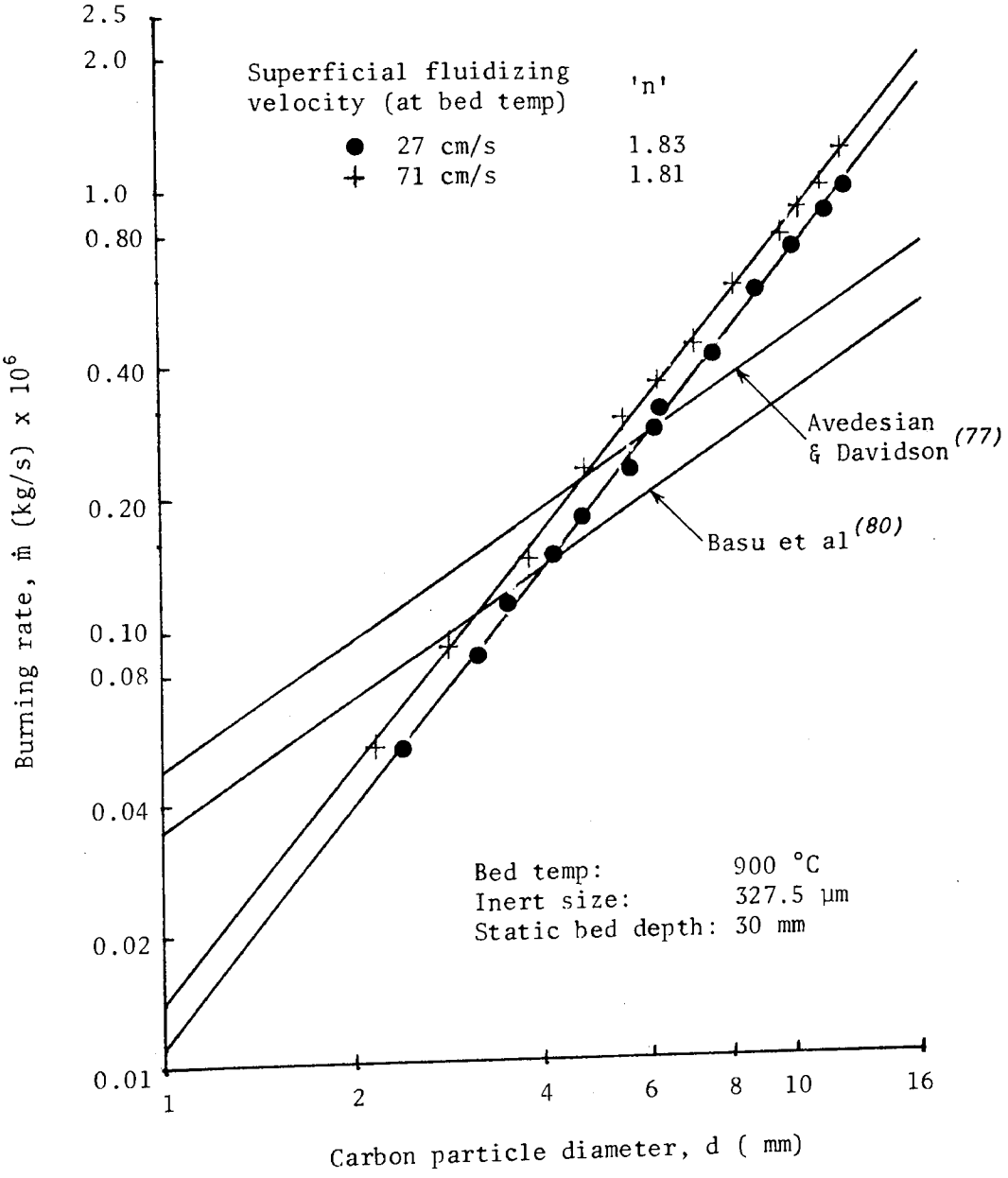

FIGURE 4.6: Variation of burning rate of carbon particles with diameter at different superficial fluidizing velocities

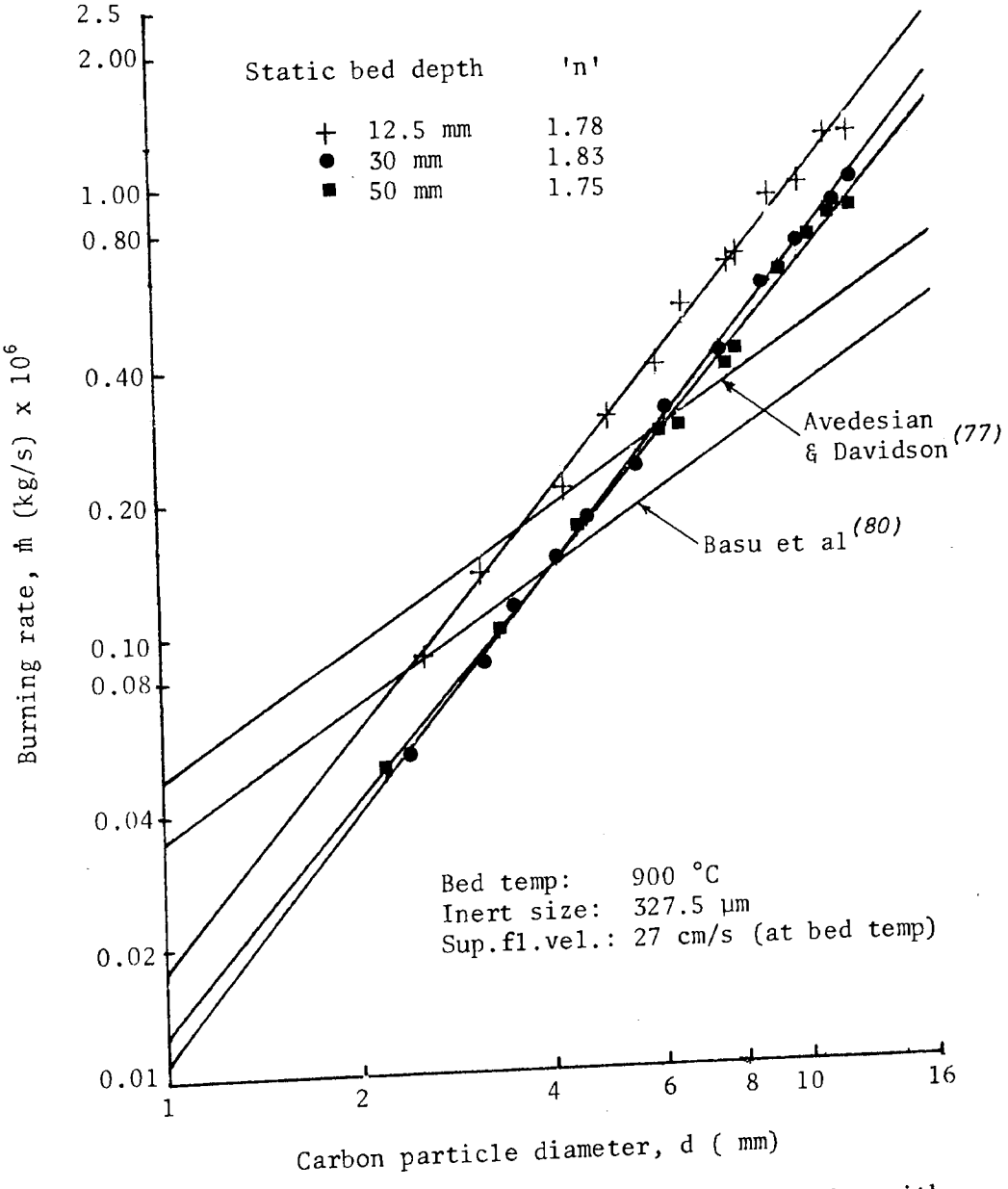

FIGURE 4.7: Variation of burning rate of carbon particles with diameter at different static bed depths

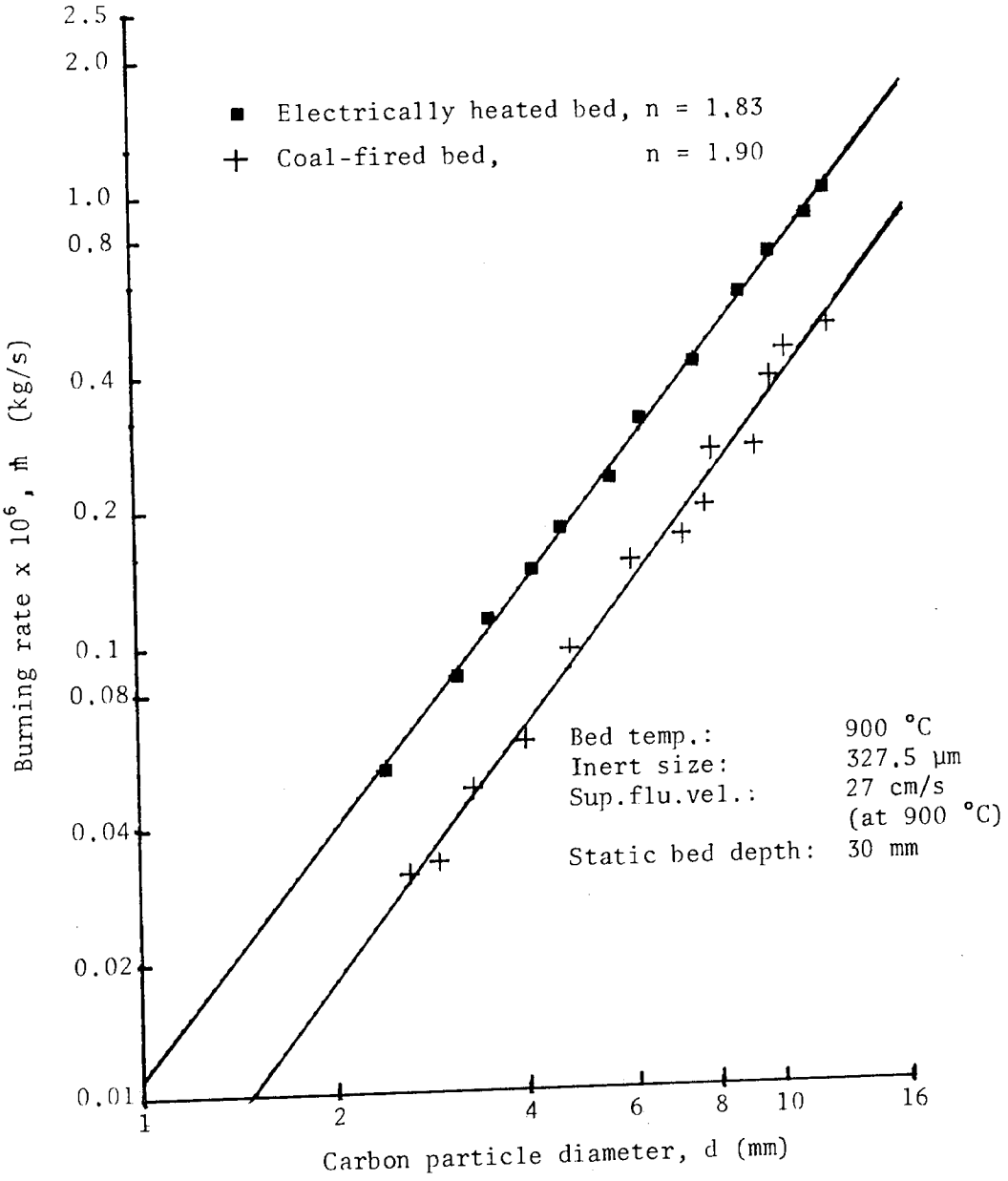

Figure 4.8 Variation of burning rate of carbon particles with diameter showing the effect of the presence of other active carbon particles in the bed

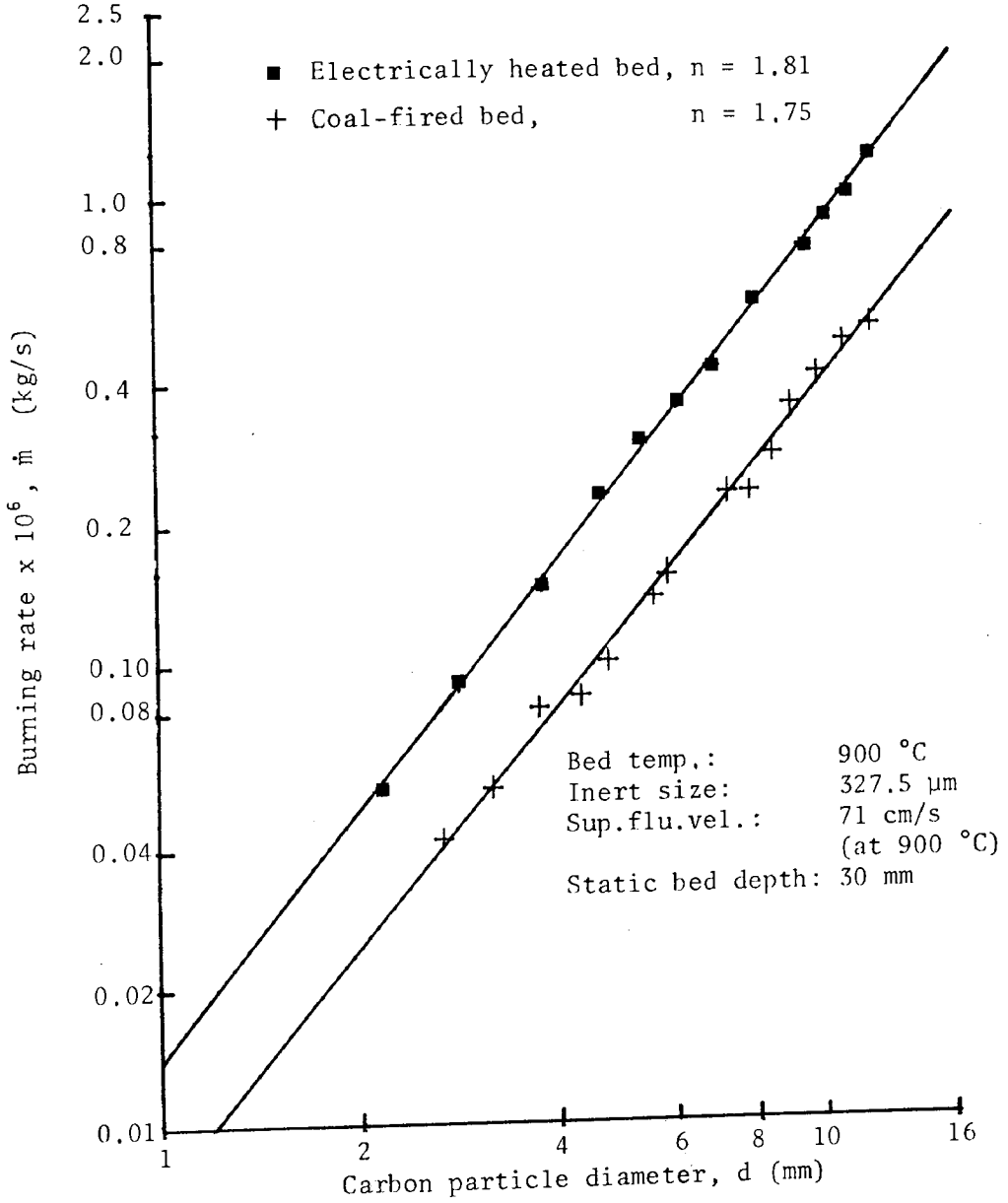

Figure 4.9 Variation of burning rate of carbon particles with diameter showing the effect of the presence of other active carbon particles in the bed

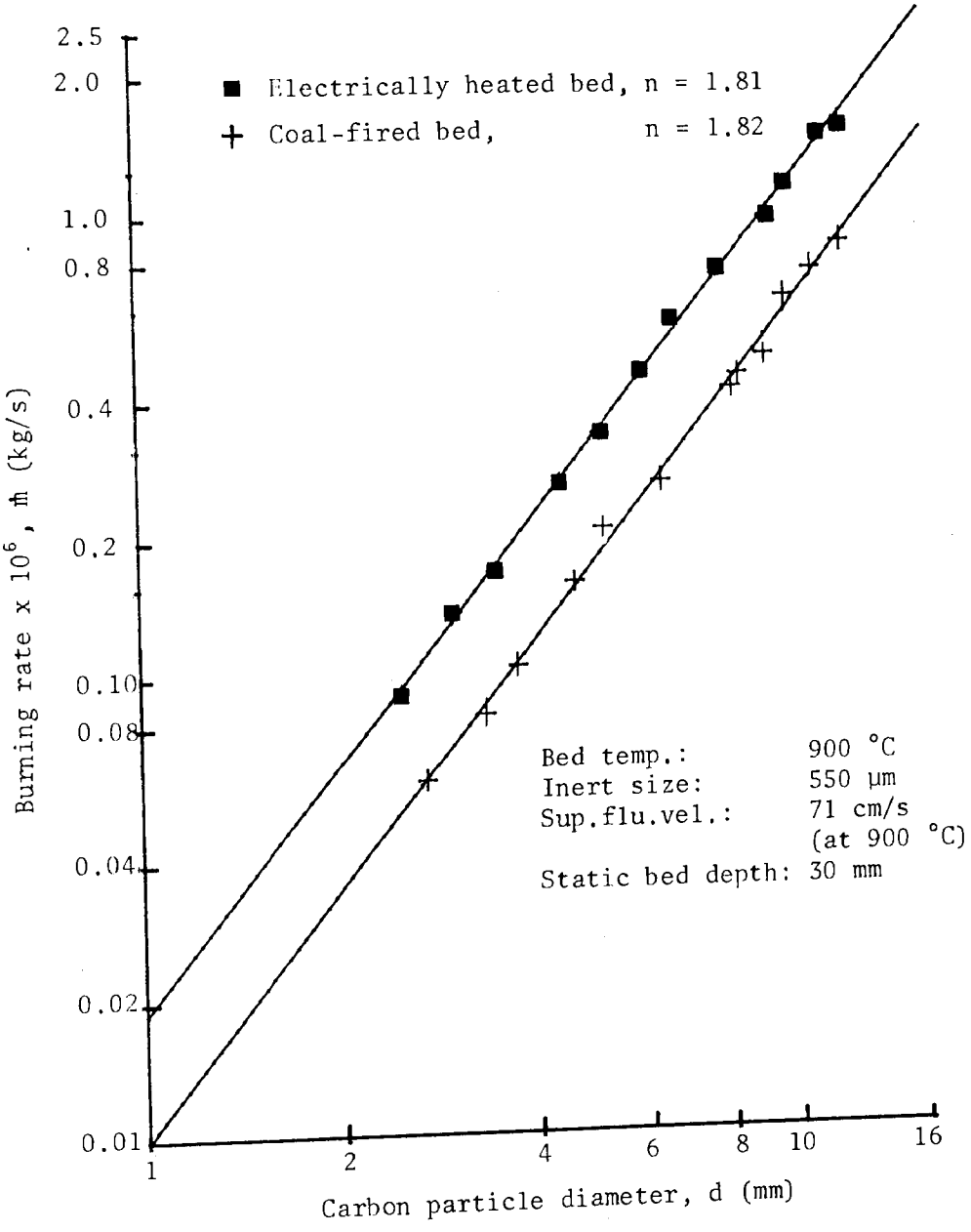

Figure 4.10 Variation of burning rate of carbon particles with diameter showing the effect of the presence of other active carbon particles in the bed

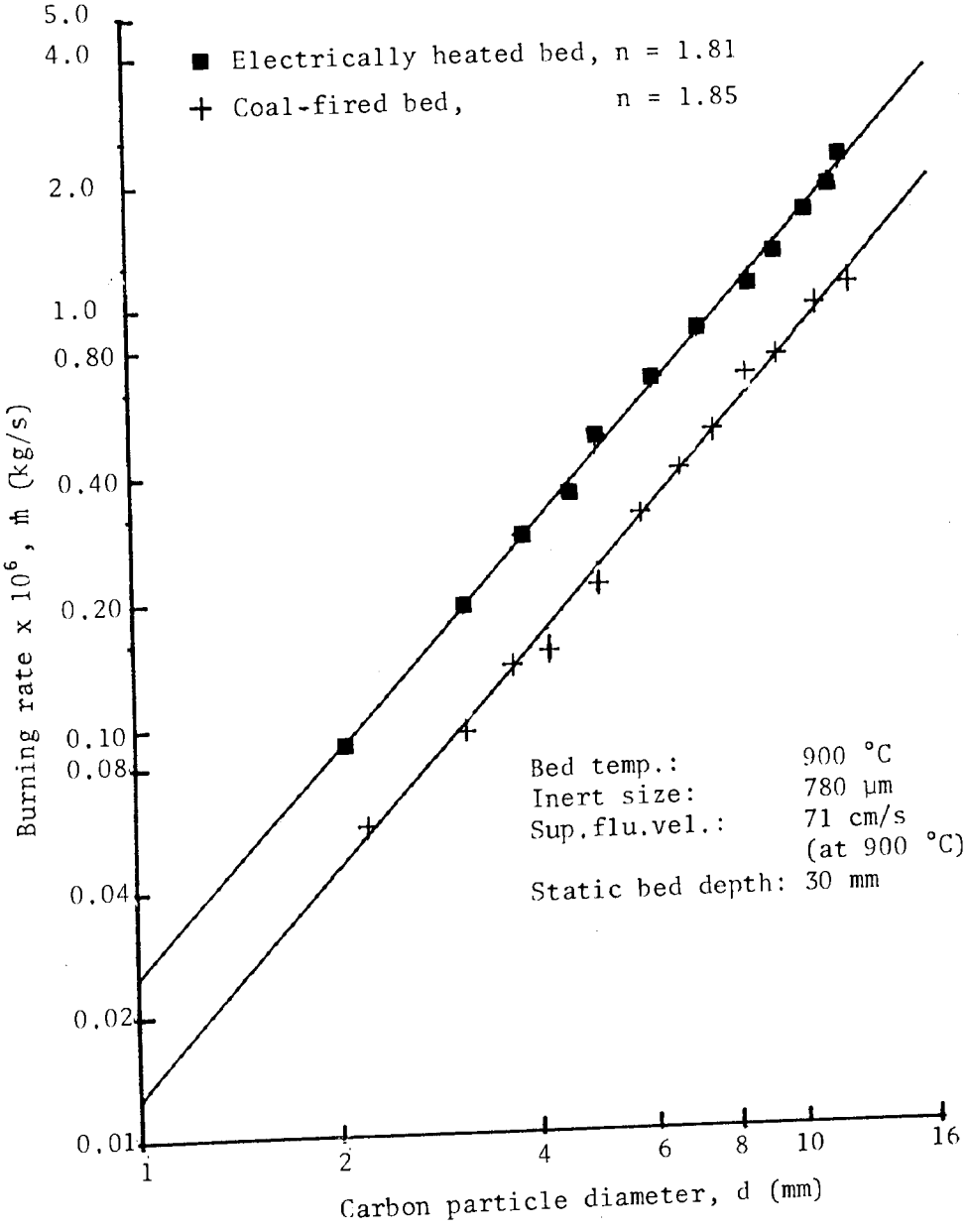

Figure 4.11 Variation of burning rate of carbon particles with diameter showing the effect of the presence of other active carbon particles in the bed

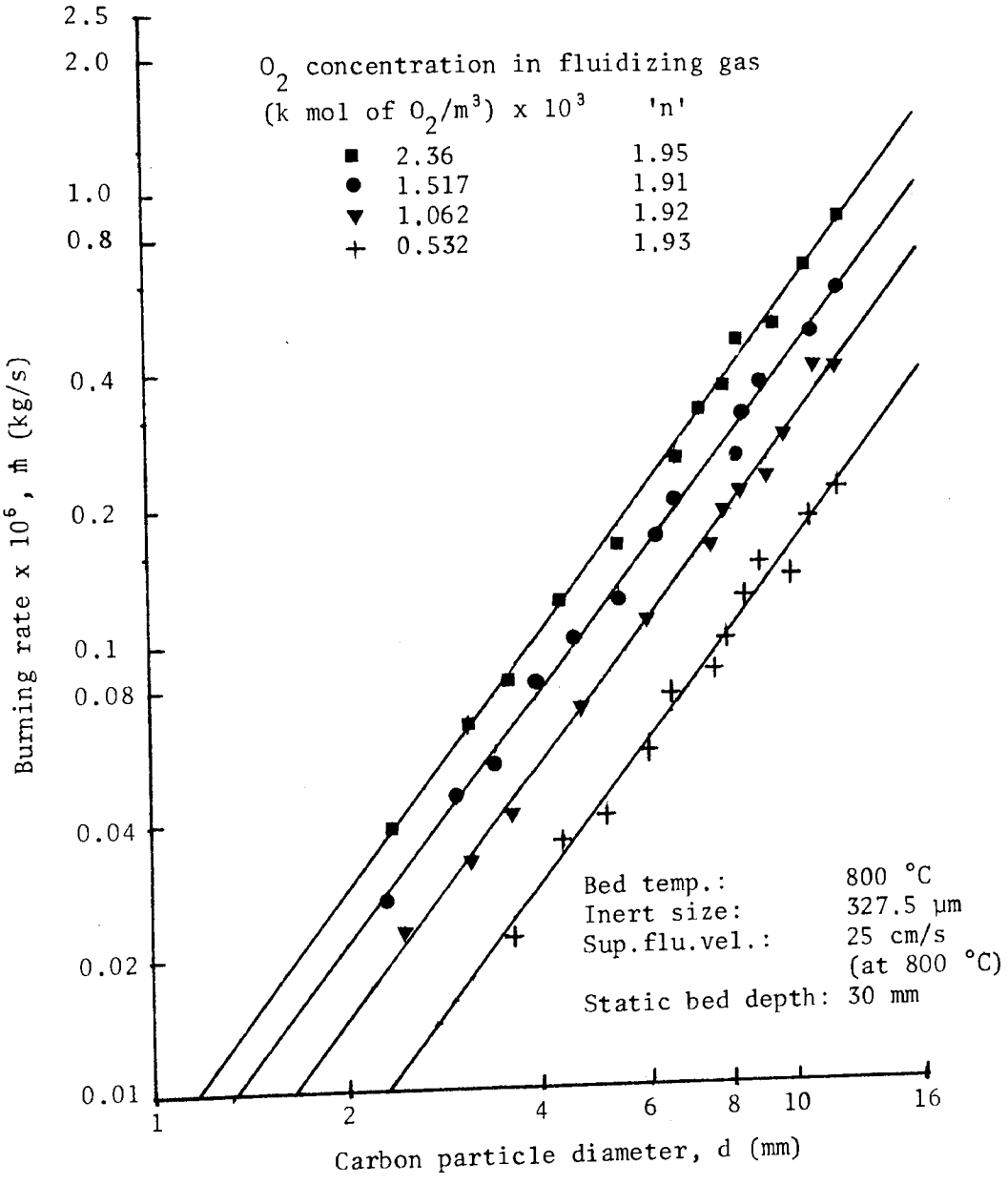

Figure 4.12 Variation of burning rate of carbon particles with diameter at different oxygen concentrations

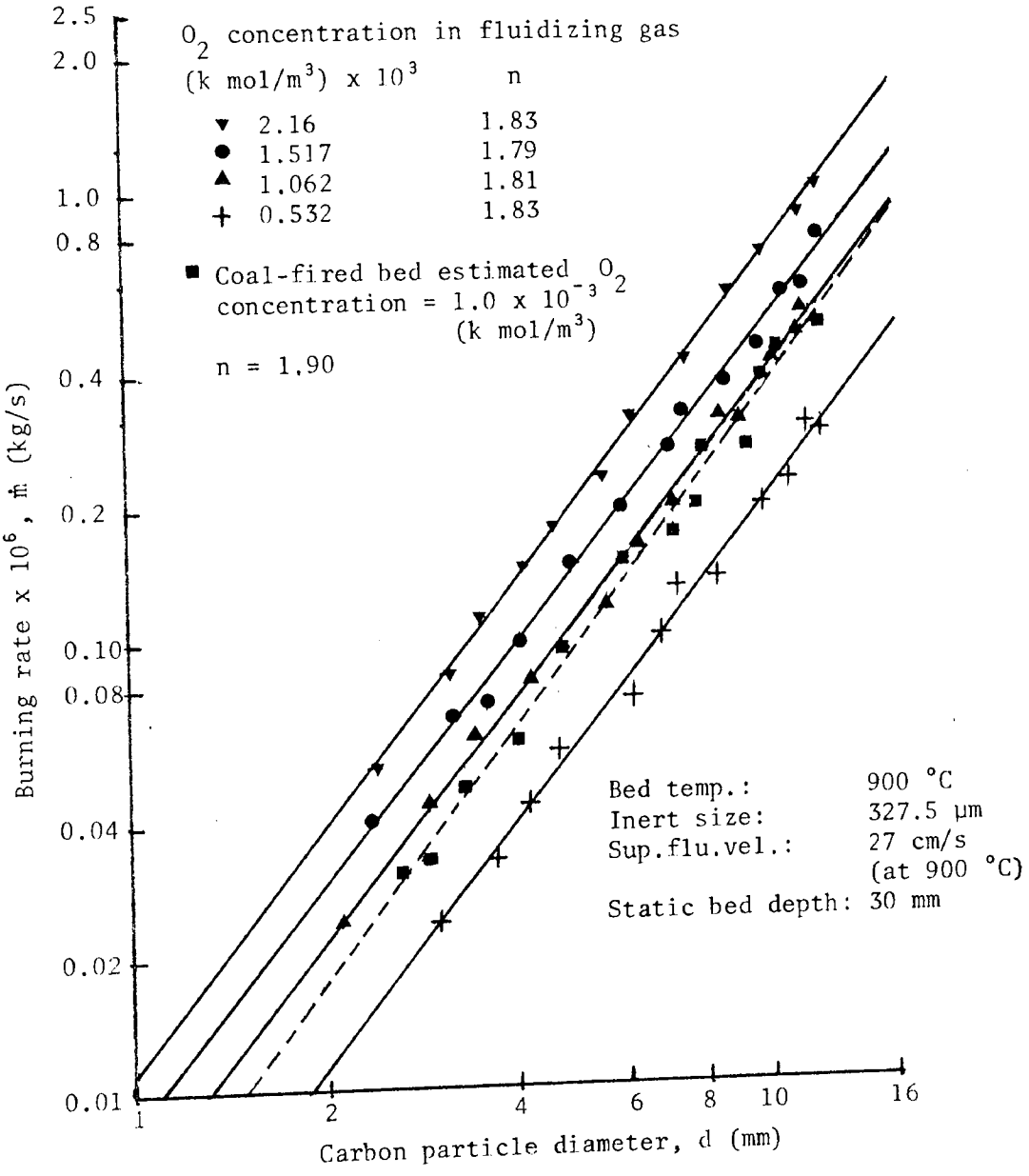

Figure 4.13 Variation of burning rate of carbon particles with diameter at different oxygen concentrations

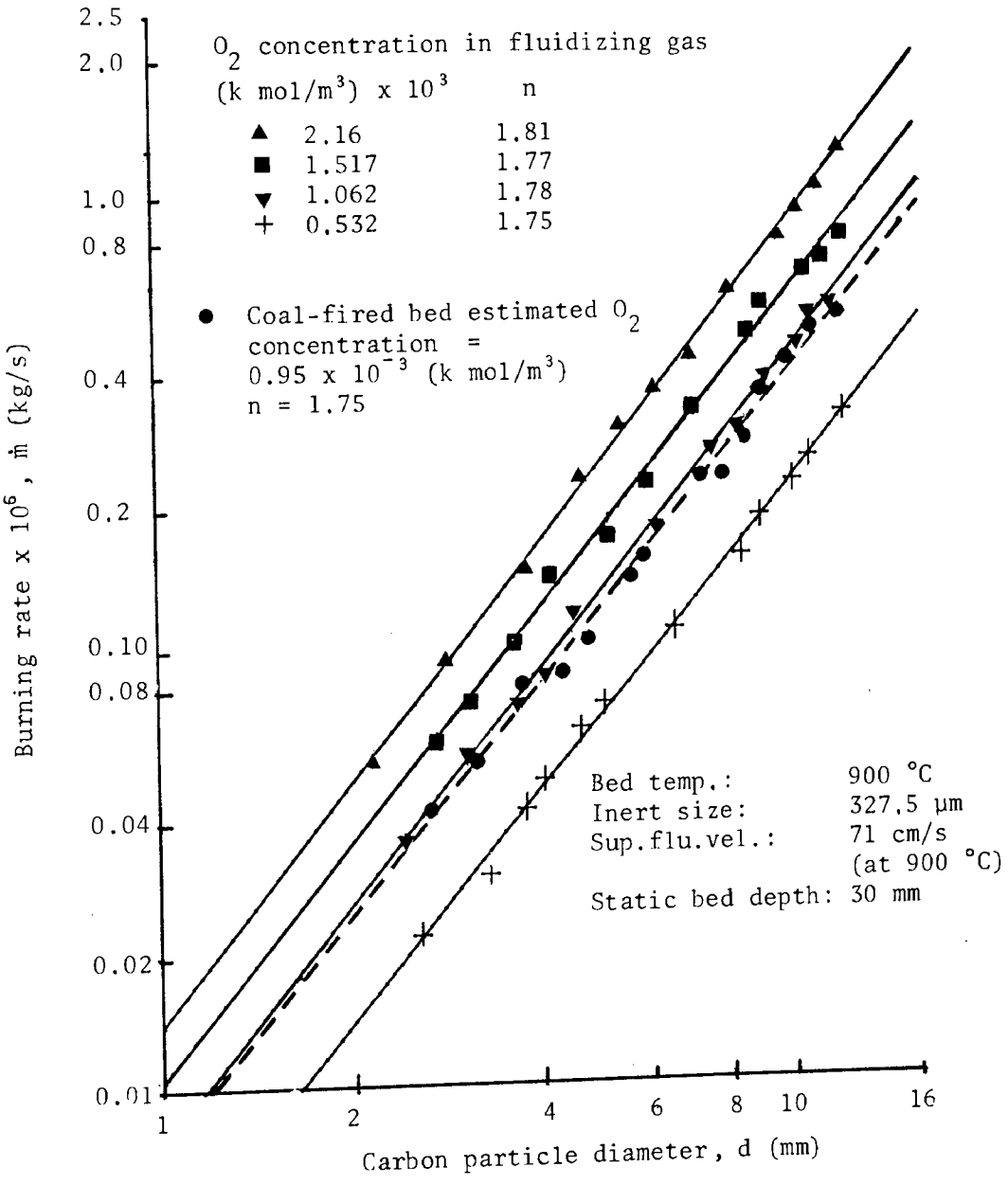

Figure 4.14 Variation of burning rate of carbon particles with diameter at different oxygen concentrations

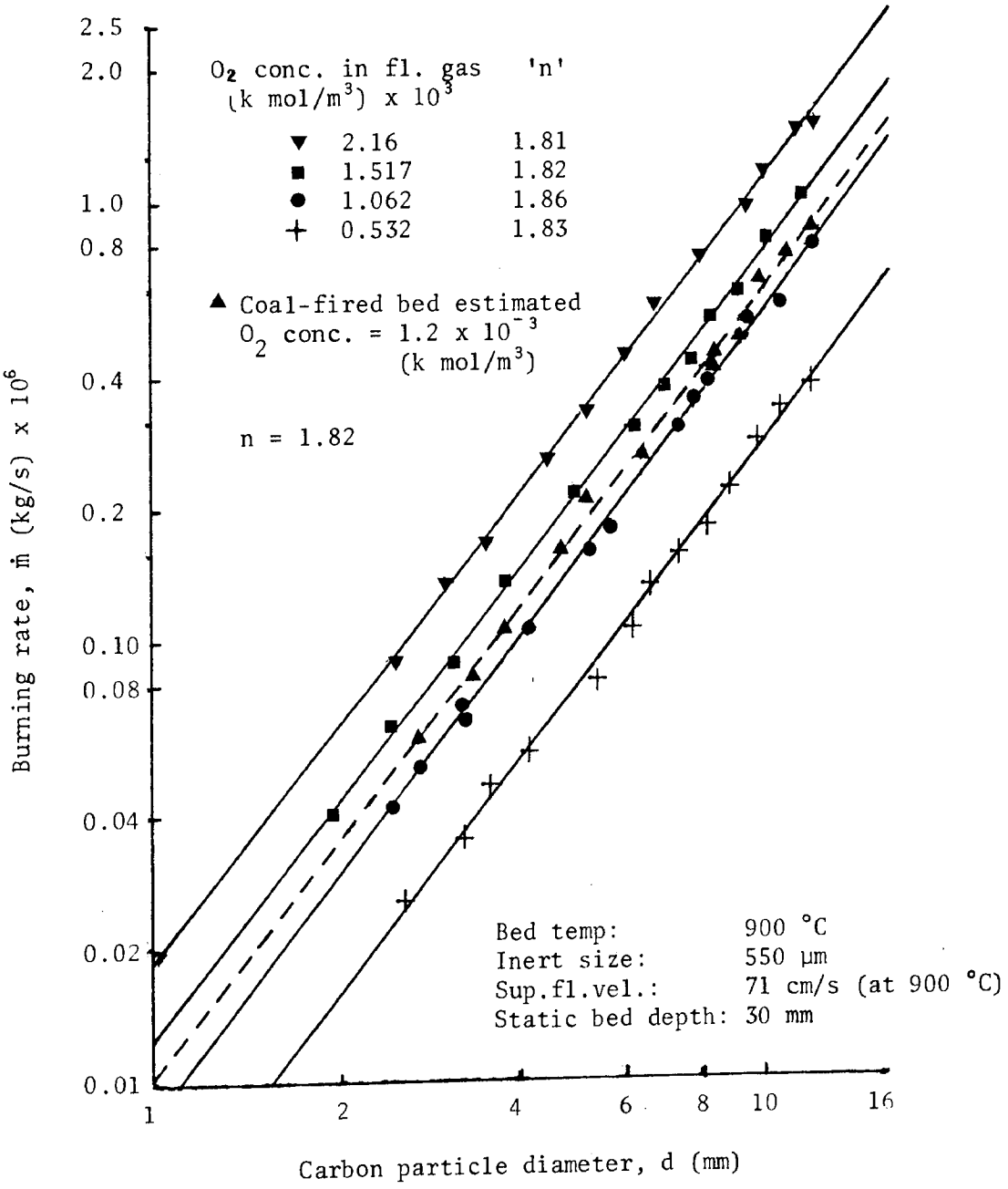

FIGURE 4.15: Variation of burning rate of carbon particles with diameter at different oxygen concentrations

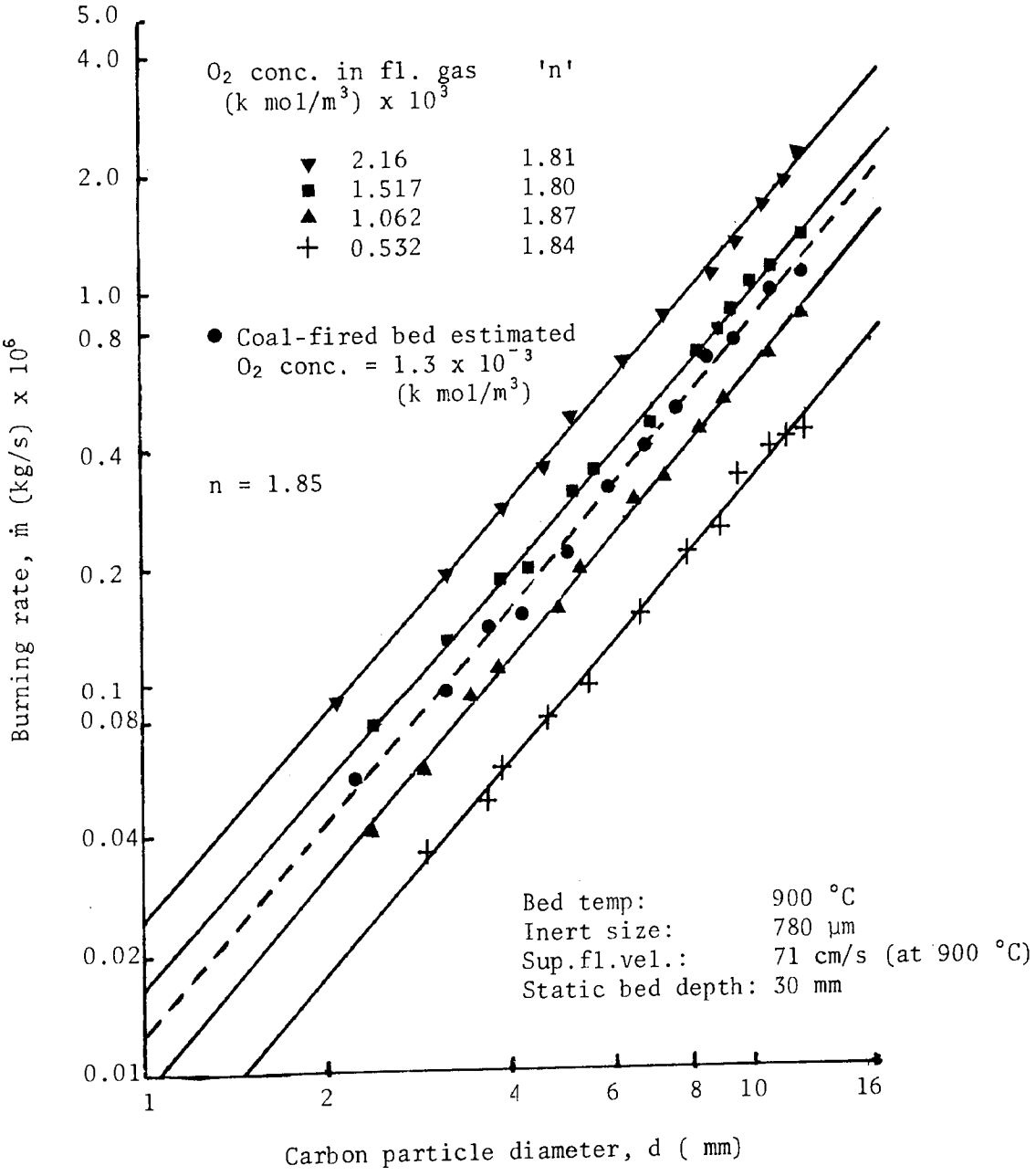

FIGURE 4.16: Variation of burning rate of carbon particles with diameter at different oxygen concentrations

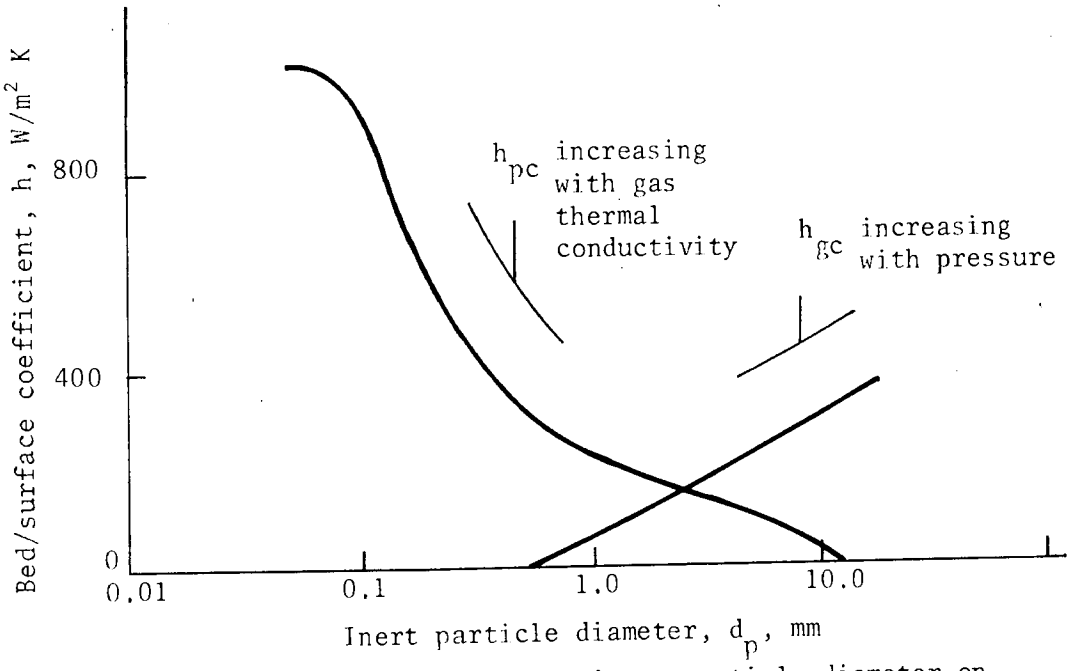

Figure 4.17 General effect of mean inert particle diameter on bed/surface heat transfer coefficient *(Botterill(104))*

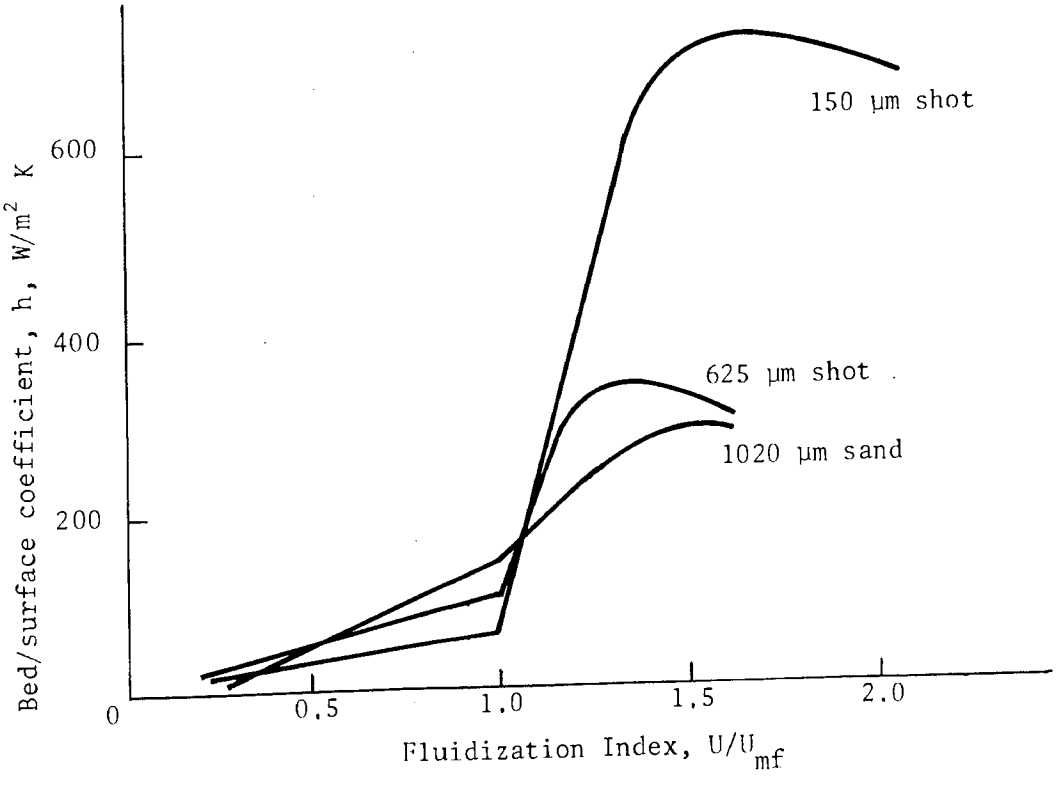

Figure 4.18 Effect of gas flow rate on bed/surface heat transfer coefficient *(Botterill(104))*

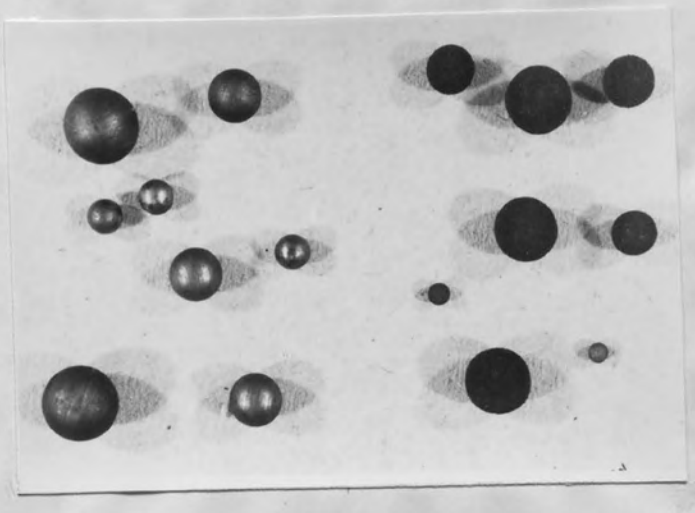

Fresh electrode carbon particles

Partially burnt electrode carbon particles

FIGURE 4.19: Photograph showing the comparison of surfaces of some fresh electrode carbon particles with those of some partially burnt ones

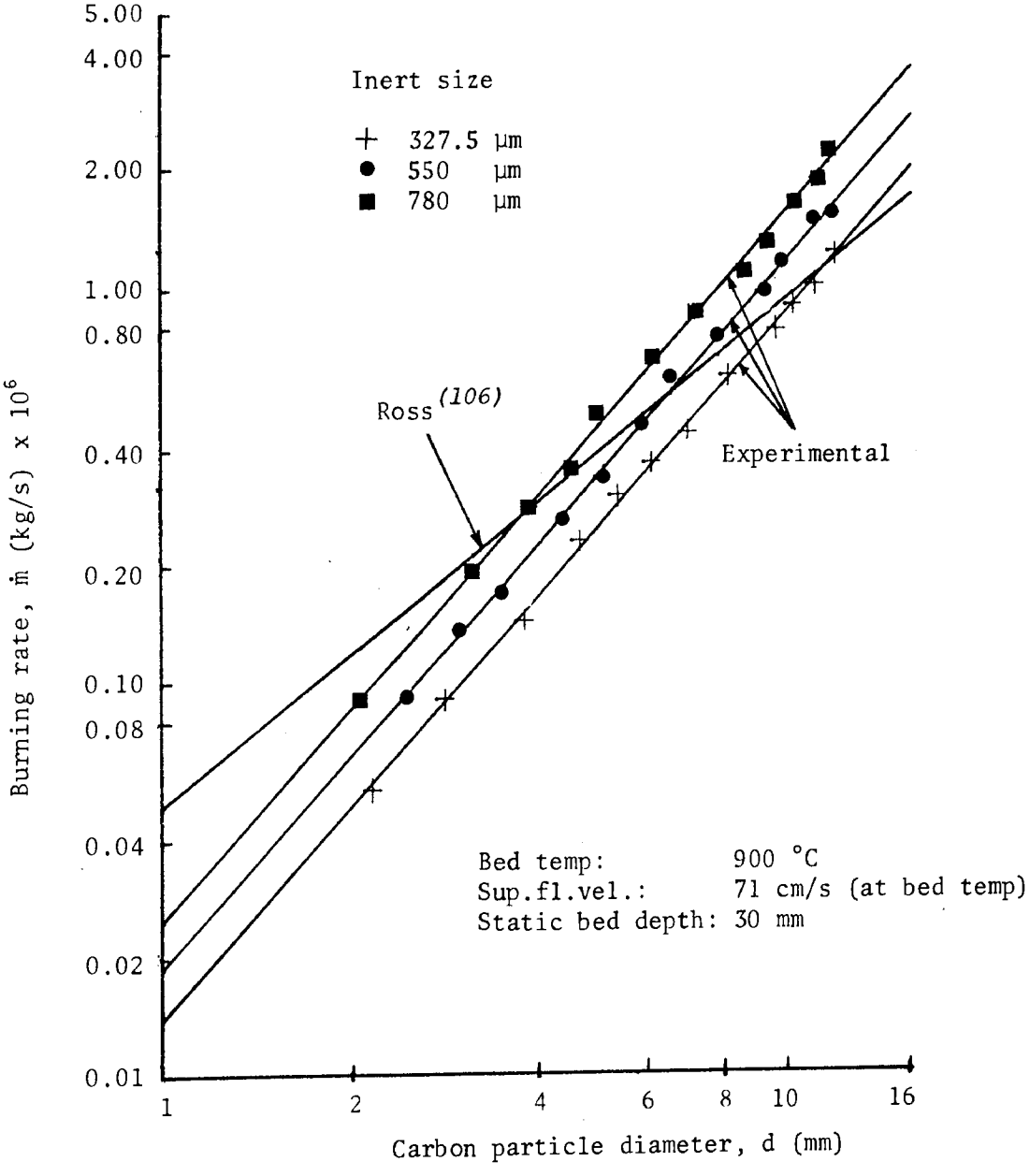

FIGURE 4.20: Comparison of experimental burning rates of single carbon particles with those predicted by the model proposed by Ross *(106)*

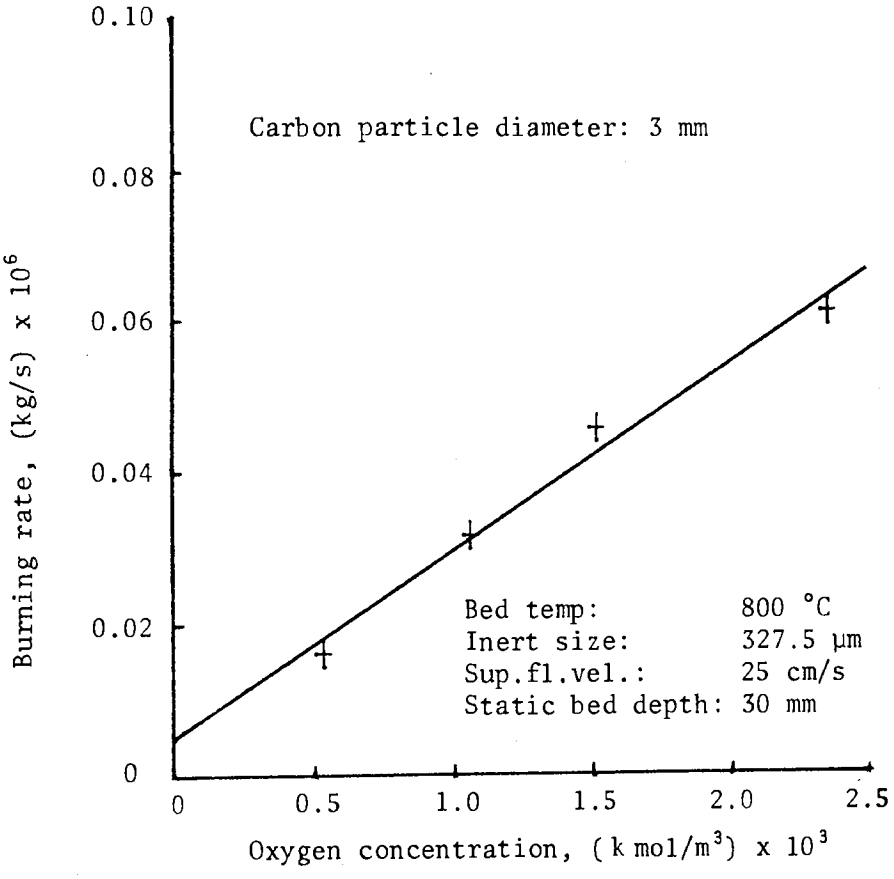

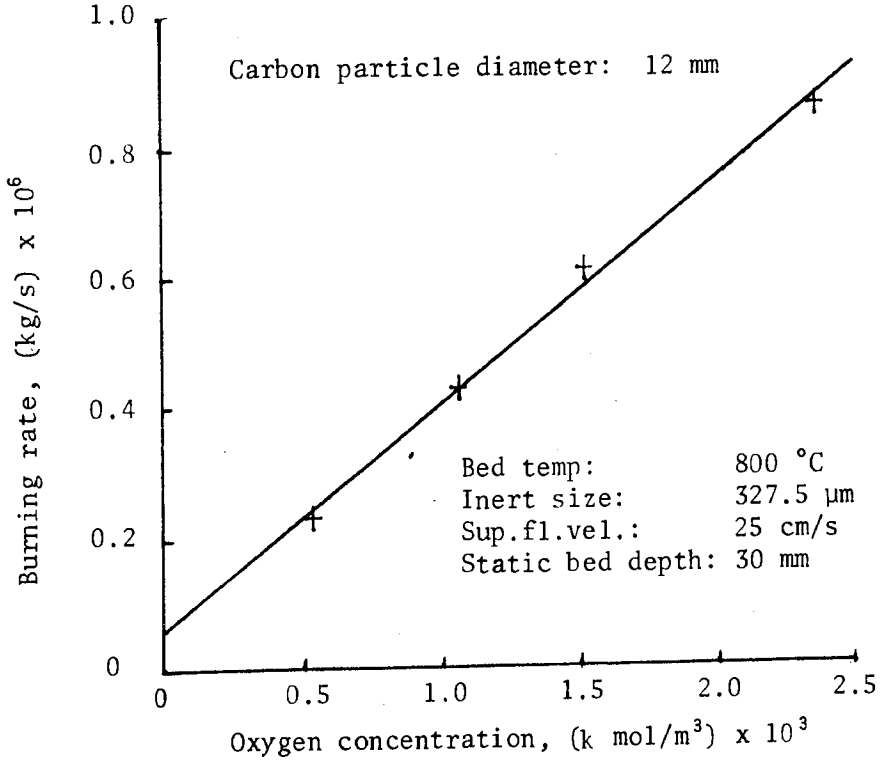

FIGURE 4.21: Variation of burning rate of carbon particle with oxygen concentration

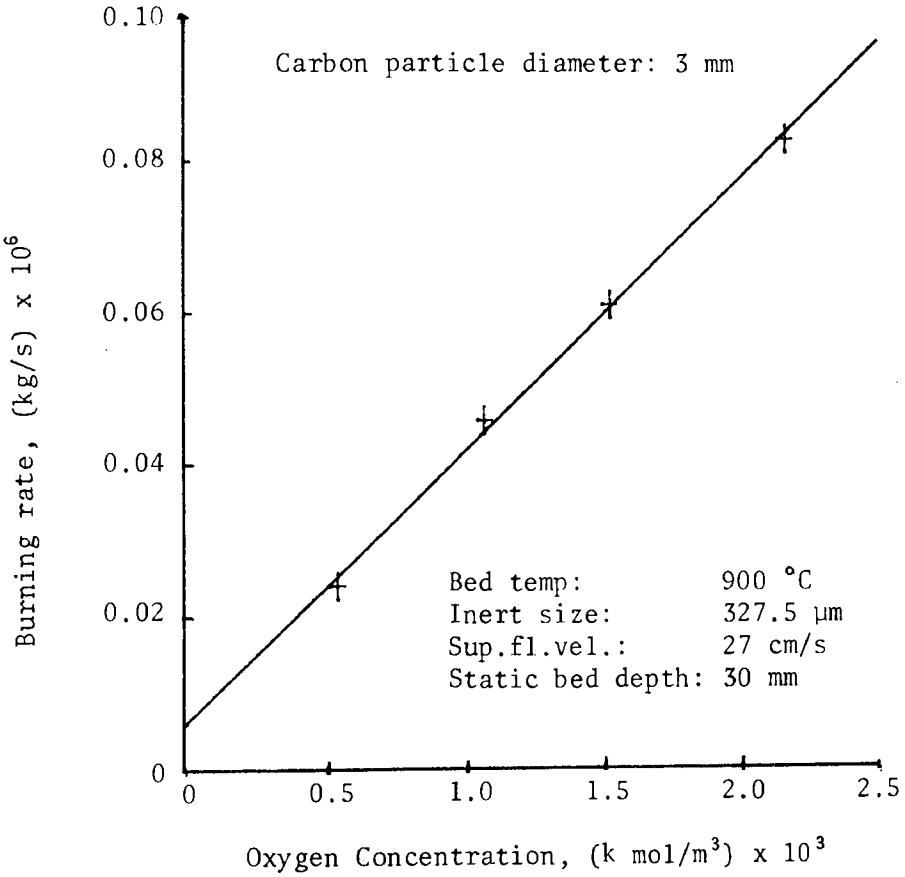

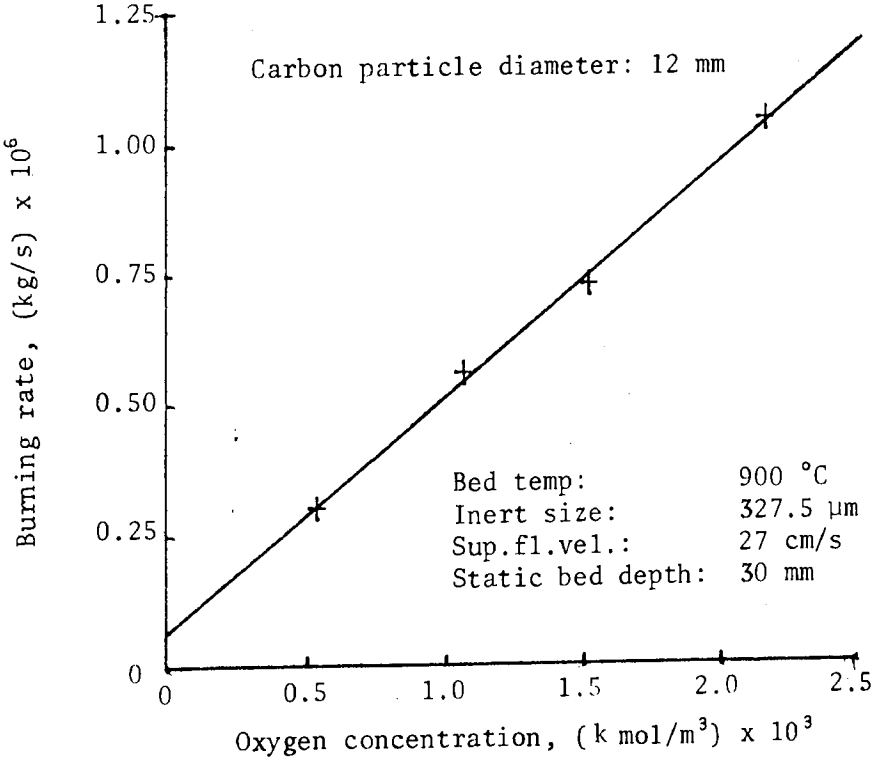

FIGURE 4.22: Variation of burning rate of carbon particle with oxygen concentration

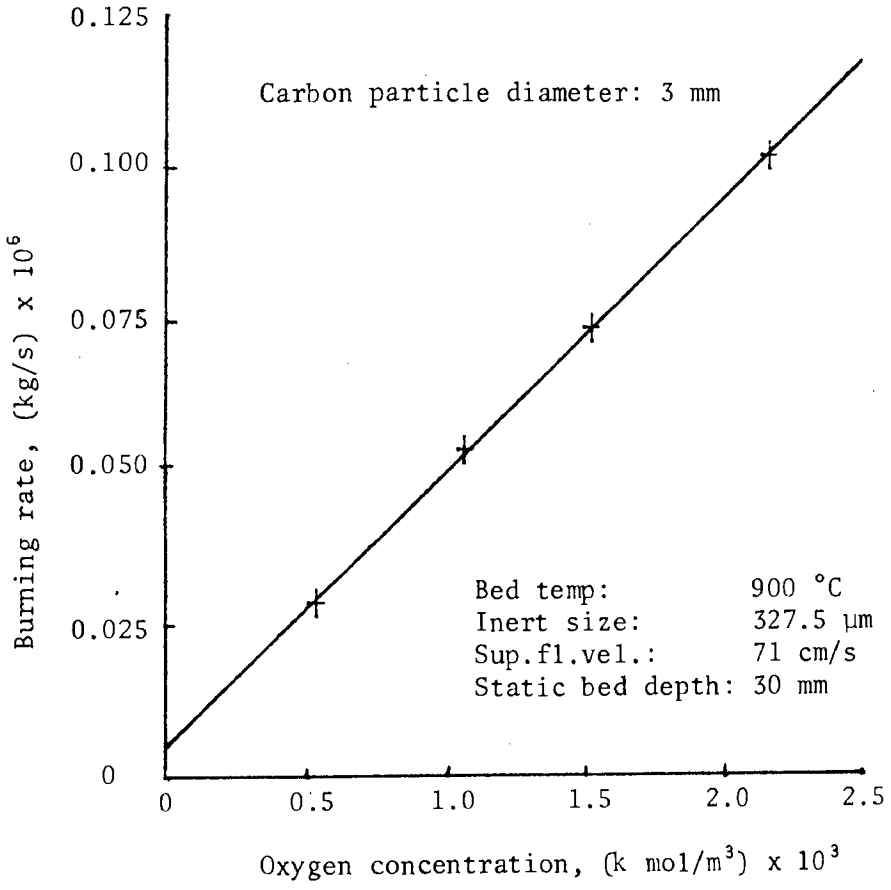

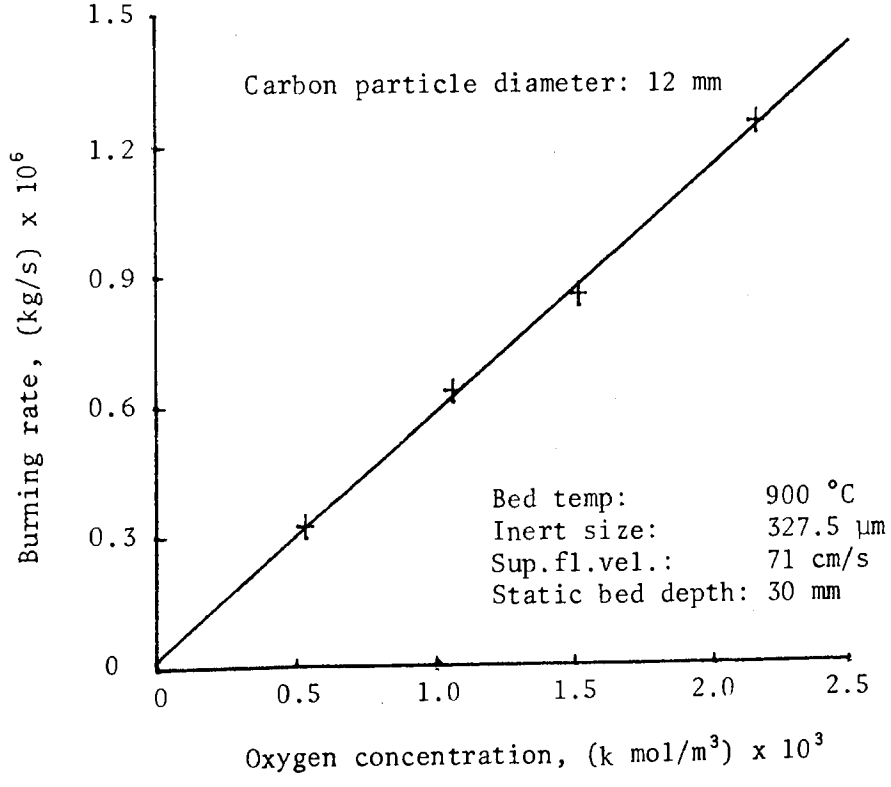

FIGURE 4.23: Variation of burning rate of carbon particle with oxygen concentration

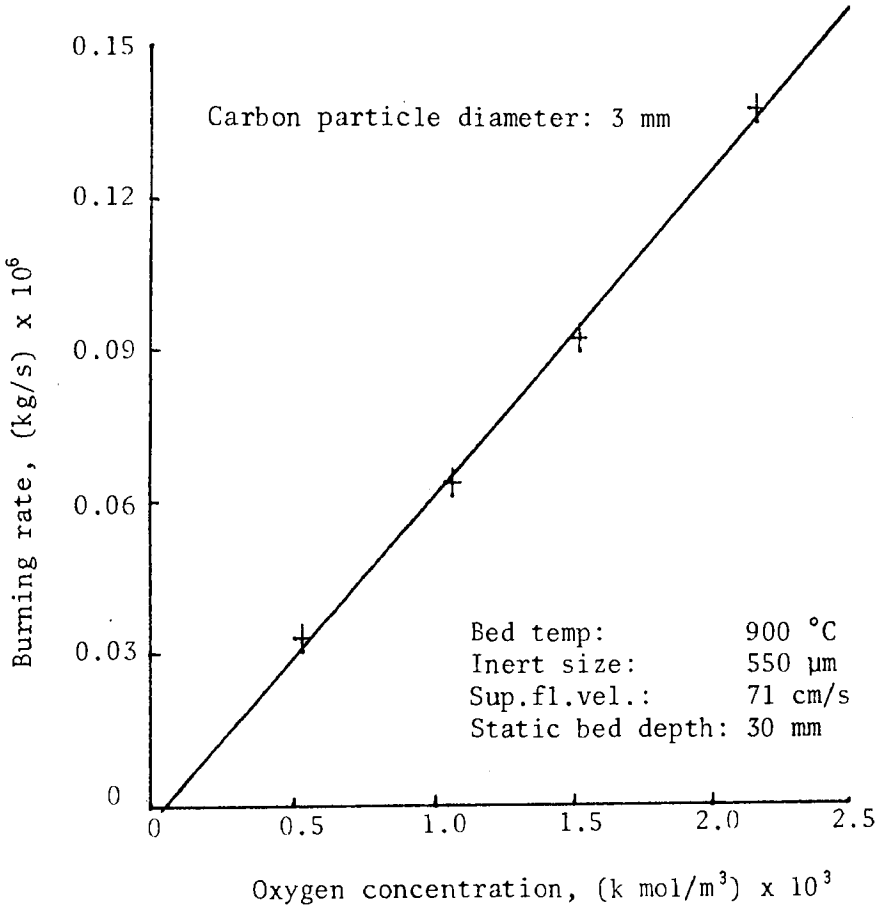

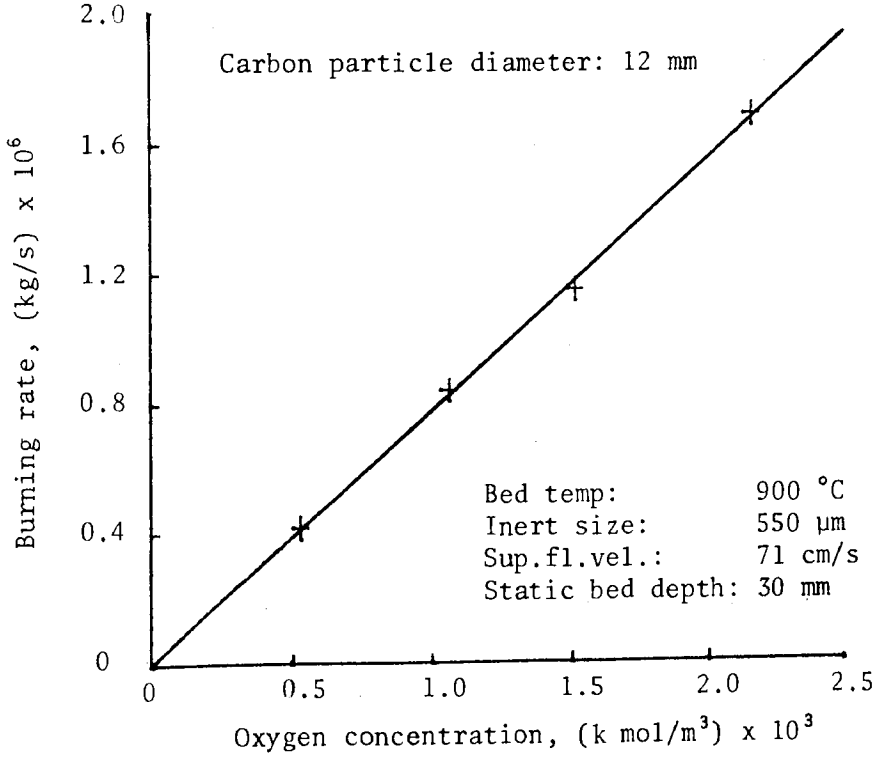

FIGURE 4.24: Variation of burning rate of carbon particle with oxygen concentration

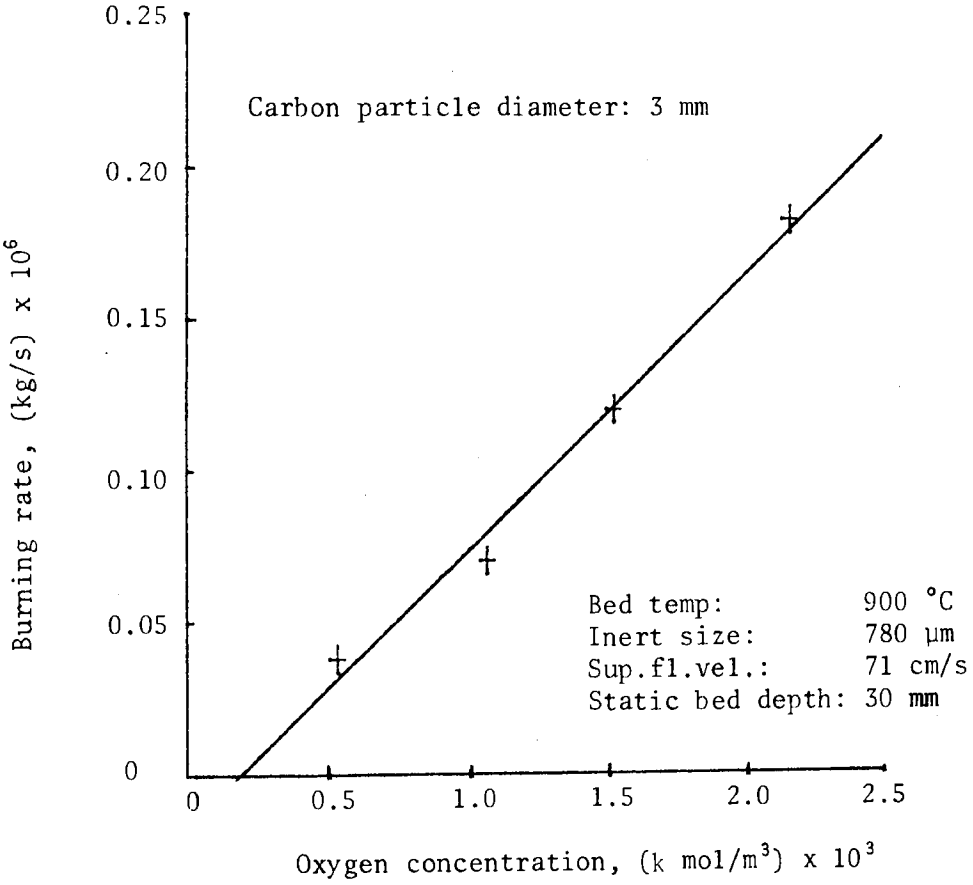

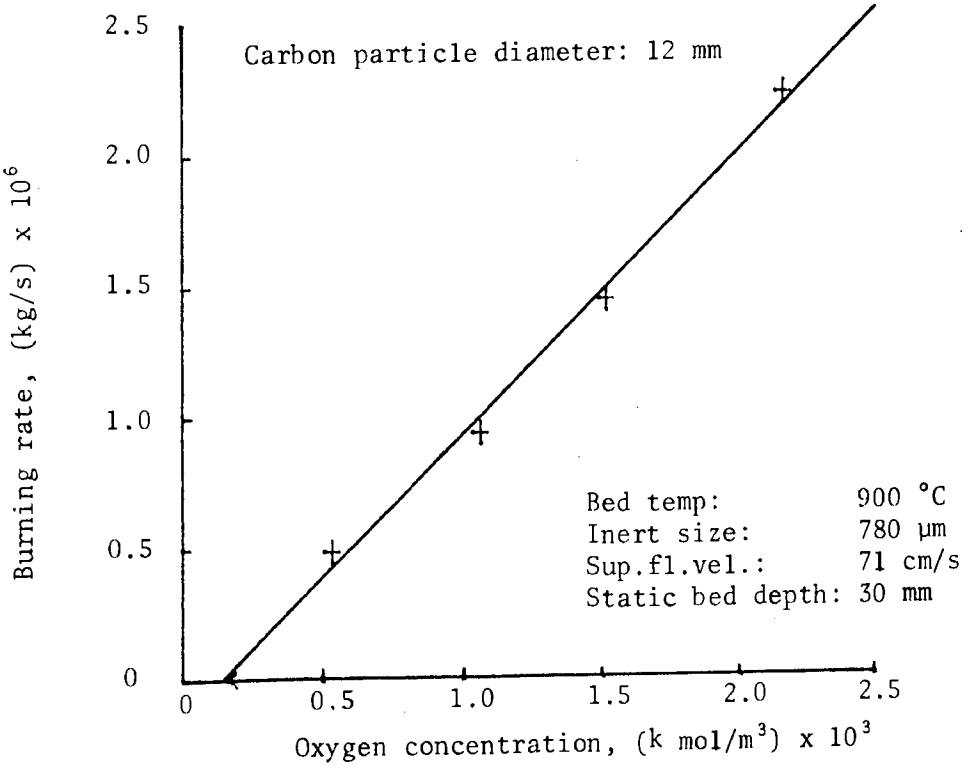

FIGURE 4.25: Variation of burning rate of carbon particle with oxygen concentration

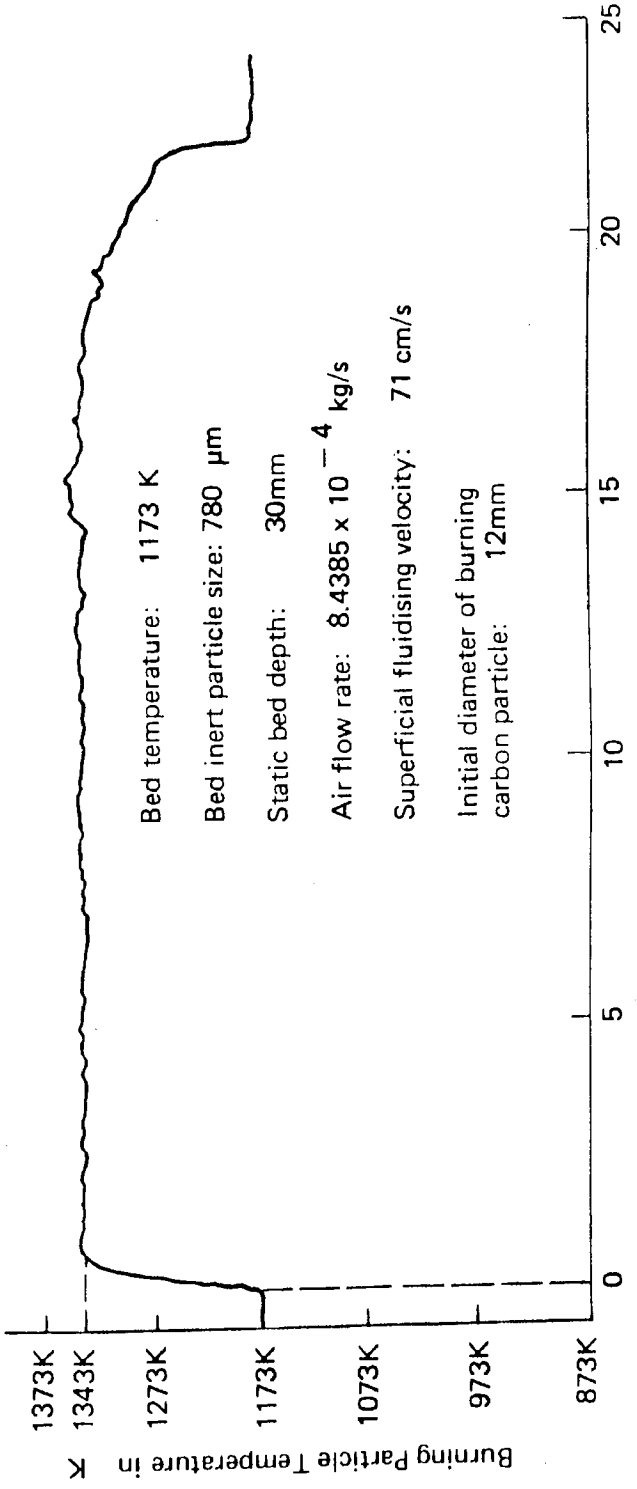

FIGURE 4.26: Temperature history of a burning carbon particle

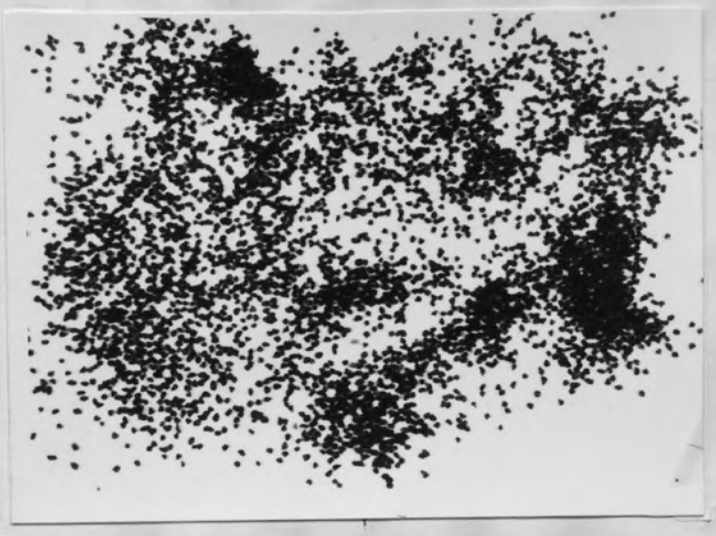

FIGURE 4.27: Photograph of some inert alumina particles

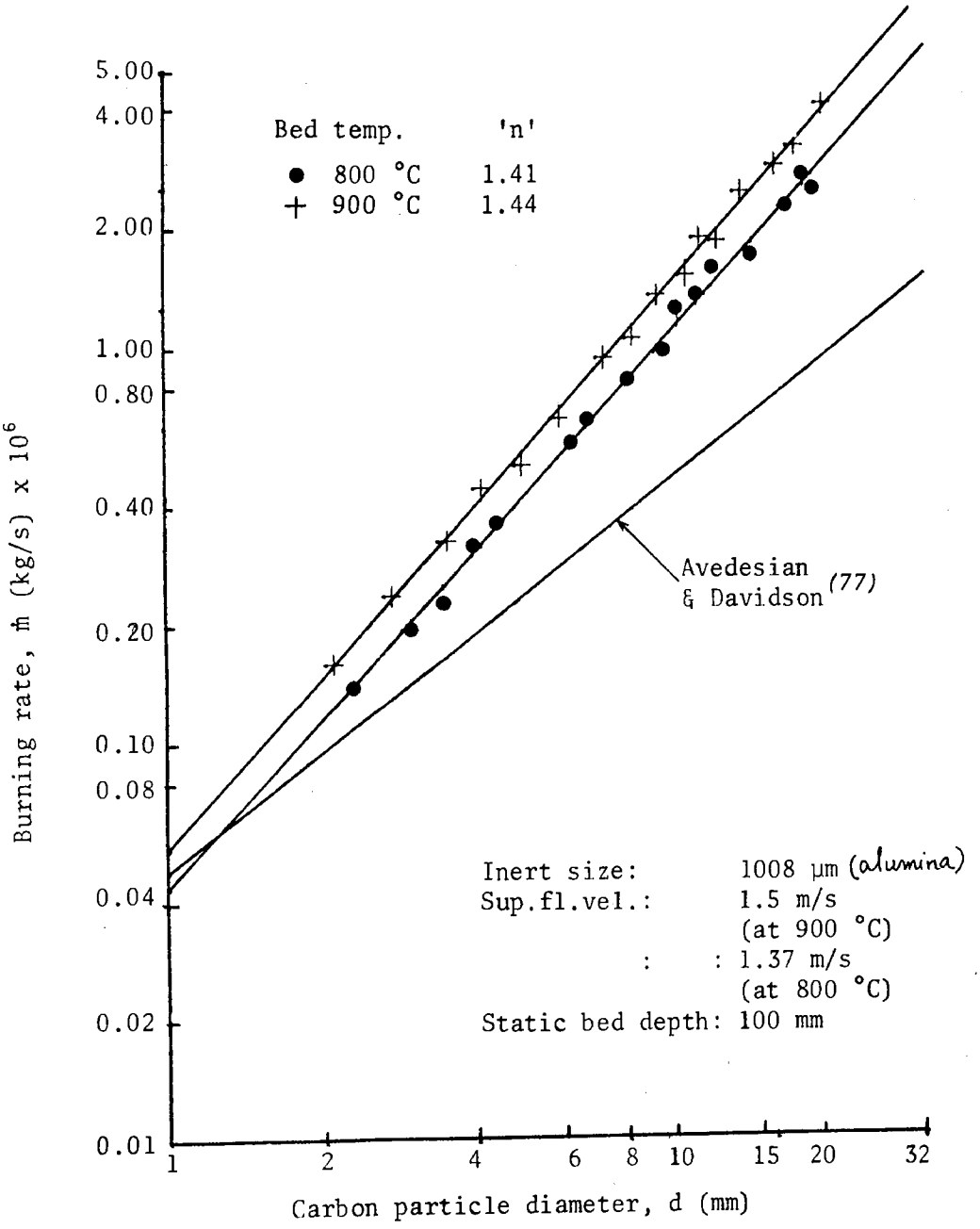

FIGURE 4.28: Variation of burning rate of carbon particles with diameter at different bed temperatures

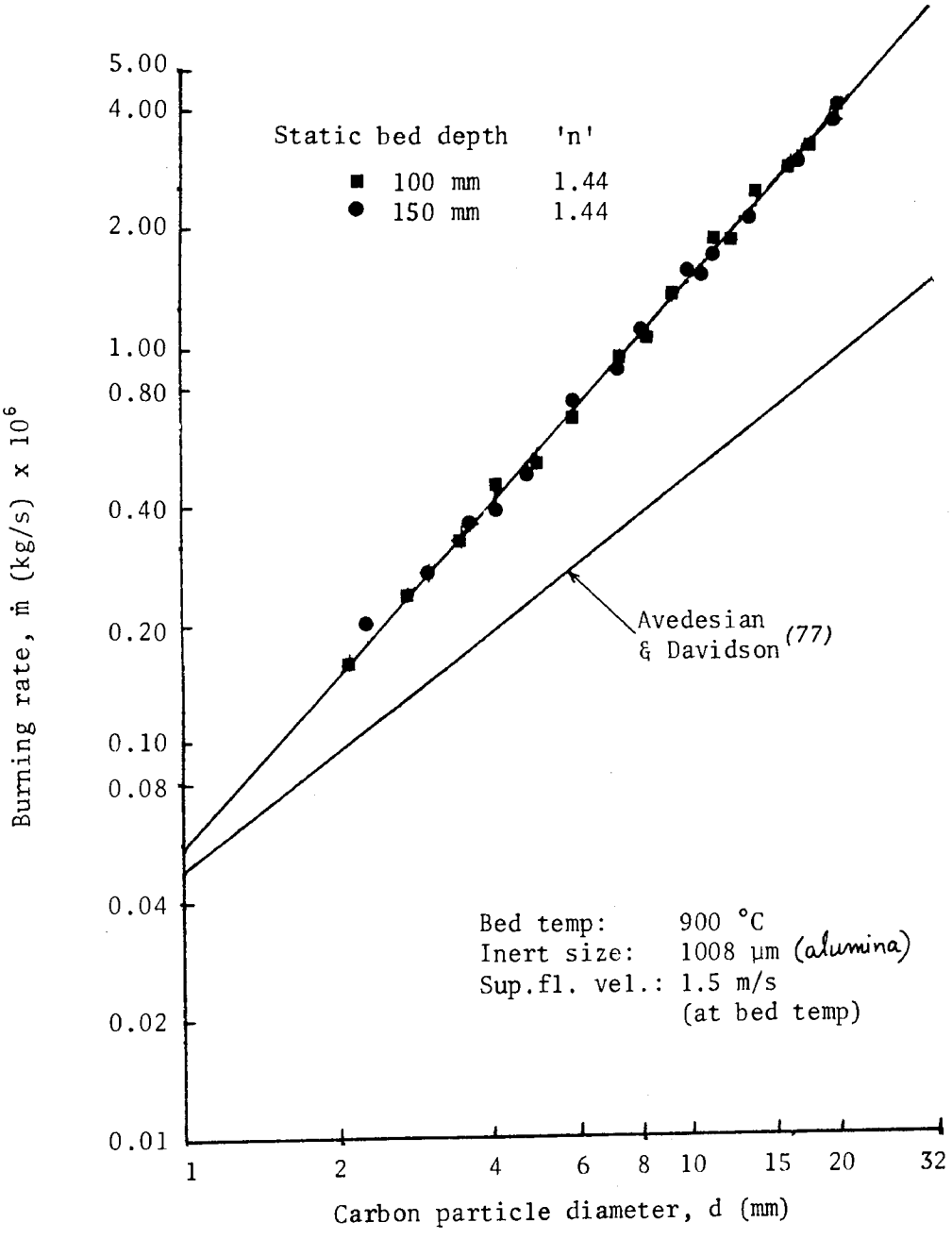

FIGURE 4.29: Variation of burning rate of carbon particles with diameter at different static bed depths

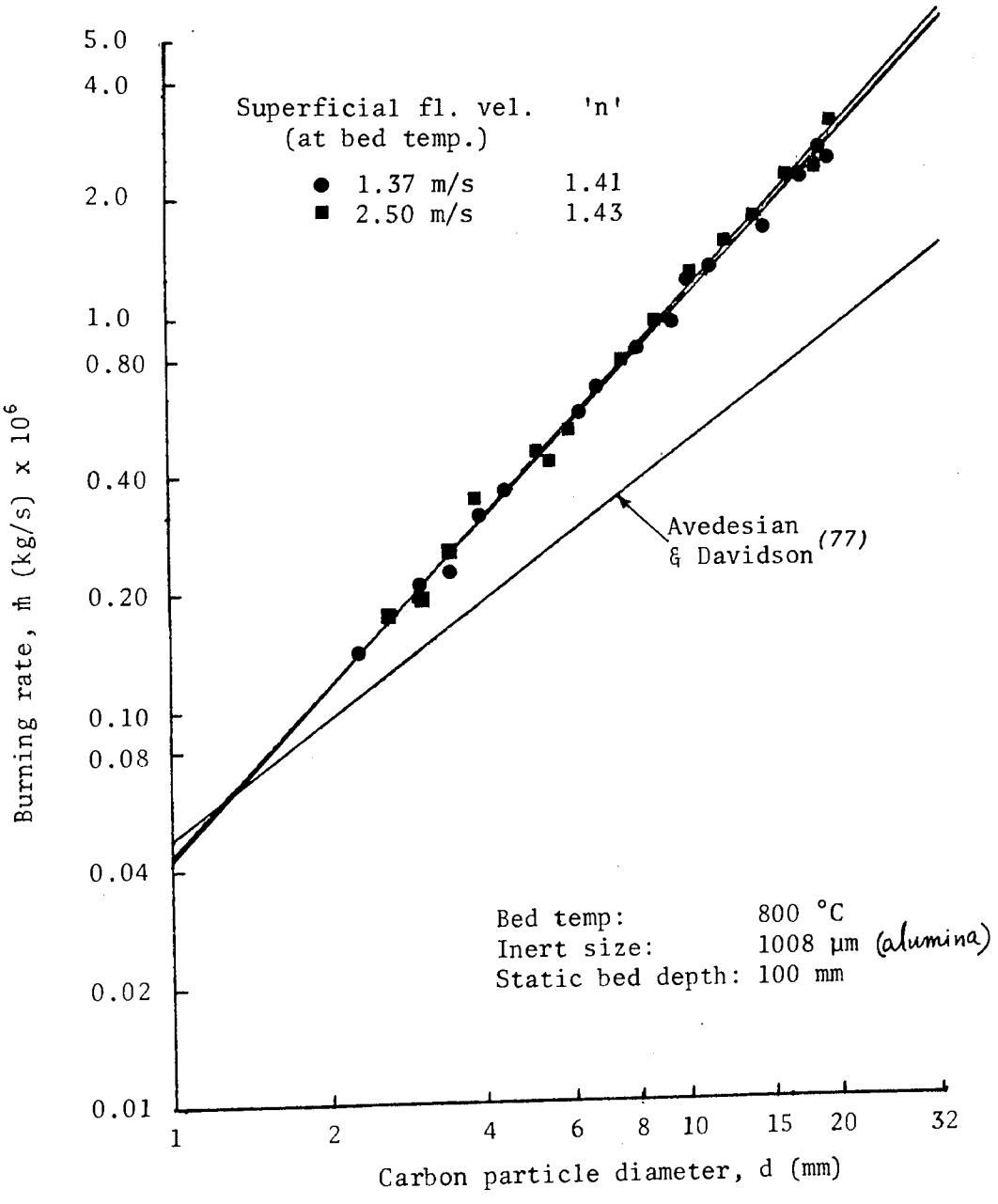

FIGURE 4.30: Variation of burning rate of carbon particles with diameter at different superficial fluidizing velocities

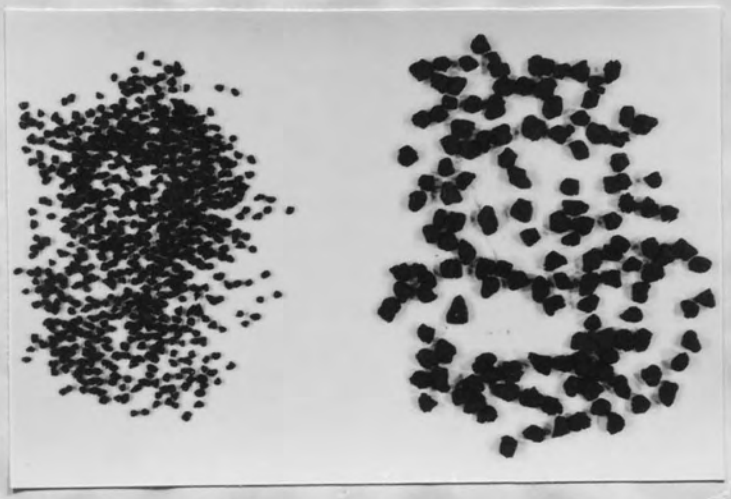

Size range:	Size range:
-2.00 mm to 1.68 mm	-4.75 mm to 4.00 mm
Mean size: 1.84 mm	Mean size: 4.375 mm

FIGURE 5.1: Photograph of some char particles

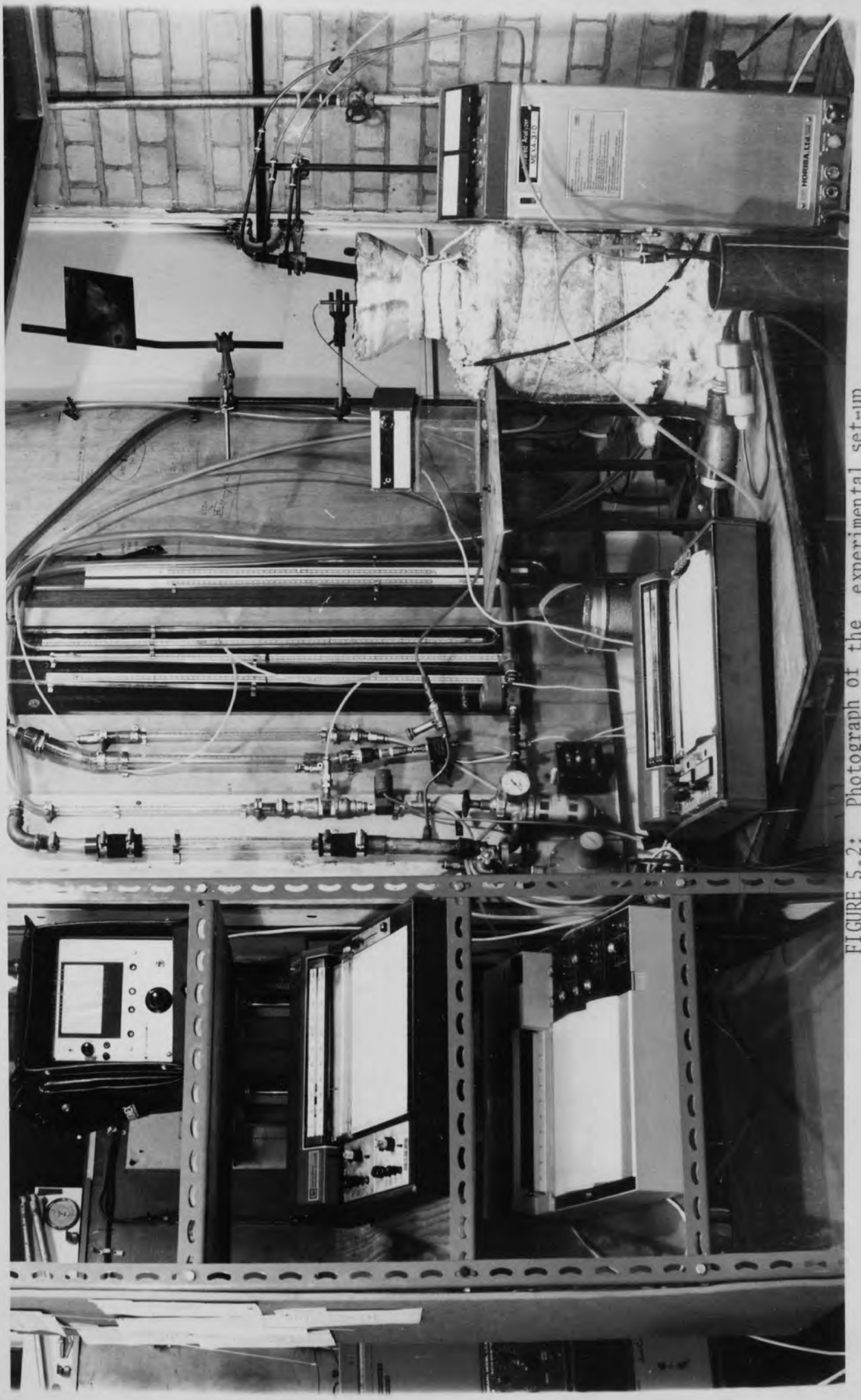

FIGURE 5.2: Photograph of the experimental set-up

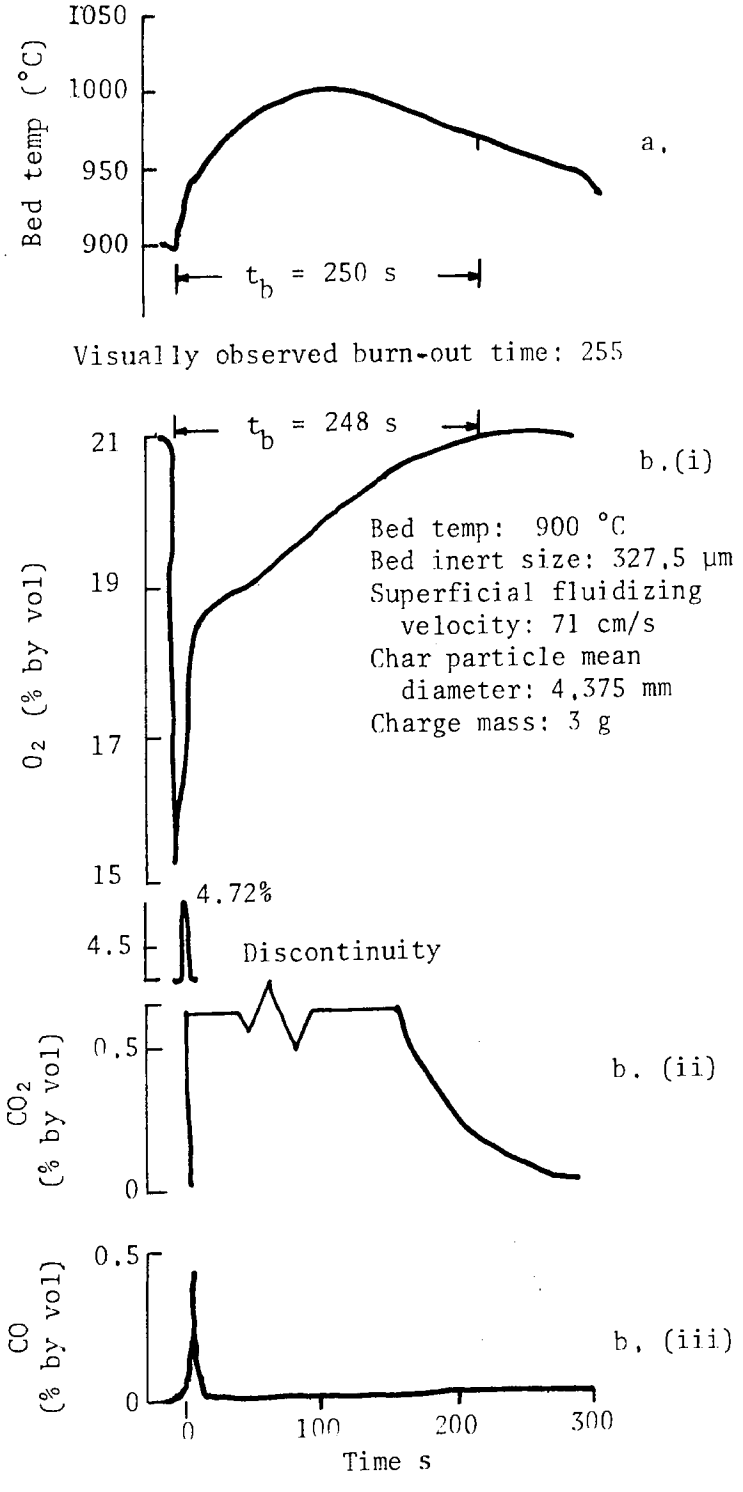

FIGURE 5.3: Typical histories (following injection of batch charges) of:
a. Bed temperature
b. Concentrations of gases in combustion products
(i) Oxygen (ii) Carbon dioxide
(iii) Carbon monoxide

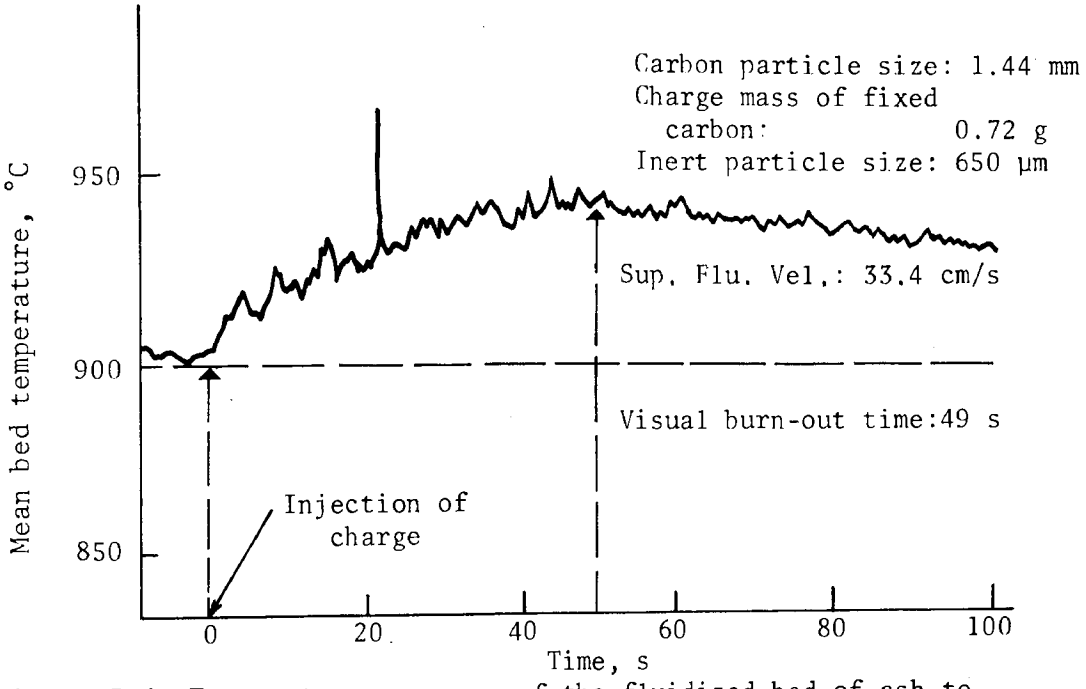

Figure 5.4 Temperature response of the fluidized bed of ash to the injection of a charge of carbon particles *(Avedesian & Davidson(77))*

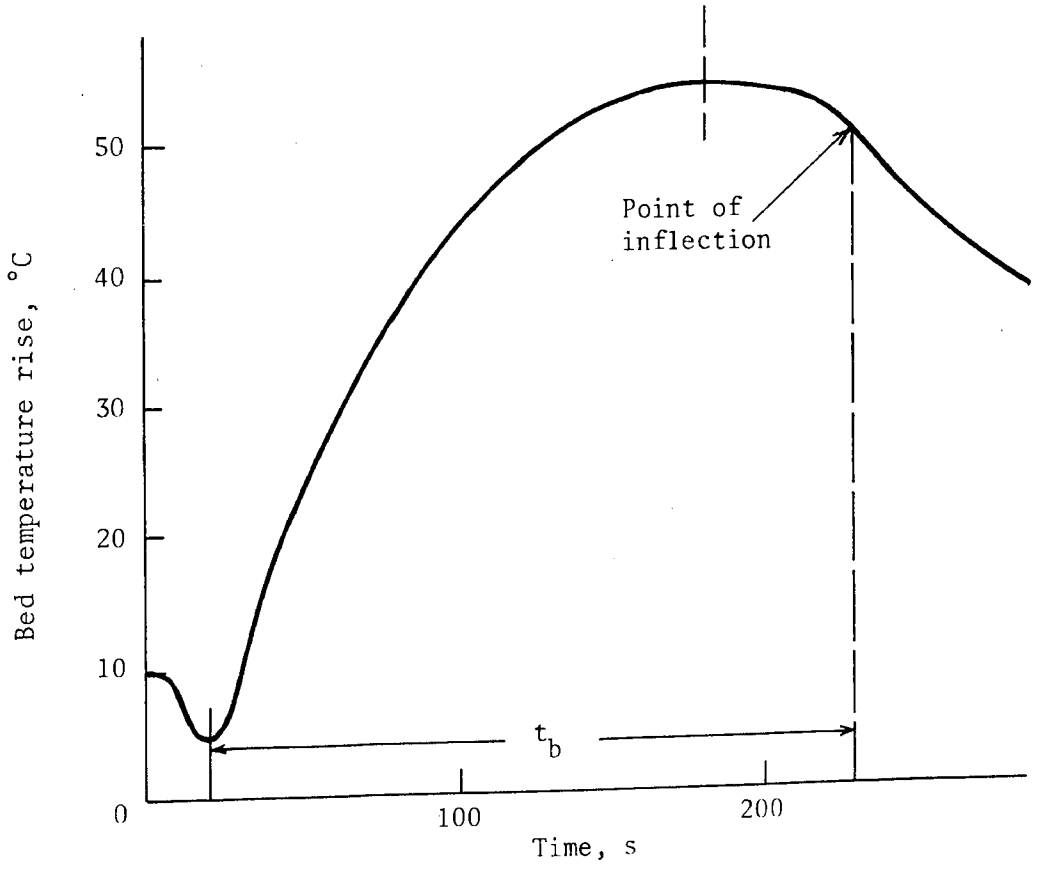

Figure 5.5 Typical temperature-time curve for batch charges *(Campbell(114))*

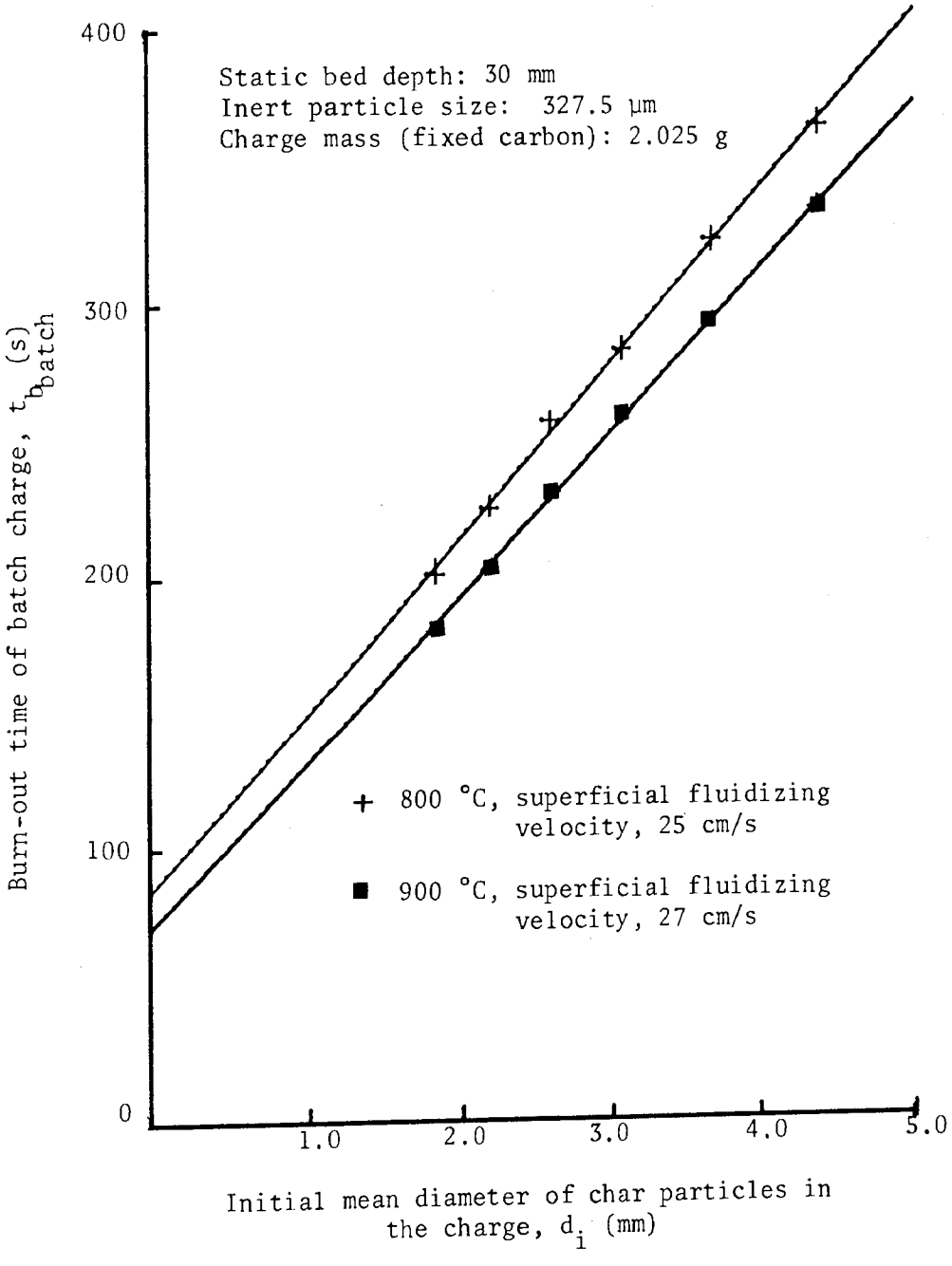

FIGURE 5.6: Burn-out time of batch charges of char particles against their initial mean diameter at different bed temperatures

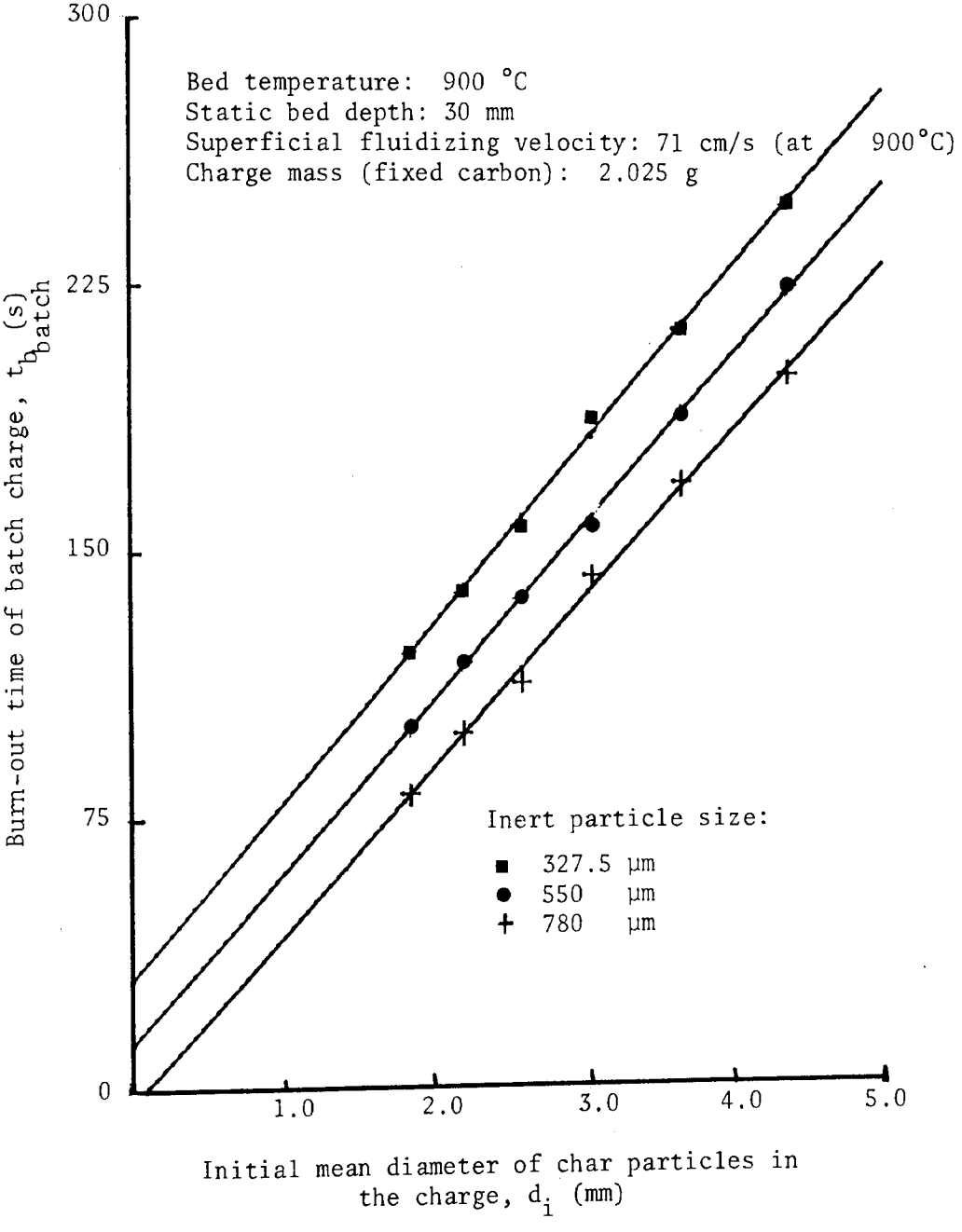

FIGURE 5.7: Burn-out time of batch charges of char particles against their initial mean diameter showing the effect of different sizes of inert particles in the bed

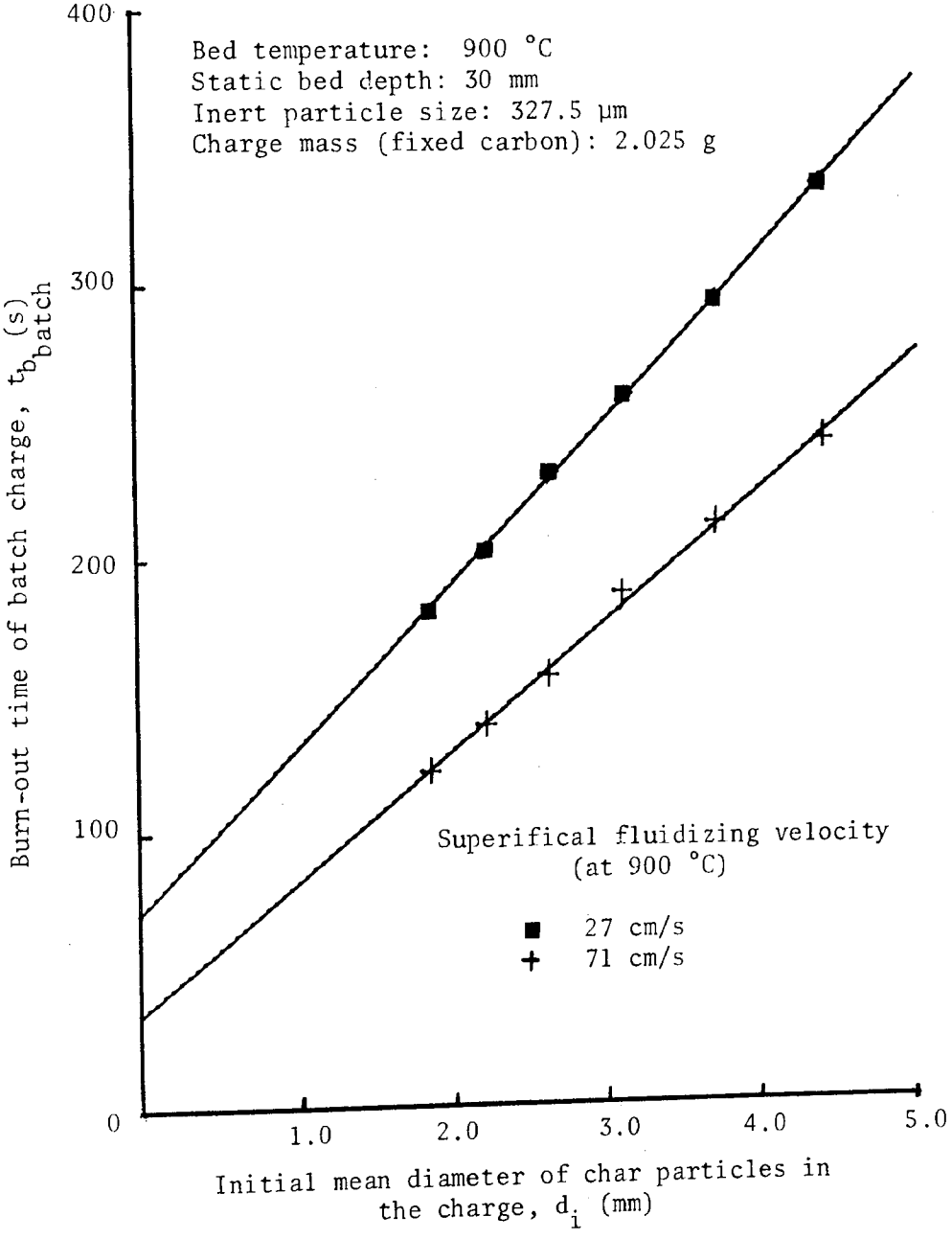

FIGURE 5.8: Burn-out time of batch charges of char particles against their initial mean diameter at different superficial fluidizing velocities

(a)

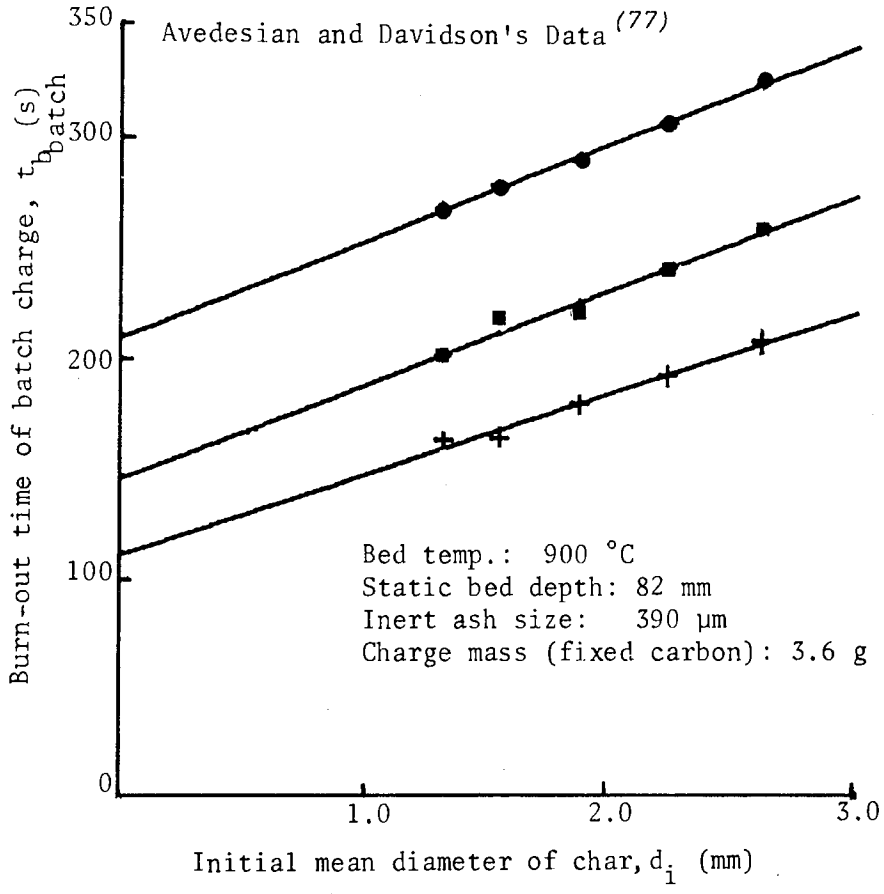

(b)

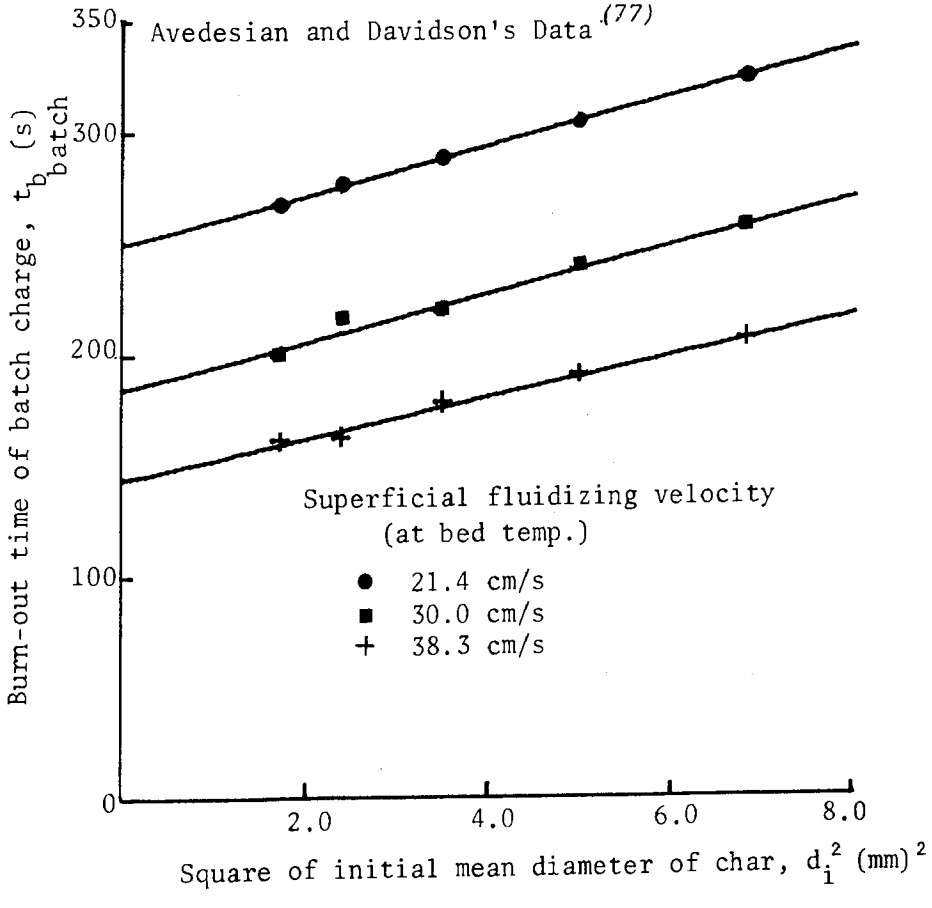

FIGURE 5.9: Burn-out time of batch charges of char particles (Avedesian & Davidson (77))

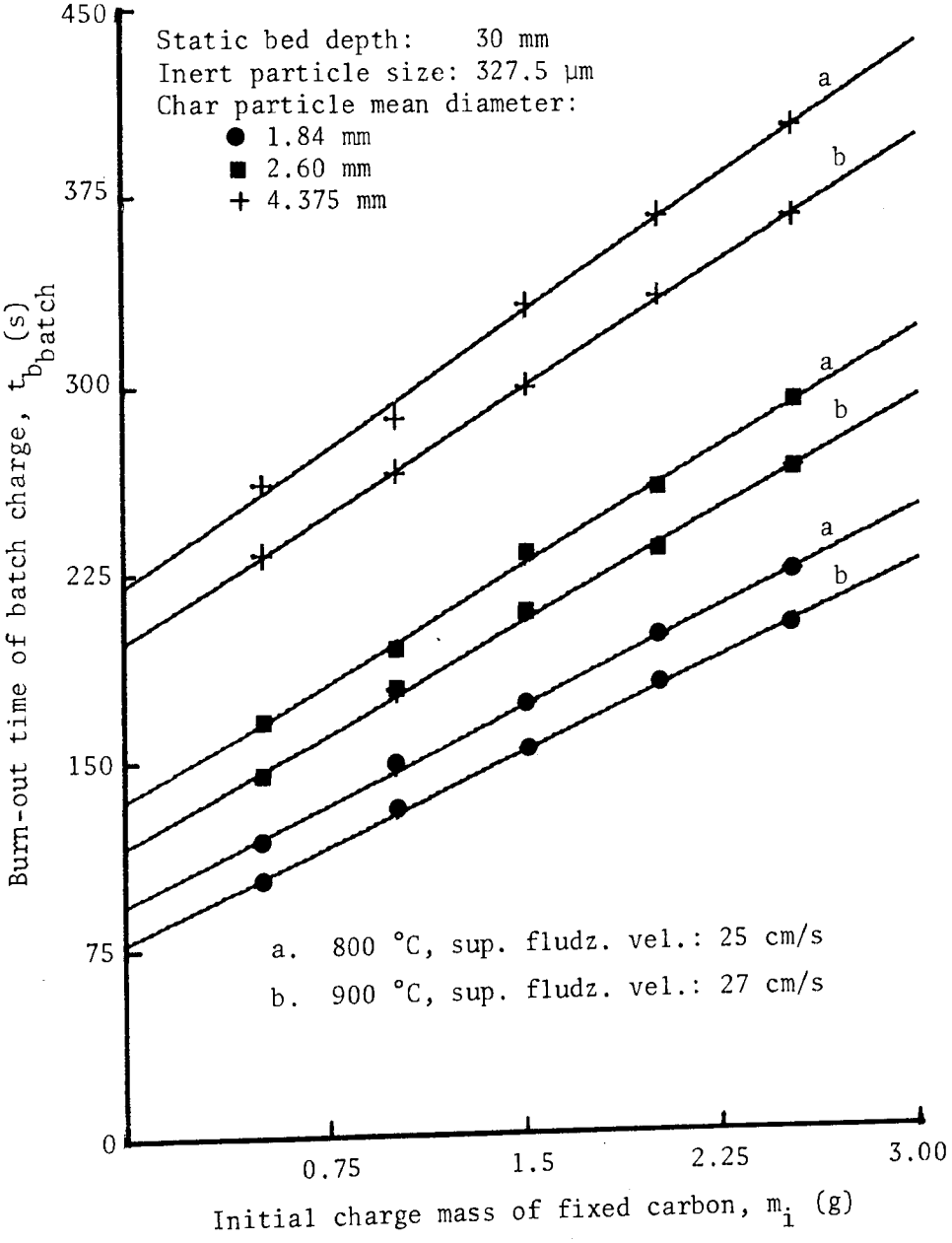

FIGURE 5.10: Burn-out time of batch charges of char particles against initial charge mass of fixed carbon at different bed temperatures

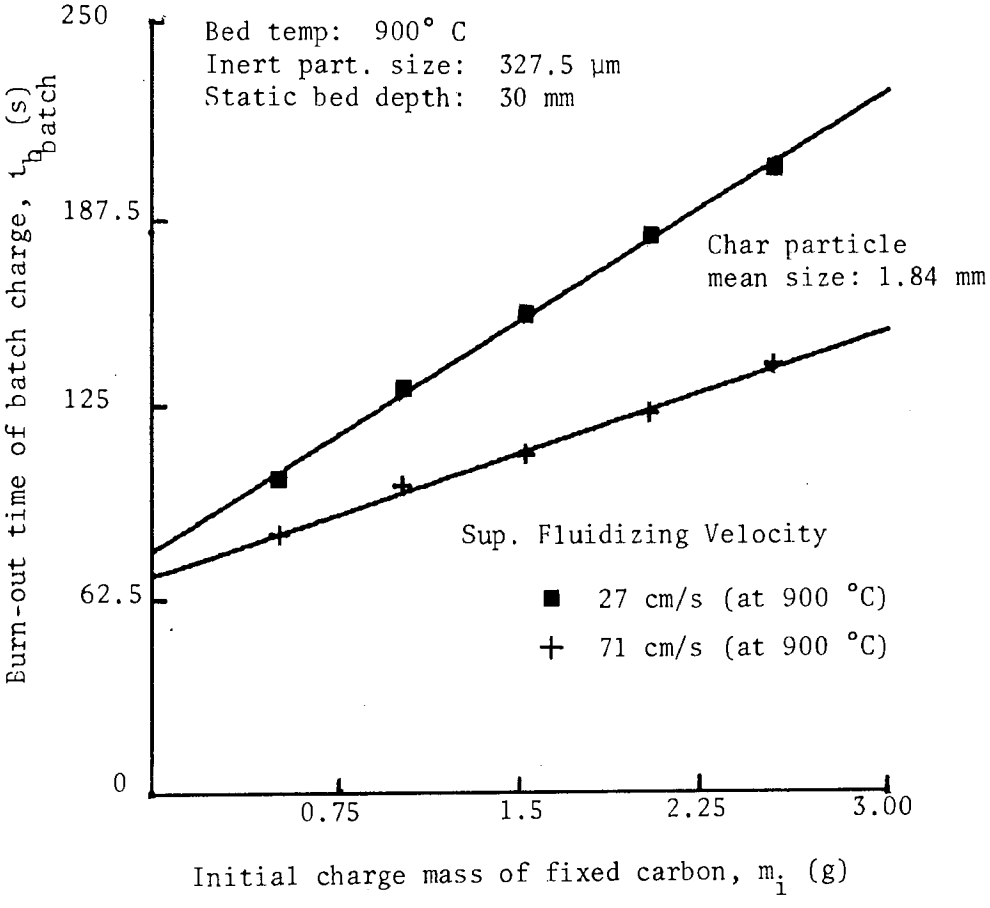

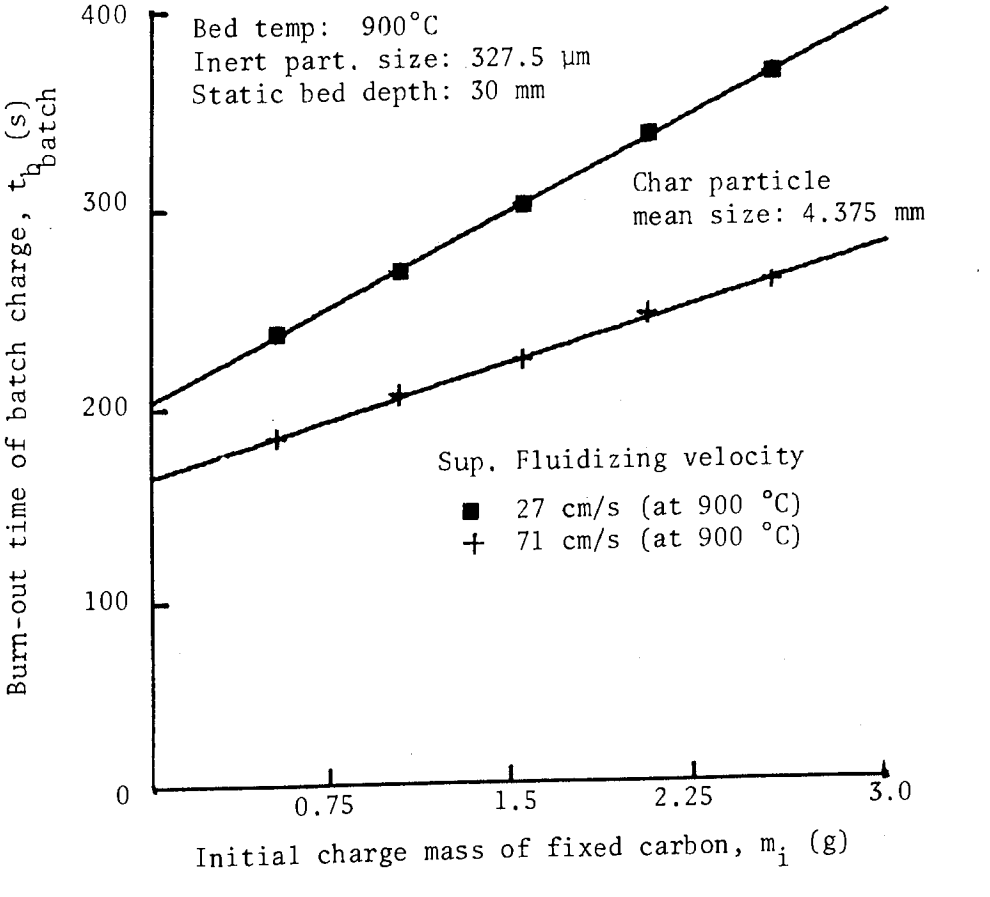

FIGURE 5.11: Burn-out time of batch charges of char particles against initial charge mass at different superficial fluidizing velocities

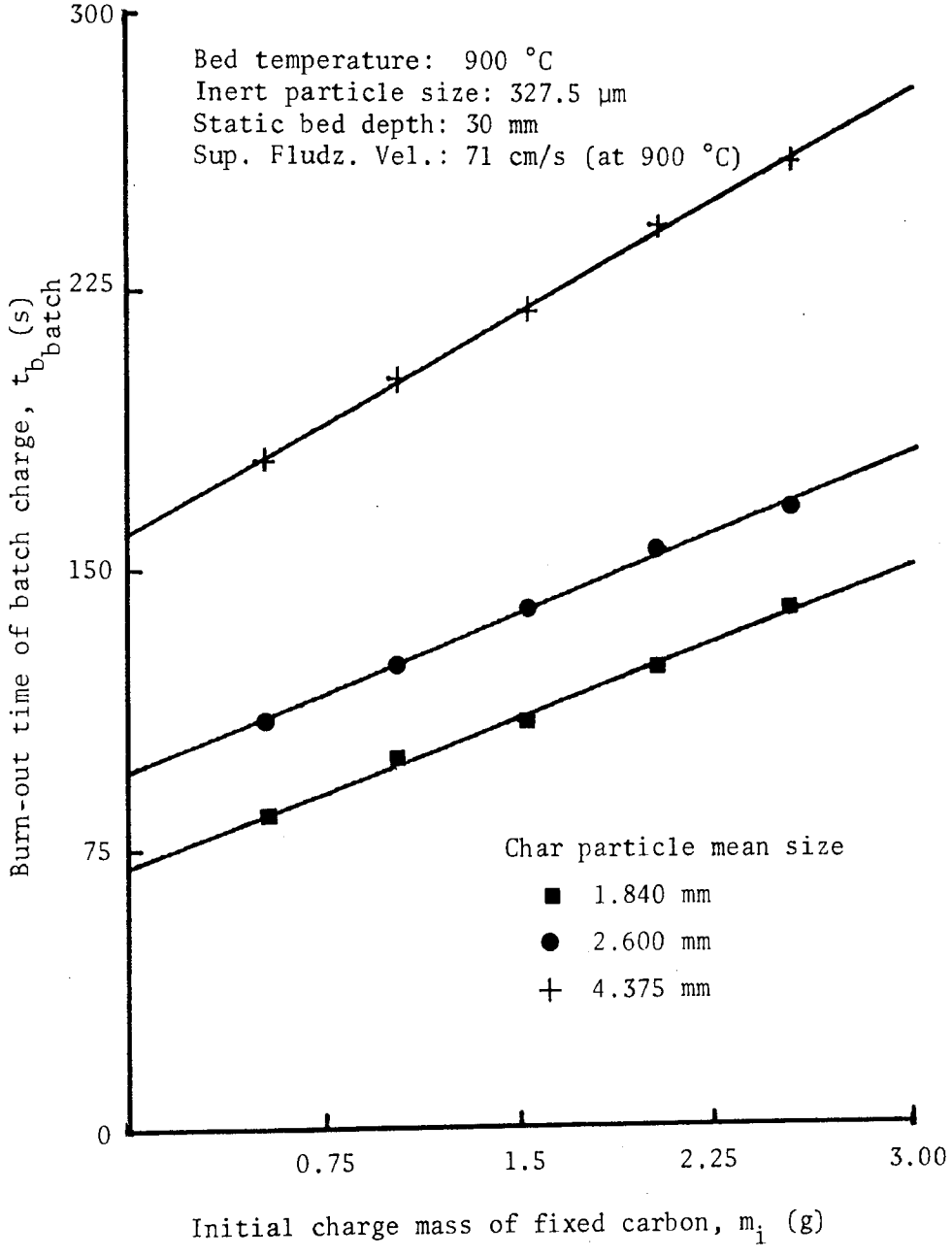

FIGURE 5.12: Burn-out time of batch charges of particles of different mean sizes against initial charge mass of fixed carbon

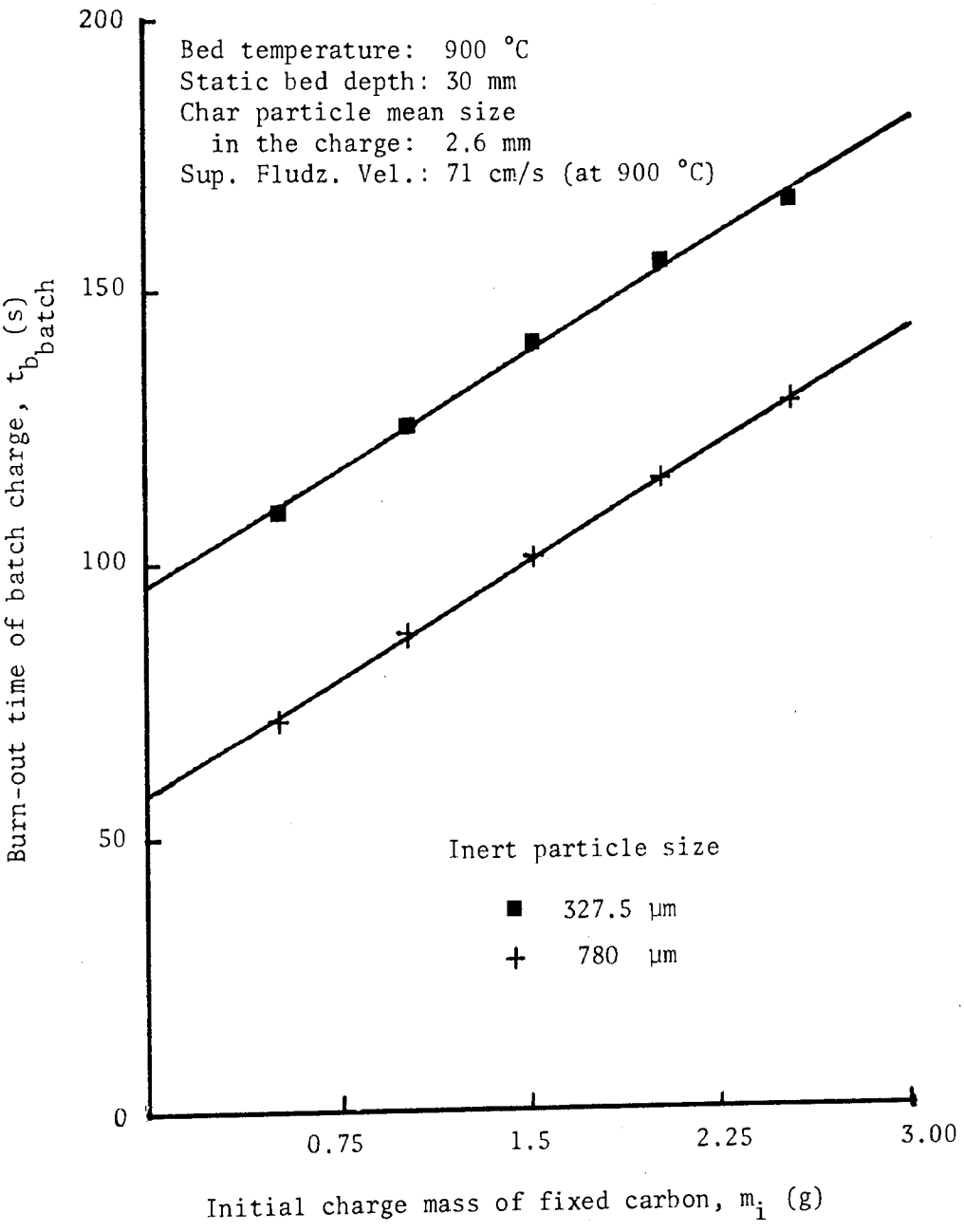

FIGURE 5.13: Burn-out time of batch charges of char particles against initial charge mass of fixed carbon showing the effect of different sizes of inert particles in the bed

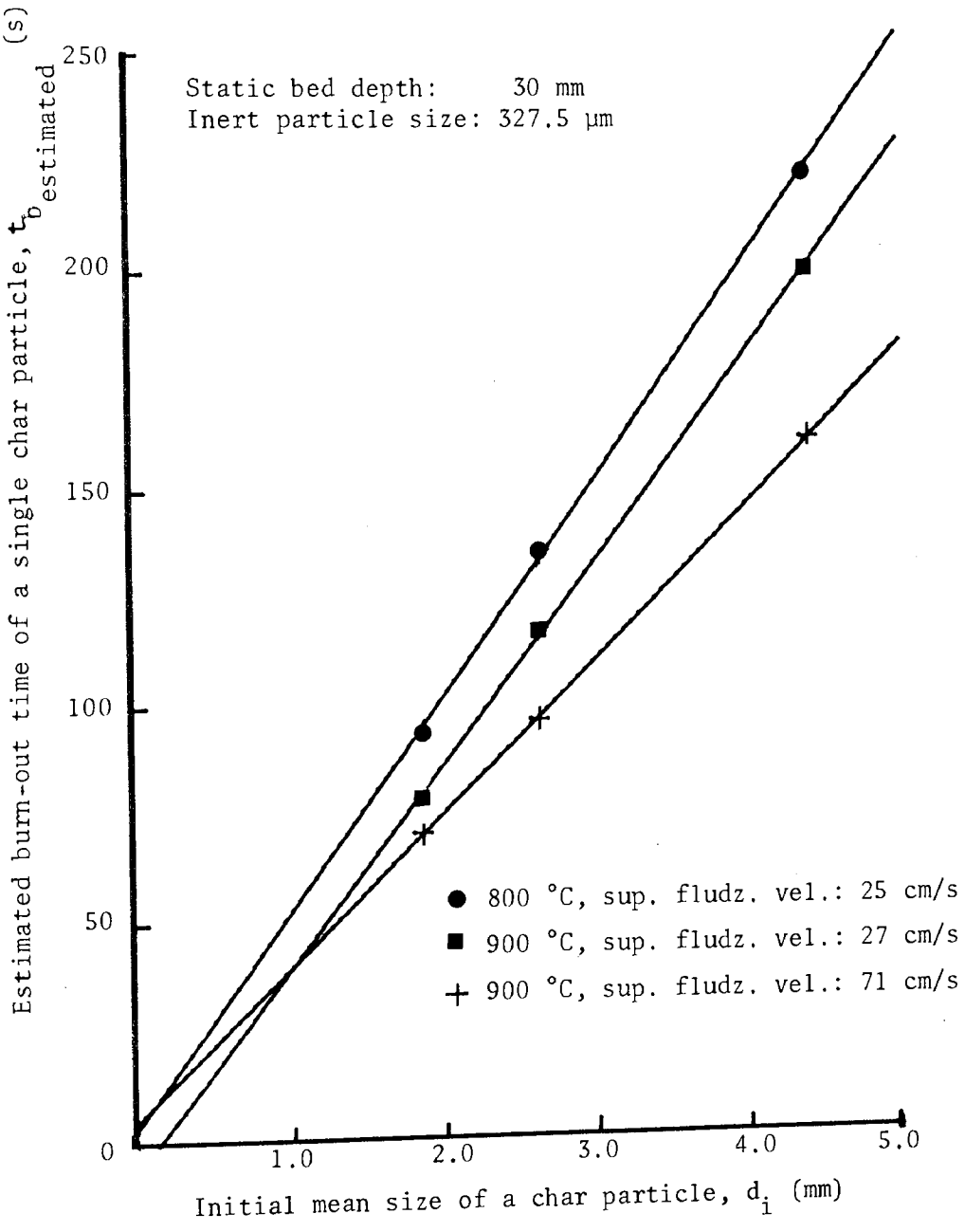

FIGURE 5.14: Estimated burn-out time of single char particles against their initial mean size at different fluidized bed operating conditions

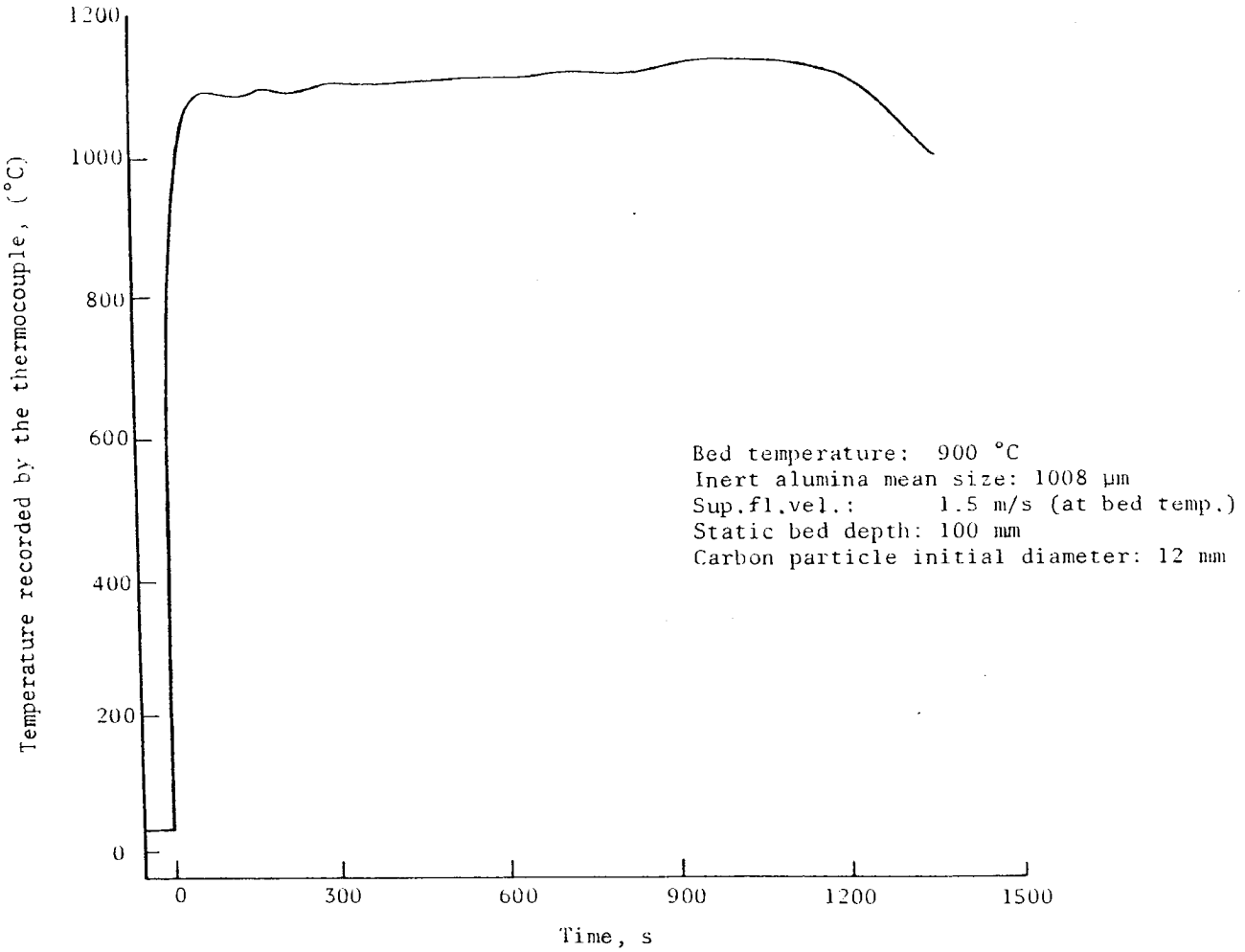

FIGURE 6.1: Temperature response of a thermocouple with its hot junction initially at the burning carbon particle surface and gradually moving away from the surface as combustion proceeded

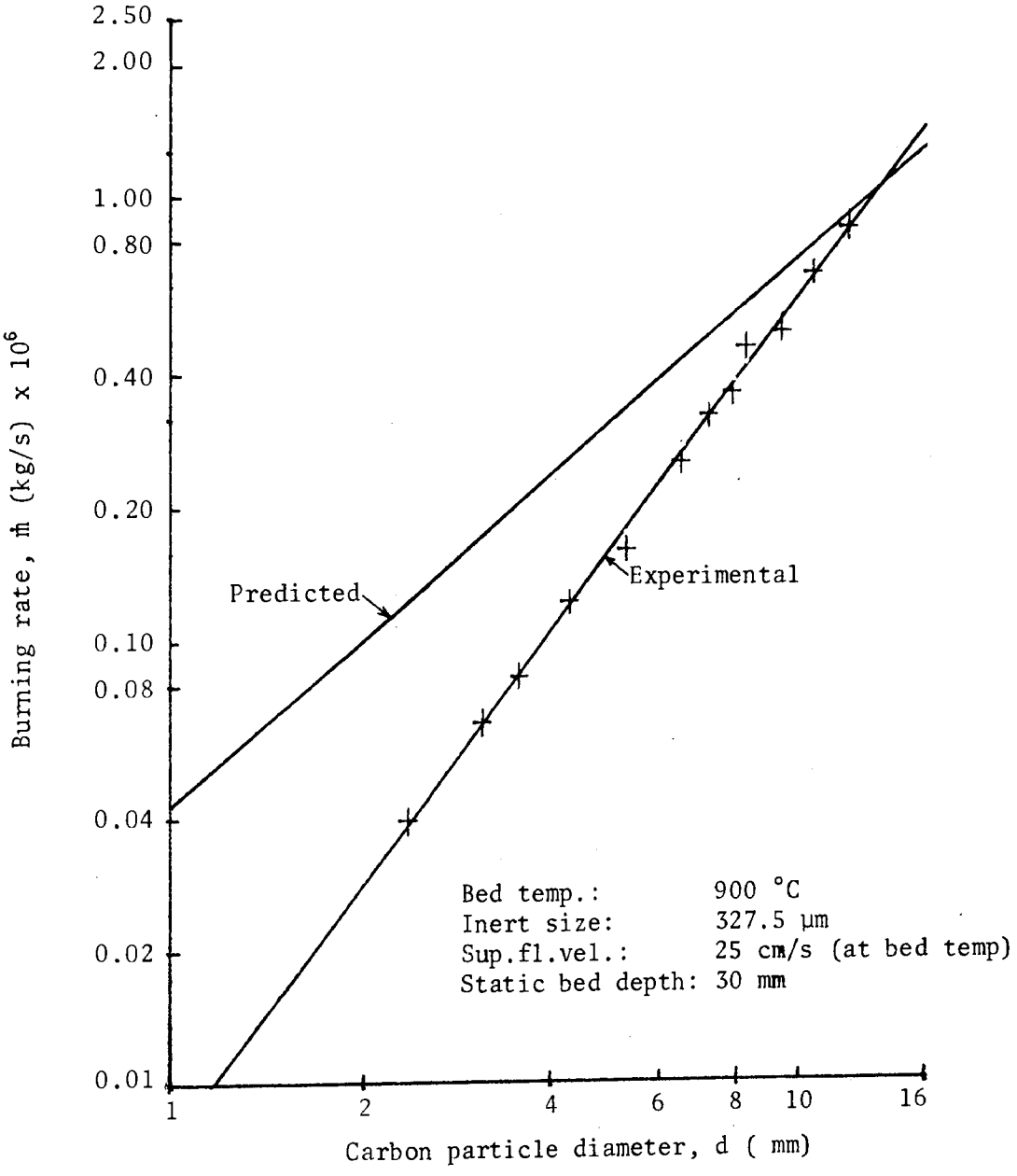

FIGURE 6.2: Comparison of experimental burning rates of single carbon particles with those predicted by the present proposed modified model

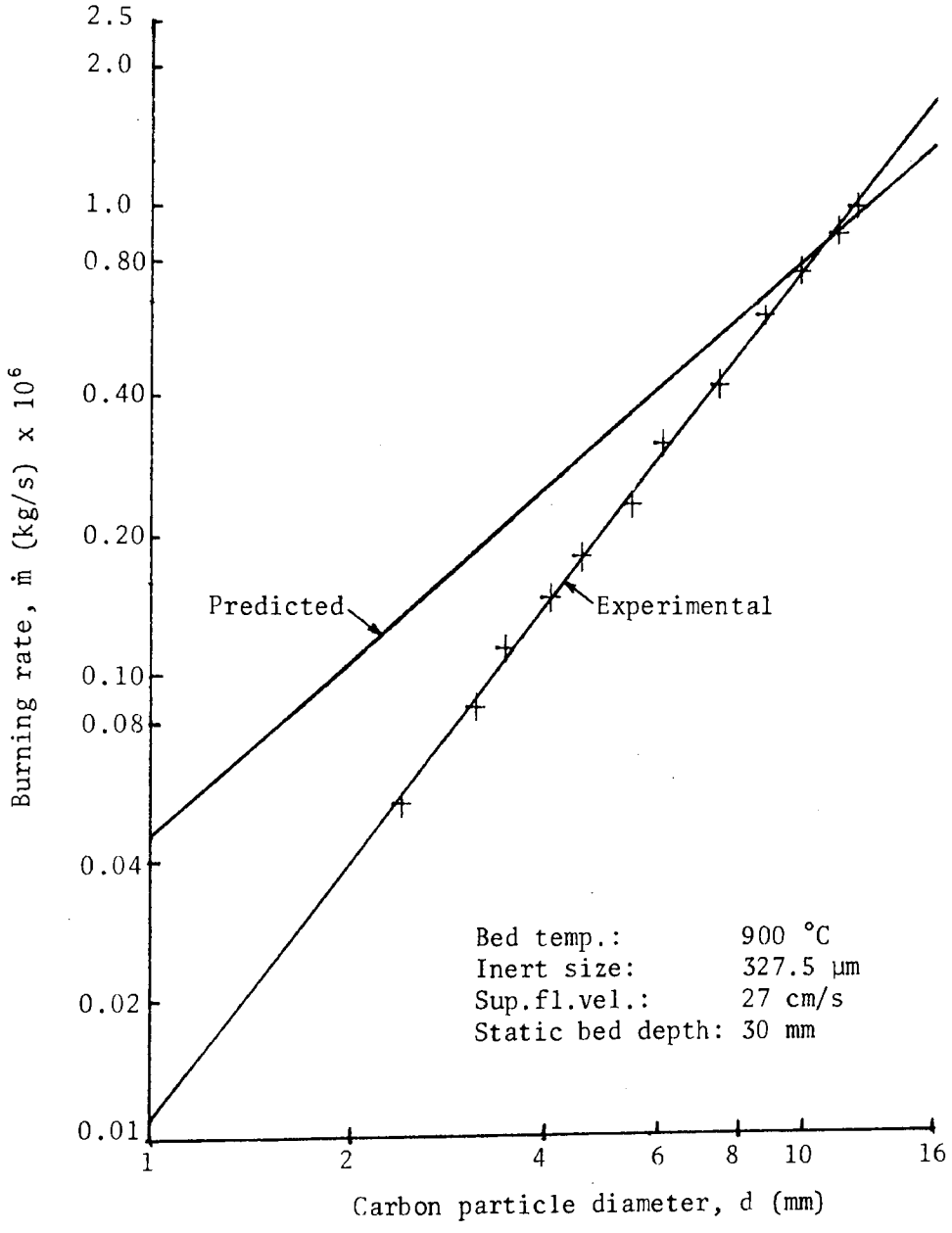

FIGURE 6.3: Comparison of experimental burning rates of single carbon particles with those predicted by the present proposed modified model

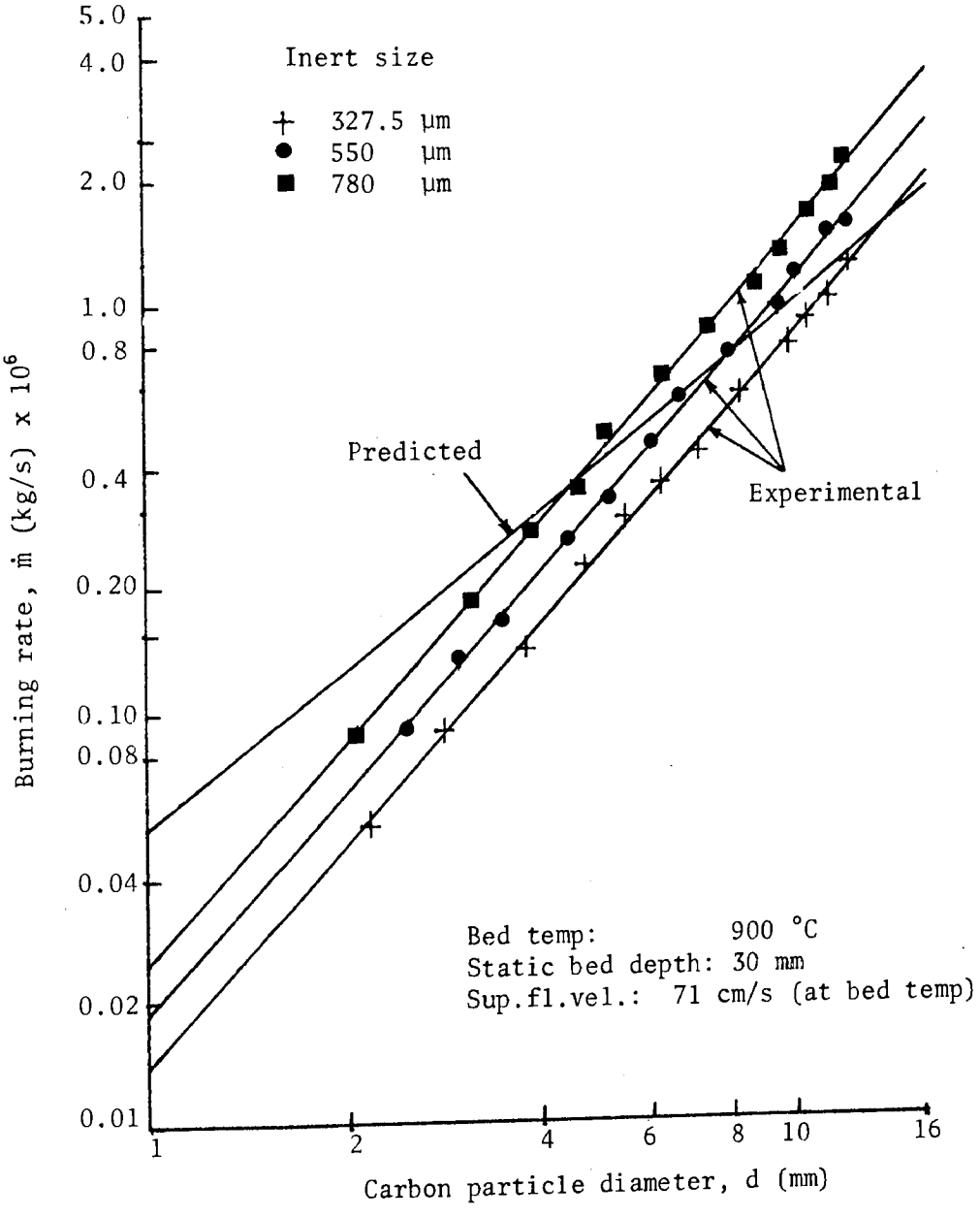

FIGURE 6.4: Comparison of experimental burning rates of single carbon particles with those predicted by the present proposed modified model

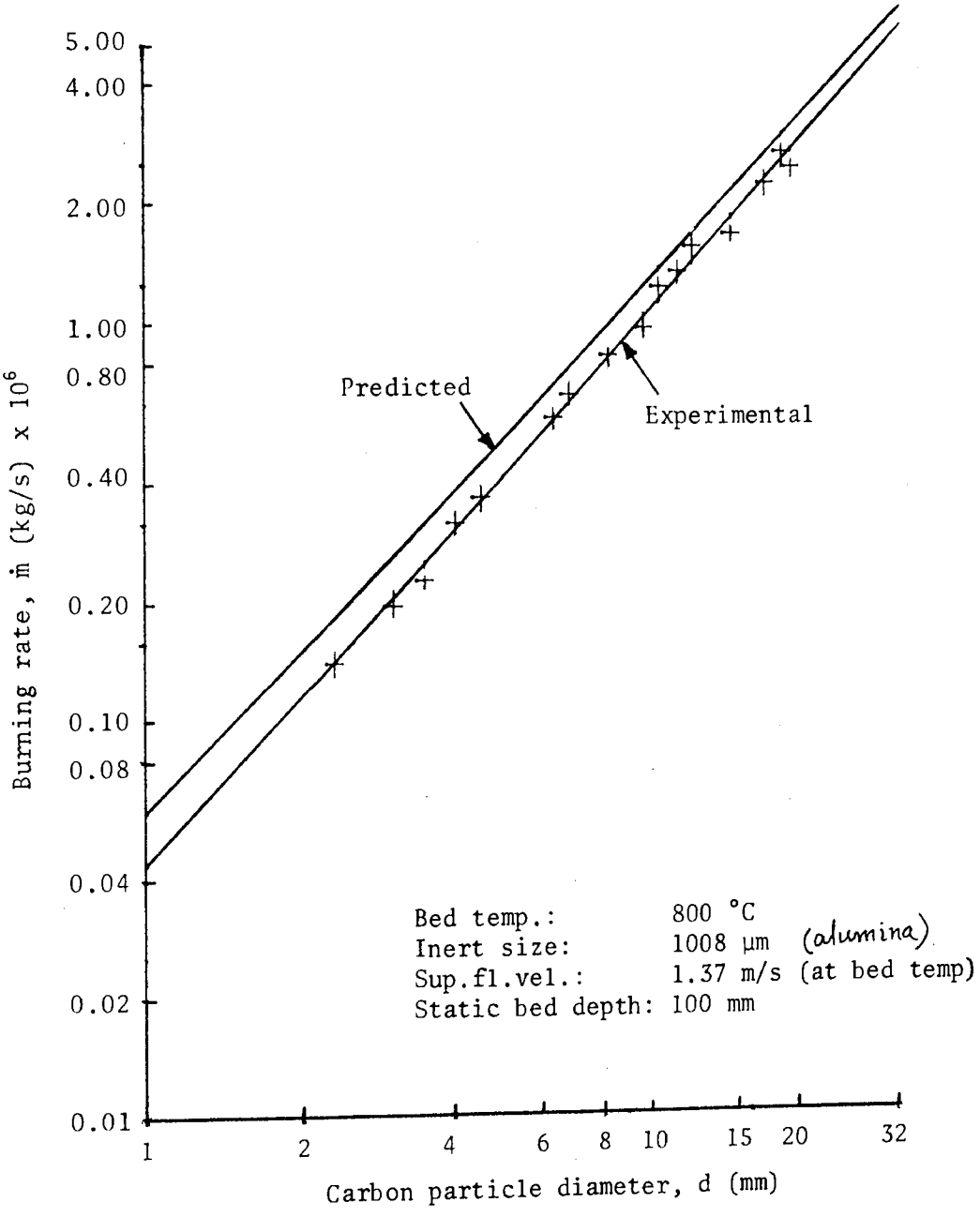

FIGURE 6.5: Comparison of experimental burning rates of single carbon particles with those predicted by the present proposed modified model

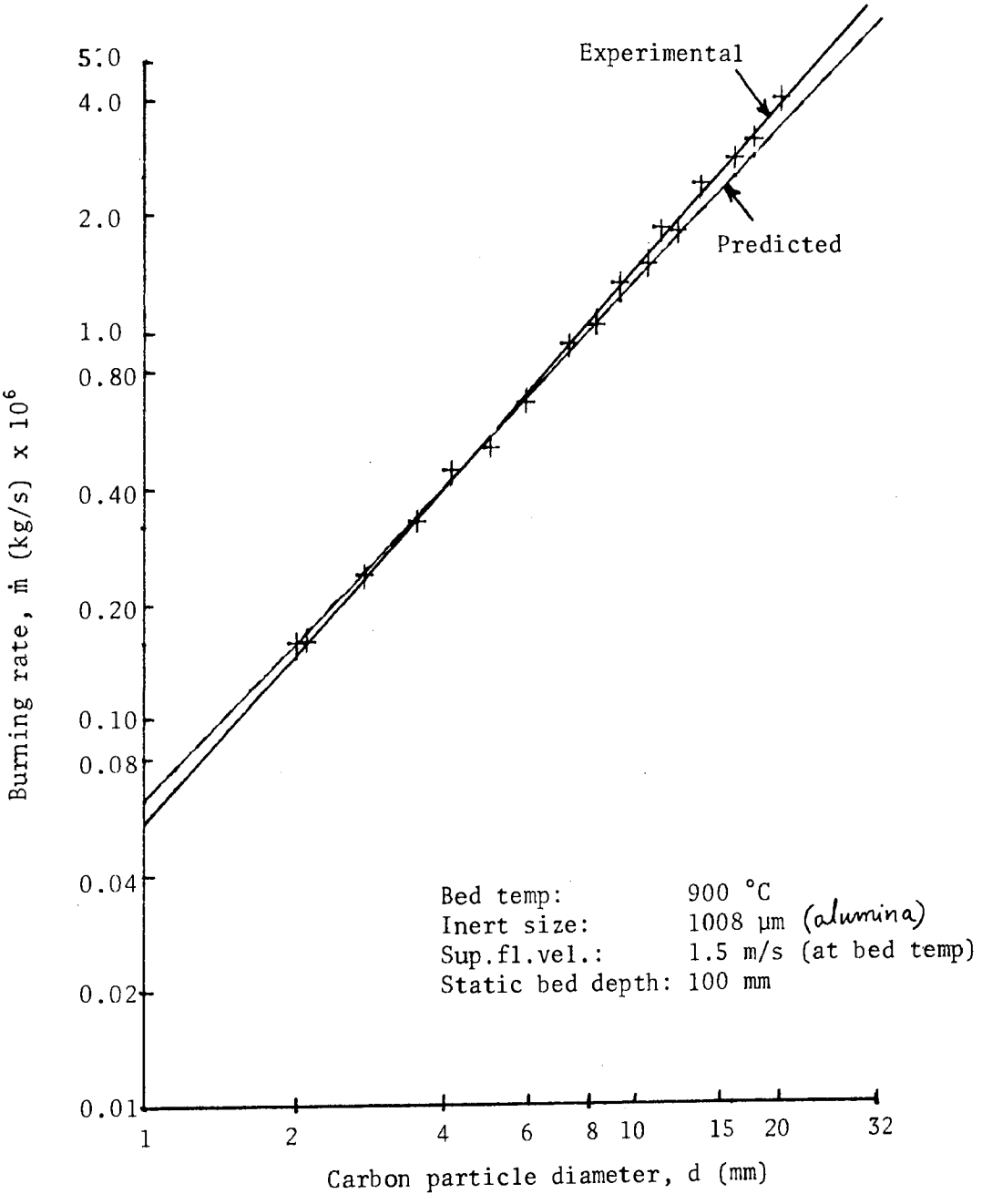

FIGURE 6.6: Comparison of experimental burning rates of single carbon particles with those predicted by the present proposed modified model

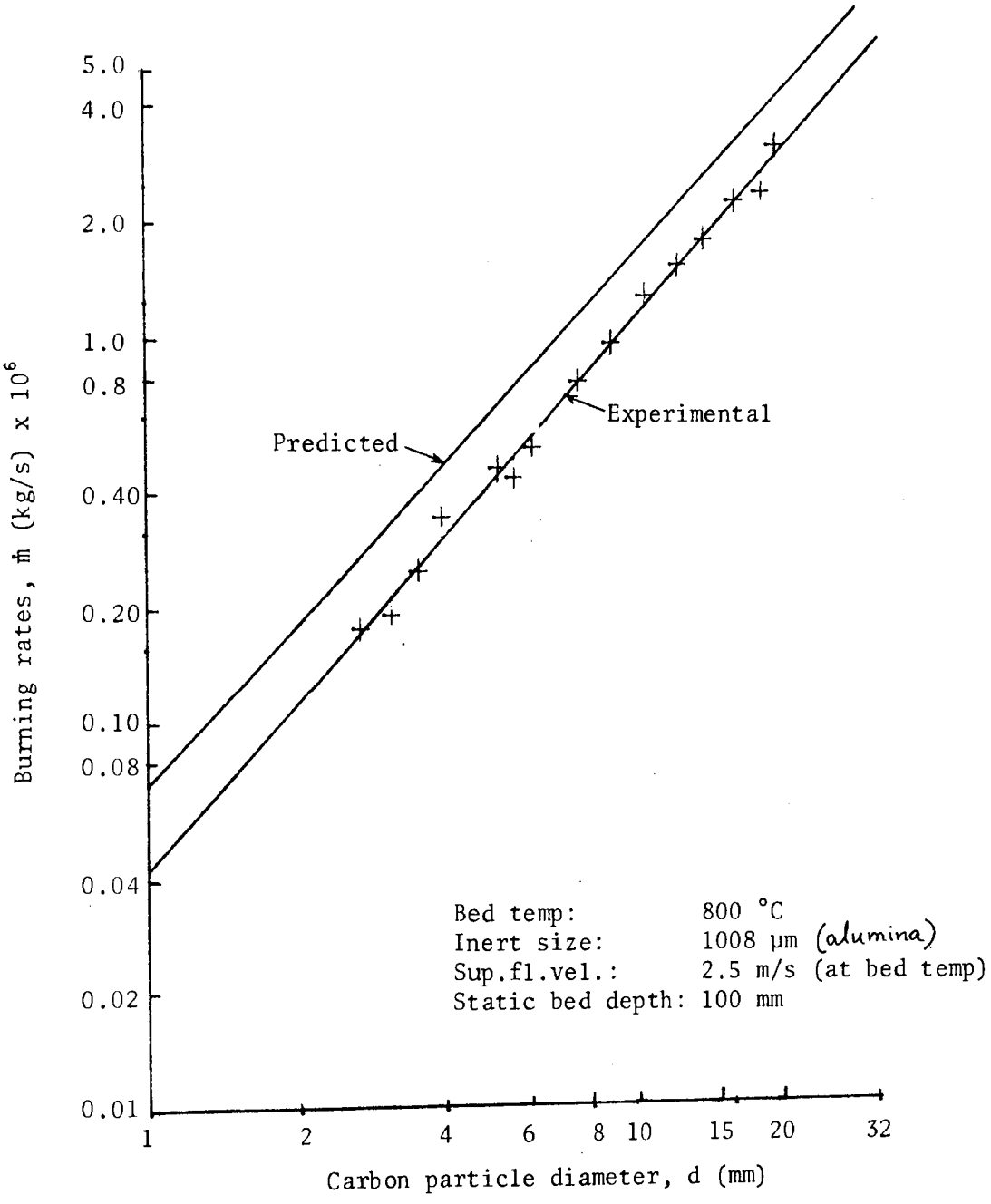

FIGURE 6.7: Comparison of experimental burning rates of single carbon particles with those predicted by the present proposed modified model

TABLE 2.1: SUMMARY OF CARBON COMBUSTION EXPERIMENTS IN FLUIDIZED BEDS

Research Workers	Carbon Particle Type and Size	Inert Particle Type and Size	Superficial Fludzg. Vel. (cm/s at Bed Temperature)	Bed Temperature °C	Combustor Dia. (mm)	Combustor Static Bed Depth (mm)	Reported Controlling Mechanism of Combustion
1. Avedesian & Davidson[77]	Coke and Char 0.23-2.61 mm	Ash 390-650 μm	21.4-38.3	900	76	82	Mass transfer by molecular diffusion
2. Campbell & Davidson[78]	Coal, char and coke 1.3-3.08 mm	Ash 390-650 μm	10-60	700-950	76	40-140	Above 850°C mass transfer by molecular diffusion
3. Basu et al[80]	Anthracite 1-6 mm	Sand 140 μm	20-30	850	100	50-100	Mainly chemical kinetics
4. Basu[81,83]	Electrode carbon 3-15 mm	Sand 100 μm	8	750-900	100	50-100	Combination of mass transfer by molecular diffusion and chem. kinetics
5. Yates & Walker[85]	Resin bonded coal dust 2-10 mm	Sand 225 μm	12.4-16.4	760-960	100	140	Mass transfer by molecular diffusion
6. Andrei[88] and Andrei et al[89]	Lignite 1.85-3 mm	Sand 200 μm	6.08-6.72	750-900	100	120	Mass transfer by forced convection at min^m. fludz. vel.
7. Present work at Aston (by Chakraborty)	a. Char 1.84-4.375 mm Electrode carbon 2-12 mm	Sand 327.5-780 μm	27-71	800-900	71.5	12.5-50	a. Mainly by chemical kinetics
	b. Electrode carbon 3-20 mm	Alumina 1008 μm	137-250	800-900	71.5	100-150	b. At 800°C: Mainly by chemical kinetics At 900°C: Mass transfer by forced convection at sup. fludzg. vel.

TABLE 4.1

BURNING ELECTRODE CARBON PARTICLE TEMPERATURES IN FLUIDIZED BEDS OF SAND

Bed Temp (°C)	Static Bed Depth (mm)	Inert Particle Size (μm)	Sup. Fludzg Vel. (cm/s)	Oxygen Concentration in the Particulate Phase ((k mol/m^3) x 10^3)	BURNING ELECTRODE CARBON PARTICLE TEMPERATURE (°C) IN			
					Electrically Heated Bed		Continuously-Fed Coal-Fired Bed	
					PARTICLE SIZE		PARTICLE SIZE	
					6 mm	12 mm	6 mm	12 mm
800 " " "	30 " " "	327.5 " " "	25 27 " "	2.36 1.517 1.062 0.532	870	850 840 830 815		
900	12.5	327.5	27	2.16	1035	1015		
900	50	327.5	27	2.16	970	950		
900	30	327.5	27	2.16 1.517 1.062 0.532	980	955 945 930 920	950	925
900	30	327.5	71	2.16 1.517 1.062 0.532	1030	1000 970 950 930	990	960
900	30	550	71	2.16 1.517 1.062 0.532	1045	1025 990 960 940	1000	975
900	30	780	71	2.16 1.517 1.062 0.532	1115	1070 1030 985 955	1075	1040

TABLE 4.2: SHERWOOD NUMBER OF BURNING CARBON PARTICLES

(Estimated from Equation (2.4) of *Avedesian & Davidson*[77] using present experimental burning rate data).

Bed temperature (°C)	Inert sand particle size (μm)	Superficial fluidizing velocity (at bed temperature) (cm/s)	Static bed depth (mm)	Estimated Sherwood Number of carbon particles of diameter		
				3 mm	6 mm	12 mm
800	327.5	25	30	0.65	1.20	2.22
900	327.5	27	12.5	1.23	2.10	3.58
900	327.5	27	30	0.81	1.45	2.57
900	327.5	27	50	0.83	1.38	2.29
900	327.5	71	30	1.00	1.76	3.07
900	550	71	30	1.35	2.38	4.20
900	780	71	30	1.76	3.12	5.50

TABLE 4.3: COMPARISON OF BURNING RATES OF SINGLE CARBON PARTICLES IN ELECTRICALLY HEATED BED AND COAL FIRED BED

Bed temperature (°C)	Inert sand particle size (μm)	Superficial fluidizing velocity (cm/s)	Burning rate of carbon particles (kg/s)x 10^6					
			Electrically heated bed Particle diameter			Coal fired bed Particle diameter		
			3 mm	6 mm	12 mm	3 mm	6 mm	12 mm
900	327.5	27	0.083	0.294	1.05	0.039	0.145	0.539
900	327.5	71	0.102	0.357	1.25	0.050	0.168	0.563
900	550	71	0.138	0.481	1.68	0.074	0.26	0.916
900	780	71	0.183	0.640	2.24	0.094	0.336	1.21

N.B. Static bed depth in all the above cases was 30 mm.

TABLE 4.4: BURNING RATES OF CARBON PARTICLES AT DIFFERENT OXYGEN CONCENTRATIONS

Bed temperature (°C)	Inert size (μm)	Sup. flu. vel. (at bed temperature) (cm/s)	Oxygen conc. in fl. gas. (k mol/m^3) x 10^3	Burning rate of carbon particles (kg/s) x 10^6 Particle diameter 3 mm	6 mm	12 mm
800	327.5	25	2.360	0.0611	0.229	0.861
			1.517	0.046	0.167	0.612
			1.062	0.032	0.116	0.430
			0.532	0.016	0.062	0.232
900	327.5	27	2.160	0.083	0.294	1.047
			1.517	0.061	0.211	0.732
			1.062	0.046	0.160	0.561
			0.532	0.024	0.085	0.302
900	327.5	71	2.160	0.102	0.357	1.249
			1.517	0.074	0.251	0.853
			1.062	0.054	0.184	0.631
			0.532	0.029	0.096	0.321
900	550	71	2.16	0.138	0.481	1.681
			1.517	0.092	0.325	1.145
			1.062	0.064	0.231	0.836
			0.532	0.033	0.118	0.418
900	780	71	2.160	0.183	0.640	2.242
			1.517	0.120	0.417	1.449
			1.062	0.070	0.257	0.938
			0.532	0.038	0.136	0.486

N.B. Static bed depth in all the above cases was 30 mm.

TABLE 4.5

BURNING ELECTRODE CARBON PARTICLE TEMPERATURES IN FLUIDIZED BEDS OF ALUMINA

Bed Temp (°C)	Static Bed Depth (mm)	Inert Particle Size (μm)	Superficial Fluidizing Velocity (m/s)	Oxygen Concentration in the Particulate Phase ((k mol/m^3) x 10^3)	BURNING ELECTRODE CARBON PARTICLE	
					Size (mm)	Temp (°C)
800	100	1008	1.37	2.36	19	1020
800	100	1008	2.5	2.36	20	1055
900	100	1008	1.5	2.16	19.7	1075
900	150	1008	1.5	2.16	20	1070

TABLE 5.1: ESTIMATED BURN OUT TIME OF SINGLE CHAR PARTICLES

1. Present work:
Inert sand particle size: 327.5 μm Static bed depth: 30 mm

Section A

Char particle mean size, (mm)	Estimated burn out time of single char particle, (s)		
	800°C-25 cm/s	900°C-27 cm/s	900°C-71 cm/s
1.84	93.85	79.03	70.81
2.6	135.63	117.33	96.81
4.375	221.84	119.43	160.71

Section B

Ratio of char particle sizes	Ratio of corresponding estimated burn out times of single char particles		
	800°C-25 cm/s	900°C-27 cm/s	900°C-71 cm/s
1.84/2.6 = 0.71	0.69	0.67	0.73
2.6/4.375 = 0.59	0.61	0.59	0.60
1.84/4.375 = 0.42	0.42	0.40	0.44

2. *Avedesian & Davidson's*[77] work:
Inert ash particle size: 390 μm Static bed depth: 82 mm

Section C

Char particle mean size, (mm)	Estimated burn out time of single char particle, (s)		
	900°C-21.4 cm/s	900°C-30 cm/s	900°C-38.3 cm/s
1.87	5315	50.1	49.9
2.61	79.6	79.5	84.1

Section D

Ratio of char particle sizes	Ratio of corresponding estimated burn out times of single char particles		
	900°C-21.4 cm/s	900°C-30 cm/s	900°C-38.3 cm/s
1.87/2.61 = 0.72	0.67	0.63	0.59

Square of ratio of char particle size = $(1.87/2.61)^2 = 0.52$

TABLE 6.1: ESTIMATED VALUES OF OVERALL RESISTANCE, MASS TRANSFER RESISTANCE AND KINETIC RESISTANCE TO COMBUSTION OF ELECTRODECARBON PARTICLES IN SHALLOW FLUIDIZED BEDS OF SAND

Bed temp. (°C)	Inert sand size (μm)	Superficial flu. vel. (at bed temp.) (cm/s)	Overall resistance to combustion, $\frac{1}{K}$ $(\frac{s}{m})$ Carbon particle diameter (mm)			Mass transfer resistance combustion, $\frac{1}{k_g}$ $(\frac{s}{m})$ Carbon particle diameter (mm)			Kinetic resistance to combustion, $\frac{1}{k_s}$ $(\frac{s}{m})$ Carbon particle diameter (mm)		
			3	6	12	3	6	12	3	6	12
800	327.5	25	13.11	13.97	14.88	4.83	8.21	13.54	8.28	5.76	1.34
900	327.5	27	8.84	9.96	11.20	4.20	7.16	11.85	4.64	2.80	-0.65
900	327.5	71	7.17	8.21	9.39	3.33	5.45	8.67	3.84	2.76	0.72
900	550	71	5.34	6.10	7.95	3.33	5.45	8.67	2.01	0.65	-0.72
900	780	71	4.02	4.59	5.23	3.33	5.45	8.67	0.69	-0.86	-3.44

N.B. Static bed depth in all the above cases was 30 mm.

TABLE 6.2: ESTIMATED VALUES OF OVERALL RESISTANCE, MASS TRANSFER RESISTANCE AND KINETIC RESISTANCE TO COMBUSTION OF ELECTRODE CARBON PARTICLES IN SHALLOW FLUIDIZED BEDS OF HIGH DENSITY ALUMINA

Bed temp. (°C)	Superficial fl. vel. (at bed temp.) (m/s)	Overall resistance to combustion, $\frac{1}{K}$ $(\frac{s}{m})$ Carbon particle diameter (mm)				Mass transfer resistance to combustion, $\frac{1}{k_g}$ $(\frac{s}{m})$ Carbon particle diameter (mm)				Kinetic resistance to combustion $\frac{1}{k_s}$ $(\frac{s}{m})$ Carbon particle diameter (mm)			
		3	6	12	18	3	6	12	18	3	6	12	18
800	1.37	3.87	5.82	8.76	11.12	3.07	4.86	7.51	9.59	0.80	0.96	1.25	1.53
800	2.50	3.92	5.80	8.59	10.82	2.51	3.89	5.90	7.47	1.41	1.91	2.69	3.35
900	1.50	2.75	4.06	5.99	7.53	2.69	4.26	6.60	8.44	0.06	-0.20	-0.61	-0.91

N.B. In all the above cases: static bed depth = 100 mm; Inert alumina size = 1008 μm